OL. 6 NO. 4 OCTOBER 1963

Journal of

ELECTROANALYTICAL CHEMISTRY

International Journal Dealing with all Aspects of Electroanalytical Chemistry, Including Fundamental Electrochemistry

ELSEVIER

GENERAL INFORMATION

See also Suggestions and Instructions to Authors which will be sent free, on request to the Publishers.

Types of contributions

(a) Original research work not previously published in other periodicals.
(b) Reviews on recent developments in various fields.
(c) Short communications.
(d) Bibliographical notes and book reviews.

Languages

Papers will be published in English, French or German.

Submission of papers

Papers should be sent to one of the following Editors:

Professor J. O'M. BOCKRIS, John Harrison Laboratory of Chemistry, University of Pennsylvania, Philadelphia 4, Pa., U.S.A.
Dr. R. PARSONS, Department of Chemistry, The University, Bristol 8, England.
Professor C. N. REILLEY, Department of Chemistry, University of North Carolina, Chapel Hill, N.C., U.S.A.

Authors should preferably submit two copies in double-spaced typing on pages of uniform size. Legends for figures should be typed on a separate page. The figures should be in a form suitable for reproduction, drawn in Indian ink on drawing paper or tracing paper, with lettering etc. in thin pencil. The sheets of drawing or tracing paper should preferably be of the same dimensions as those on which the article is typed. Photographs should be submitted as clear black and white prints on glossy paper.
All references should be given at the end of the paper. They should be numbered and the numbers should appear in the text at the appropriate places.
A summary of 50 to 200 words should be included.

Reprints

Twenty-five reprints will be supplied free of charge. Additional reprints can be ordered at quoted prices. They must be ordered on order forms which are sent together with the proofs.

Publication

The *Journal of Electroanalytical Chemistry* appeared monthly and has six issues per volume and two volumes per year, each of approx. 500 pages.

Subscription price (post free): £ 10.15.0 or $ 30.00 or Dfl. 108.00 per year; £ 5.7.6 or $ 15.00 or Dfl. 54.00 per volume.

Additional cost for copies by air mail available on request.
For advertising rates apply to the publishers.

Subscriptions

Subscriptions should be sent to:

ELSEVIER PUBLISHING COMPANY, P.O. Box 211, Spuistraat 110-112, Amsterdam-C., The Netherlands.

SUMMARIES OF PAPERS PUBLISHED IN JOURNAL OF ELECTROANALYTICAL CHEMISTRY

Vol. 6, No. 4, October 1963

CATHODIC CHRONOPOTENTIOMETRY OF PEROXYDISULFATE AT PLATINUM ELECTRODES

The electro-reduction of the peroxydisulfate anion has been studied chronopotentiometrically. It was found that two distinct sets of potential oscillations or fluctuations occurred in the wave under certain conditions in the absence of a supporting electrolyte. The effects of electrode pre-treatment, electrode material, pH, and supporting electrolyte on the wave characteristics are described. A possible explanation of the types of reactions involved in the reduction mechanism is proposed.

H.B. MARK, JR. AND F. C. ANSON,

J. Electroanal. Chem., 6 (1963) 251–260

THE EFFECT OF THE CONCENTRATION OF LIGAND ON THE POLAROGRAPHIC REDUCTION WAVES PALLADIUM

The effect of the ligand concentration on the polarographic reduction waves of the platinum metals has been studied using pyridine as the ligand and palladium as a representative of the platinum metals. The shift in the reduction peak with increase in ligand concentration is used to calculate formation constants of the complexes formed in solution. The results obtained are discussed on the basis of statistical, symmetry- and d-level splitting-considerations.

R. J. MAGEE AND W. H. DOUGLAS,

J. Electroanal. Chem., 6 (1963) 261–266

CHARACTERISTICS AND PROPERTIES OF A PLATINUM IMMERSION ELECTRODE I

(in French)

We have studied the instantaneous values of the currents set up when a platinum electrode which can be raised and lowered is used as the anode in 10^{-3} *M* $K_4Fe(CN)_6$ and 0.1 *N* NaOH solutions.

It has been established that only diffusion currents are produced when the electrode is totally immersed. When the electrode is being levelled, and emerges from the solution, currents due to localised convectional movements near the electrode are associated with these diffusion currents.

The results obtained under different working conditions have been compared. It has been shown that it is possible to calculate the currents formed when the electrode is totally immersed only if the area of the small platinum sphere in contact with the solution is known.

D. COZZI, G. RASPI AND L. NUCCI,

J. Electroanal. Chem., 6 (1963) 267–274

CHARACTERISTICS AND PROPERTIES OF A PLATINUM IMMERSION ELECTRODE II

(in French)

We have investigated the behaviour of hemispherical bubbling platinum electrodes of surface areas 0.02–0.08 cm^2 at different rates of bubble formation. Results are given for an electrode of surface area 0.049 cm^2. It was found that the relationship between the value of the instantaneous current and $1/\sqrt{t}$ was in approximate agreement with the theoretical relationship calculated on the basis of the equation governing spherical diffusion. We have calculated from experimental and theoretical values of the limiting diffusion currents, a value t_0 for each electrode. This value expresses the difference between experimental and theoretical behaviour.

D. Cozzi, G. Raspi et L. Nucci,
J. Electroanal. Chem., 6 (1963) 275–282

THE CHRONOPOTENTIOMETRIC REDUCTION OF OXYGEN AT GOLD ELECTRODES

Oxygen reduction at gold cathodes was studied chronopotentiometrically. In sodium hydroxide solutions two waves are observed. The first of these, due to the reduction of oxygen to hydrogen peroxide, is longer than the 2-electron value due to the surface-catalyzed disproportionation of hydrogen peroxide which regenerates more oxygen. This effect is most pronounced at an electrode which has been recently anodized and cathodized (pre-treated). The effect diminishes as the electrode is allowed to stand in contact with the test solution. The total transition time for the two waves is unaffected by electrode treatment. In sulfuric acid a single wave due to the 2-electron reduction is observed at a pre-treated electrode. In other media of pH between 1.6 and 12, two oxygen reduction waves are observed.

D. H. Evans and J. J. Lingane,
J. Electroanal. Chem., 6 (1963) 283–299

THE EFFECT OF ELECTRICAL MIGRATION ON THE CHRONOPOTENTIOMETRIC TRANSITION TIME

Sand's theory of electro-migration in chronopotentiometry has been re-derived and extended. The theory, although approximate, satisfactorily describes the enhancement of cathodic transition times. The behavior of thallous sulfate in the presence of little or no supporting electrolyte agrees well with that predicted by the equation $i\tau^{1/2}/AC = (n_1\pi^{1/2}FD_{11}{}^{1/2}/2(1 - T_1))$. The enhancement of the cupric ion transition time for the reduction of cupric sulfate in the presence of little or no supporting electrolyte is less than predicted by this equation. As expected, the transition time for the reduction of benzoquinone is little affected by the concentration of supporting electrolyte.

M. D. Morris and J. J. Lingane,
J. Electroanal. Chem., 6 (1963) 300–313

SOME APPLICATIONS OF ULTRA-VIOLET SPECTROPHOTOMETRY TO STUDIES OF ADSORPTION AT COPPER, NICKEL AND SILVER ELECTRODES

A spectrophotometric method developed previously has been applied to the examination of the adsorption of several organic adsorbates in neutral and ionic form at various solid electrode materials. Standard free energies and isosteric heats of adsorption have been evaluated and their apparent dependence on coverage examined. The behaviour of the adsorbates at the solid metals is compared with that of similar compounds at the mercury electrode. As in previous work, difficulties are encountered when adsorption at non-noble metals is studied over a range of potentials.

R. G. BARRADAS AND B. E. CONWAY,
J. Electroanal. Chem., 6 (1963) 314–325

RADICAL ION INTERMEDIATES IN THE ELECTROREDUCTION OF TRIPHENYLMETHANE DYES

The existence of radical intermediates in the reduction of several triphenylmethane dyes has been proved by observation of their EPR spectrum. Certain solvation effects concerning the reduction of the dyes have also been substantiated. Under equivalent conditions however, the expected spectra from the reduction of other similar triphenylmethane dyes have not been produced.

T. MILLER, B. LAMB AND R. N. ADAMS,
J. Electroanal. Chem., 6 (1963) 326–327

CURRENT–VOLTAGE CURVES FOR ZIRCONIUM AND URANIUM IN MOLTEN FLUORIDES

(Short Communication)

D. L. MANNING AND G. MAMANTOV,
J. Electroanal. Chem., 6 (1963) 328–329

ERRATUM

The Summary of the paper published in the September issue on pages 245–249 should read:

THE CATALYTIC REDUCTION OF NITRITE IONS DURING POLAROGRAPHIC REDUCTION OF VANADIUM(V)

Enhanced limiting currents for the polarographic reduction of vanadium(V) in NH_3-NH_4Cl electrolyte are observed in the presence of nitrite ions. The limiting current is independent of the head of mercury and is proportional to the square root of the nitrite ion concentration. The enhanced current is attributed to the catalytic reduction of nitrite ion, involving the following reactions:

$$V(V) + 3\,e \rightarrow V(II)$$

$$V(II) + NO_2^- \rightarrow V(IV) + \text{reduction of products of } NO_2^-$$

$$V(IV) + 2\,e \rightarrow (VII)$$

F. BAUMANN,
J. Electroanal. Chem., 6 (1963) 245–249

CATHODIC CHRONOPOTENTIOMETRY OF PEROXYDISULFATE AT PLATINUM ELECTRODES*

HARRY B. MARK Jr.** AND FRED C. ANSON

Division of Chemistry and Chemical Engineering, California Institute of Technology, Pasadena, California (U.S.A.)

(Received June 7th, 1963)

INTRODUCTION

The polarographic reduction of the peroxydisulfate anion, $S_2O_8^{2-}$, has received a great deal of attention in the past few years[1-10] because the current–voltage curves, under certain conditions, exhibit a pronounced potential minimum and the apparent transfer coefficient can become negative.

There has been no published report of a chronopotentiometric investigation of $S_2O_8^{2-}$ reduction and the present study was undertaken to see if the behavior to be expected on the basis of the polarographic data would be observed. The chronopotentiometric behavior obtained at platinum electrodes was quite unusual and could not be readily correlated with the polarography of $S_2O_8^{2-}$. Periodic oscillations of potential are observed under certain conditions. Similar periodic electrochemical and chemical phenomena have been reported in the literature, but the mechanisms of these reactions is not well understood[11-26].

This paper reports our experimental observations. Thus far the data has proved too complicated for more than a qualitative interpretation but, because of the unusual phenomena observed, we considered it would be worthwhile to present our findings in their present state.

EXPERIMENTAL

Apparatus

The chronopotentiometric circuitry followed the standard practice, and complete descriptions of the circuit components have been previously reported[28,29]. A Moseley Authograph Model 3-S recorder was employed.

A standard two-compartment (working and auxiliary electrode in one, reference electrode in the other) H-cell was used. The platinum electrode was a 0.020 in. diam. platinum wire sealed in soft glass with an exposed surface area of approximately 0.1 cm^2. The gold electrode was a 0.030-in. diam. wire sealed in soft glass (exposed surface area $\approx$ 0.7 cm^2) and the palladium electrode was a 0.040-in. diam. wire extending into the solution (surface area in solution $\approx$ 0.6 cm^2).

* Contribution No. 2976 from the Gates and Crellin Laboratories of Chemistry.

** Present address: *Department of Chemistry, The University of Michigan, Ann Arbor, Michigan.*

Preparation of solutions

All solutions were prepared with triply distilled water, and reagent grade chemicals were used without further purification.

Procedure

The sample solutions were de-aerated in the electrolysis cell by bubbling nitrogen gas through the solution prior to the experiment. A nitrogen atmosphere was maintained over the surface of the solution during the actual determination. The solutions were allowed to become quiescent for 1 min before measurement. Between successive trials with the same solution, stirring was carried out for 1 min by means of a magnetic stirrer (N_2 gas was also bubbled through the solution) and the solution was then allowed to stand 1 min. before measurement.

All potentials were measured with respect to the saturated calomel electrode (S.C.E.) and all measurements were made at room temperature (25° ± 2.0°).

As the condition of the surface of the platinum electrode appears to be an important factor in the characteristics of the reduction of $S_2O_8^{2-}$, it is necessary to define the procedures employed to obtain three types of reproducible electrode surface conditions (a) an *active* electrode, (b) a *pre-oxidized* electrode, and (c) an *aged* electrode. An *active* electrode is one which has been successively anodized and cathodized to +1.6 and —0.2V, respectively in approximately 1 *F* H_2SO_4 in a cyclic manner, about 10–20 times. The final cycle is cathodic and the current is interrupted as soon as the potential reaches the background potential (approximately —0.2 V *vs.* S.C.E.). This pre-treatment results in the formation of finely divided platinum on the surface[33]. A *pre-oxidized* electrode is one treated in the same manner as the *active* electrode except that it is anodized in the sample solution for a duration of 0.5–5 sec. This treatment produces a film of platinum oxide(s) on the surface of the electrode[16,28–33]. An *aged* electrode is obtained by soaking the active electrode in 1 *F* H_2SO_4 for a period of 24 h[16,33]. The pre-treated electrodes were always submerged in the sample solution 1 min prior to measurement.

Unless otherwise stated in the text, all measurements were made in the *absence* of supporting electrolyte. The potential oscillations are observed only in the absence of supporting electrolyte.

EXPERIMENTAL RESULTS

General observations

Active electrodes were partially oxidized when soaked in 0.1–0.001 *F* $K_2S_2O_8$ solutions. The electrodes were soaked in the solutions for periods varying from one second to half an hour, removed and washed quickly with distilled water, and then placed in a cell which contained a de-aerated 0.1 *F* Na_2SO_4 electrolyte at pH 7. The electrodes were allowed to stand a few minutes in the stirred electrolyte and then a cathodic current (0.4 mA/cm²) was passed. Waves were obtained whose quarter-wave potentials (—0.3 V *vs.* S.C.E.) corresponded to those for platinum oxide. The extent of surface oxidation (150–300 μcoulombs/cm²) did not correspond to total surface oxidation (about 500–1000 μcoulombs/cm²) for a fully oxidized surface[16,31–33]). Experiments indicated that most of this oxide formed very rapidly (within one or two sec) and that the quantity of oxide did not then increase appreciably with further exposure. It was found qualitatively that the extent of surface oxidation of the platinum by $S_2O_8^{2-}$

was not appreciably changed by the addition of either nitrate or sulfate salts to the $S_2O_8^{2-}$ solution.

The pH of $S_2O_8^{2-}$ solutions initially at pH $\leqq$ 7 slowly drifted to more acidic values over a period of a few hours (pH $\leqq$ 4 after 3–4 h); the decomposition of $S_2O_8^{2-}$ in aqueous medium produces HSO_4^- and O_2[34-36] which explains this slow change in pH. The rate of pH decrease was accelerated by the presence of the platinum electrodes.

Experiments showed that the potentials as well as the characteristic shapes of the $S_2O_8^{2-}$ chronopotentiograms were affected by pH (these effects will be explained in detail below) even though the overall electrochemical reduction reaction does not involve protons[8]:

$$S_2O_8^{2-} + 2\,e^- \rightarrow 2\,SO_4^{2-} \qquad (1)$$

The discussion of the characteristics of the chronopotentiograms given below, unless otherwise stated, refers to results obtained for neutral solutions (pH = 7 ± 0.3). It was necessary to monitor continuously the pH of the test solution in order to obtain reasonable reproducibility. NaOH was added when necessary in sufficient quantity to bring the pH slightly above 7 and measurements were made when the pH had drifted back to 7. The small amount of $S_2O_8^{2-}$ decomposed during the 10–40 min of the measurements did not result in a detectable change in $S_2O_8^{2-}$ concentration. The addition of the small quantities of NaOH did not affect the chronopotentiograms.

Effect of the electrode condition

The general characteristics of the cathodic chronopotentiograms of a 0.01 *F* $K_2S_2O_8$ solution are shown in Fig. 1. The chronopotentiograms were recorded successively

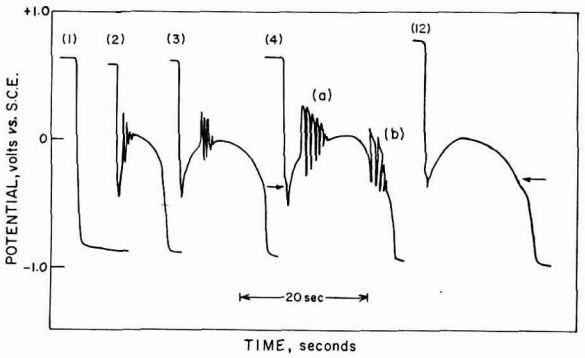

Fig. 1. The reduction of 0.01 *F* $K_2S_2O_8$, current density 2 mA/cm², pH = 7. The measurements were made successively with the same solution (see text for procedure). Curve (1) represents an *aged* electrode. Curves 5–11 of series are omitted.

using the same solution in the manner described above. The applied current was 2 mA/cm². Curve (1) represents the wave obtained for an *aged* electrode. The potential drops immediately to the background potential and $S_2O_8^{2-}$ does not, therefore, appear to be reduced before the background, at an *aged* electrode. In curve (2), the

potential drops rapidly to about −0.45 V *vs.* S.C.E. and then begins to rise until the wave reaches a potential of about −0.2 V. At this point, the potential shifts very rapidly to about +0.2 V and then undergoes a few oscillations before reaching a steady value of about 0.0 V. Curve (3) is similar to curve (2), except the transition time τ, has increased. In curve (4), a second set of oscillations (b) are observed and τ is slightly larger than that of curve (3). In waves 2–4 a small wave (indicated by the arrow in curve (4)) is observed, at −0.35 V just prior to the minimum potential of the initial *dip*. In the successive chronopotentiograms (curve 5–11, which are not shown) the general characteristics of curve (4) are repeated. Although τ remains constant for all successive waves after (4), in general the frequency of the oscillations increases while the initial amplitude decreases.

Eventually after several successive chronopotentiograms (10–15 in most cases), a chronopotentiogram of $S_2O_8^{2-}$ was obtained which did not exhibit either set of oscillations, (see curve (12) of Fig. 1). All subsequent successive measurements yielded identical waves. The minimum potential of the *dip* is more positive than that of the other curves of Fig. 1. Also, a small wave, indicated by the arrow, is observed at about the potential where the second set (b) of oscillations was previously observed. *Active* electrodes always yielded waves similar to curve (12). Thus, successive cathodic chronopotentiograms seem to result in an electrode condition similar to that obtained by cycling in 1 *F* H_2SO_4.

The potential fluctuations of set (a), (see Fig. 1), oscillated around the smooth potential value observed when the electrode was in the *active* condition. Set (b), however, oscillated between a cathodic potential limit corresponding to the potential observed during the latter portion of the wave of an active electrode and an anodic potential which is approximately the most positive limit of a wave obtained with an *active* electrode. In general, as shown in Fig. 1, the amplitude and the frequencies of both sets of fluctuations decreased with time during a wave in a manner similar to a damped oscillation. While the qualitative characteristics of the sequence of measurements shown in Fig. 1 as well as the initial amplitude of both sets of fluctuations were more or less reproducible, the number of oscillations per set, initial frequency, rate of change of frequency and the rate of change of amplitude (*damping*) were not reproducible. It was not possible, therefore, to determine with any degree of certainty how the oscillations varied with current density.

A *pre-oxidized* electrode gave initial waves which were somewhat different from the initial waves obtained for *active* electrodes. Figure 2 compares the characteristics of the first portion of the initial waves of (i) an *active* electrode, (curve 1); (ii) an electrode which had been anodized for a period of about 0.5 sec at a current density of 2 mA/cm^2 to cover the surface partially with a film of platinum oxide[33], (curve 2); and (iii) an electrode which was anodized for 5 sec at a current density of 2 mA/cm^2 to cover its surface completely with platinum oxide[33], (curve 3). In each case a small cathodic wave (indicated by arrow) is observed before the potential reaches the minimum value at the *dip*. The magnitude of this wave increases with the extent of surface oxidation and the potential ($\sim$ − 0.3 V *vs.* S.C.E.) corresponds to the potential for platinum oxide reduction in neutral unbuffered electrolyte[32]. The rate of the anodic potential rise after the initial potential *dip* decreases with increasing extent of surface oxidation. Also, the maximum potential reached by the anodic rise is always 0.1–0.2 V more negative than that observed for an *active* electrode.

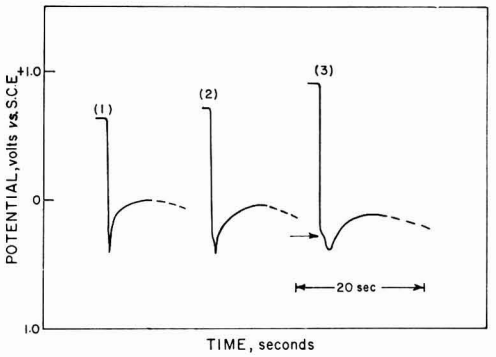

Fig. 2. The initial portion of chronopotentiograms of 0.01 F $K_2S_2O_8$ employing electrodes which have different extents of surface oxidation. Current density 2 mA/cm², pH = 7. Curve (1), an *active* electrode which was in contact with sample solution 2 min; curve (2), a *preoxidized* electrode which was anodized in the sample solution for 0.5 sec; curve (3), as for curve (2) except that the anodic current was passed for 5 sec.

A series of *active* electrodes were potentiostated during the two-minute interval between successive runs, at potentials more cathodic than the normal rest potential of the electrode (about + 0.6 V *vs.* S.C.E.). Potentials from 0.0 to +0.5 V *vs.* S.C.E. were employed. It was found that the characteristics of the potential *dip* changed as the initial controlled potential was varied. Although the minimum potential reached during this *dip* did not appear to change appreciably, the rate of the anodic potential shift following the minimum, increased as the potential was controlled at more cathodic values.

Details of the initial portion of the chronopotentiogram and first set of fluctuations obtained with a $2 \cdot 10^{-3}$ F $K_2S_2O_8$ solution are shown in part A of Fig. 3. The current

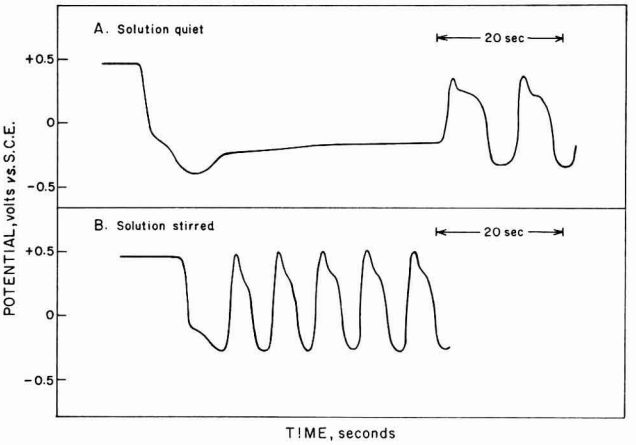

Fig. 3. The reduction of $2 \cdot 10^{-3}$ F $K_2S_2O_8$ solutions at a current density of 0.4 mA/cm² at a platinum electrode, pH ≈ 6.5. A, solution at rest; B, solution stirred.

density was 0.4 mA/cm². The anodic portion of the oscillation is very rapid, while the cathodic portion resembles a miniature chronopotentiogram. Part B of Fig. 3 shows

the initial portion of a chronopotentiogram obtained under the same conditions except that the solution was stirred with a magnetic stirrer. The anodic shift of potential after the initial potential dip is now rapid. The potential oscillation starts immediately after the initial dip and the oscillations in the stirred cases have the same general characteristics as in the unstirred cases, except the frequency has increased. To determine if this frequency increase was the result of two different surface conditions or the result of stirring, several measurements were made in which the rate of stirring was varied. Qualitatively it was found that the frequency of oscillation varied inversely with the rate of stirring. Also the amplitude of oscillation slowly decreased and the frequency increased steadily with time even though constant stirring was continued. The oscillations usually ceased after a few minutes (4–10 min). All subsequent measurements showed no potential oscillation. In unstirred solutions this electrode then behaved like an *active* electrode. In both stirred and unstirred solutions, the potential oscillated between approximately the rest potential of the electrode and the potential at the *bottom* of the initial *dip*.

Effect of pH

The chronopotentiograms of $S_2O_8^{2-}$ were measured at different pH values varying from 9.5–4.0. Oscillations were found to occur at all pH values in this range. The only effects observed were that the rate of the anodic shift of potential following the initial potential *dip* increased, and the overpotential for the reduction of $S_2O_8^{2-}$ and the potential of the small wave preceding the minimum potential of the *dip* decreased as the pH decreased. The magnitude of the shift of this wave with pH is identical to the shift of the reduction potential of platinum oxide with pH[32].

Effect of variation of electrode material

The reduction of 0.01 *F* $K_2S_2O_8$ solutions at gold and palladium electrodes was also studied. Potential oscillations were observed to occur with both electrodes.

Two distinct sets of fluctuations were observed with gold at a constant current density of 1.4 mA/cm^2. The fluctuations had the same characteristics as the two sets of oscillations observed for platinum electrodes (see Fig. 1). The cathodic limit of oscillation was about 0.0 V *vs.* S.C.E. at the gold electrode compared to about −0.3 V *vs.* S.C.E. for the reduction at platinum electrodes. Experiments showed that the potential pause in the cathodic wave for the reduction of gold oxide, occurred at about 0.0 V *vs.* S.C.E. in neutral Na_2SO_4 solution. The initial portion of the chronopotentiogram always exhibited a brief potential *dip* similar to that found for platinum electrodes. The *dip* in the case of gold electrodes was considerably sharper and the minimum potential reached was about −0.05 V *vs.* S.C.E.

Potential oscillations were observed on palladium only when the solution was stirred. Figure 4 illustrates the initial portion of the chronopotentiograms obtained for the reduction of a 0.01 *F* $K_2S_2O_8$ solution (pH = 6) at a palladium electrode using a constant current density of 3 mA/cm^2. Curve (1) was obtained for the solution at rest (electrode cycled once), curve (2) for a stirred solution (note that the potential oscillations slowly decrease in amplitude and increase in frequency until they finally cease, which is similar to the behavior of a platinum electrode), and curve (3) represents the wave obtained either for the measurement subseqeunt to curve (2) (2 min interval between measurements) in a stirred solution or the wave obtained with an *active* elec-

trode in a stirred solution. Experiments showed that there were two potential pauses in the cathodic wave of a *pre-oxidized* palladium electrode in a 0.1 F Na_2SO_4 solution

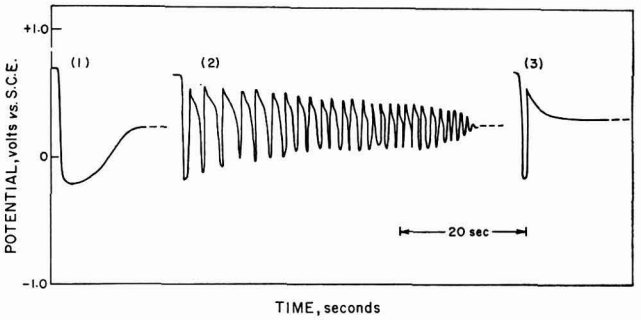

Fig. 4. The reduction of 0.01 F $K_2S_2O_8$ at a current density of 3 mA/cm² at a palladium electrode, pH = 6.0. Curve (1), solution at rest; curve (2), solution stirred; curve (3), solution stirred, measurement made subsequent to curve (2).

(pH $\lesssim$ 6) occurring at about + 0.20 and − 0.30 V *vs.* S.C.E., which is in reasonable agreement with values reported in the literature for the reduction of palladium oxides[37].

Effect of supporting electrolyte

The general characteristics of the cathodic chronopotentiograms of a 0.01 F $K_2S_2O_8$ solution in 0.1 F $NaNO_3$ are shown in Fig. 5. The chronopotentiograms were recorded

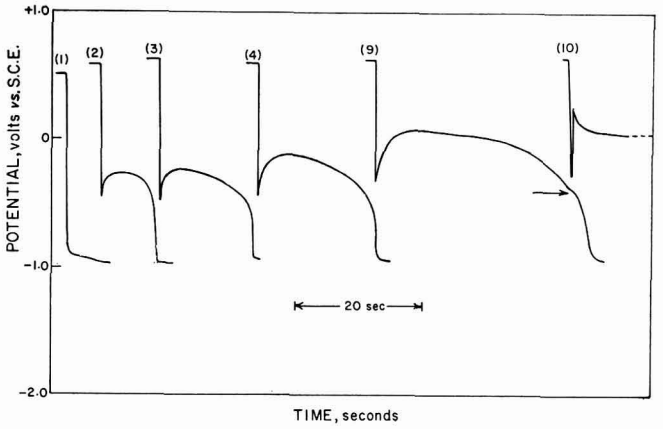

Fig. 5. The reduction of 0.01 F $K_2S_2O_8$ in 0.1 F $NaNO_3$ at a current density of 2 mA/cm², pH = 7. The measurements were made successively with the same solution (see text for procedure) Curve (1) represents an *aged* electrode. Curves (5)–(8) of the series are omitted.

successively using the same solution in the manner described in the experimental section. The applied current was 2 mA/cm². Curve (1) represents the wave obtained for an *aged* electrode. The potential drops immediately to the background potential and $S_2O_8^{2-}$ does not, therefore, appear to be reduced before background at an *aged* electrode even in the presence of a supporting electrolyte. In curve (2), a wave is ob-

served. The potential drops rapidly to about — 0.45 V *vs.* S.C.E. and then begins to rise until the wave reaches a potential maximum of about — 0.3 V *vs.* S.C.E. The potential then falls off slowly at first and then rapidly drops to background. During the successive measurements, curves 3 through 8 (curves 5–8 not shown), the potential of the sharp minimum and of the rounded maximum move anodic with each successive run. The transition time of each successive wave increases. Curve (9) represents the reproducible wave obtained after the electrode had undergone the series of successive measurements. A small second wave (indicated by arrow) is observed just before the potential drops to background. The potential of the wave is about — 0.4 V *vs.* S.C.E. and corresponds closely to the potential minimum observed at the beginning of the wave. Curve (10) represents the initial portion of the wave obtained using an electrode which was in a reproducible condition (same history as the electrode of curve (9)), but, the sample solution was stirred vigorously by means of a magnetic stirrer. The potential drops rapidly to about the same minimum value as in curve (9) but the subsequent anodic shift in potential is much faster. The potential reaches a maximum of about + 0.3 V *vs.* S.C.E. and then drops somewhat more slowly to a constant value of + 0.05 V *vs.* S.C.E.

The chronopotentiograms of 0.01 *F* $K_2S_2O_8$ solutions in 0.1 *F* H_2SO_4 at pH $\approx$ 7 were found to be almost identical to those described above for 0.1 *F* $NaNO_3$ (see Fig. 5).

DISCUSSION

The experimental results have shown that the $S_2O_8^{2-}$ anion is capable of partially oxidizing the surface of the platinum electrode. The magnitude of the cathodic potential attained during the platinum oxide wave (potential pause observed immediately prior to the potential minimum of the *dip*, see Figs. 1, 2 and 3) indicates that most or all of the surface oxide film must be removed before $S_2O_8^{2-}$ can be electrochemically reduced. ANSON AND KING[38] and DAVIS[39] have reported similar potential *dips* in the reduction of vanadium(V) and iodate ion in the presence of supporting electrolyte.

When the oxide has been essentially removed from the electrode, the surface consists of finely divided platinum metal (partially *active*) at which reduction of the $S_2O_8^{2-}$ ion can proceed more rapidly. As a result the potential becomes more anodic. This rise in potential is relatively slow in unstirred solution (as can be seen by curves 2–12 of Fig. 1 and 1–9 of Fig. 5) but is rapid when the solution is stirred (curve B of Fig. 3 and curve (10) of Fig. 5). The slow anodic rise appears, therefore, to be caused by the presence at the electrode of some chemical species that is produced during the initial portion of the wave and which causes the reduction of $S_2O_8^{2-}$ to occur at this more cathodic potential. Hydroxide ion produced from the reduction of platinum oxide[37] is probably the substance in question. The pH dependence of the rate of the slow anodic potential shift following the potential *dip* and its instantaneous shift when the solution is stirred supports this possibility. The potential rises more slowly in unstirred solutions because of the much longer time needed for the hydroxide to diffuse away from the electrode surface.

It seems reasonable to postulate a mechanism for the oscillations which is based on two of the properties of $S_2O_8^{2-}$ observed in this study: (i) the ability of $S_2O_8^{2-}$ to oxidize the platinum electrode surface to a finite extent, and (ii) the ability of this oxide film to inhibit completely the reduction of $S_2O_8^{2-}$. The surface of the electrode follow-

ing the initial potential *dip*, is probably free of all or most of the platinum oxide and the potential of the electrode rises to the value at which $S_2O_8^{2-}$ is reduced on an oxide-free (active) electrode. This shift (as argued above) is not instantaneous because of the diffusion of the OH^- at the electrode produced by the reduction of the platinum oxide, but as the OH^- concentration at the electrode drops, the potential climbs to +0.3 to + 0.5 V *vs.* S.C.E. At these potentials the electrode surface is oxidized by the $S_2O_8^{2-}$ at the electrode surface in excess of that necessary to carry the constant current. Thus, the surface area of the electrode available for the electrochemical reduction of $S_2O_8^{2-}$ at the more anodic potentials rapidly decreases (current density increases rapidly) and a very short $S_2O_8^{2-}$ wave is observed (see Fig. 1). The potential then falls to the reduction potential of the platinum oxide, at which point the oxide film is reduced to form the *active* metal surface. The $S_2O_8^{2-}$ can now react at the oxide-free electrode, the potential climbs back to +0.3 to 0.5 V, and the cycle starts over again.

The damping of the first set (a) of potential fluctuations (see curve (4) of Fig. 1) may result from the accumulation of SO_4^{2-} ions at the electrode (two sulfate ions are produced for each $S_2O_8^{2-}$ reduced, see eqn. 1) because the addition of supporting electrolyte was shown to eliminate the potential oscillations.

At the conclusion of the first set (a) of oscillations, the steady potential probably represents the reduction of $S_2O_8^{2-}$ at a very slightly oxidized electrode (the controlled potential experiments showed that a finite quantity of oxides is present at + 0.05 V). The reduction of $S_2O_8^{2-}$ on this surface continues until the surface concentration of $S_2O_8^{2-}$ approaches zero. At this point the potential starts to become more cathodic until the platinum oxide potential is reached. The residual oxide is then reduced (see wave marked with arrow in Fig. 1) which results in new metal surface available for the reduction of $S_2O_8^{2-}$ and effectively decreases the current density. The transition time corresponding to this lower current density having not been reached, the potential again becomes more anodic. A few oscillations are again seen at this point (set (b) of curve (4), Fig. 1) which corresponds to the re-oxidation of the platinum and subsequent reduction of the oxide. The oscillations rapidly become *damped* because the total surface concentration of $S_2O_8^{2-}$ at all sites soon becomes zero near the end of the wave and the potential is forced to background reduction potential.

The observations that the potential at the initial *dip* and the cathodic limits of the oscillations for platinum, gold, and palladium electrodes all coincide with the potentials at which the corresponding oxides are reduced in neutral Na_2SO_4 solution support this theory for the mechanism of the oscillations.

ACKNOWLEDGEMENT

This research was sponsored in part by the National Science Foundation.

SUMMARY

The electro-reduction of the peroxydisulfate anion has been studied chronopotentiometrically. It was found that two distinct sets of potential oscillations or fluctuations occurred in the wave under certain conditions in the absence of a supporting electrolyte. The effects of electrode pre-treatment, electrode material, pH, and supporting electrolyte on the wave characteristics are described. A possible explanation of the types of reactions involved in the reduction mechanism is proposed.

REFERENCES

1 A. N. FRUMKIN, O. A. PETRII AND N. V. NIKOLAEVA-FEDOROVICH, *Dokl. Akad. Nauk SSSR* 128 (1959) 1006.
2 A. N. FRUMKIN, *Z. Elektrochem.*, 59 (1955) 807.
3 A. N. FRUMKIN AND G. M. FLORIANOVICH, *Zh. Fiz. Khim.*, 29 (1955) 1827.
4 N. V. NIKOLAEVA, N. S. SHAPIRO AND A. N. FRUMKIN, *Dokl. Akad. Nauk SSSR*, 86 (1952) 581; N. V. NIKOLAEVA AND A. A. GROSSMAN, *Dokl. Akad. Nauk SSSR*, 95 (1954) 1013.
5 N. V. NIKOLAEVA-FEDOROVICH AND L. A. FOKINA, *ibid.*, 118 (1958) 987.
6 T. V. KALISH AND A. N. FRUMKIN, *Zh. Fiz. Khim.*, 28 (1954) 473.
7 A. N. FRUMKIN AND N. V. NIKOLAEVA-FEDOROVICH, Vestuik Moskovskogo Universiteta (1957) 169.
8 L. GIERST, *Cinétique d'approche et réactions d'electrodes irreversibles*, Thèse d'aggrégation. Université Libre de Bruxelles, 1958.
9 A. N. FRUMKIN, *Z. Physik. Chem. (Leipzig)*, 35 (1933) 792.
10 R. PARSONS, *The Structure of the Electrical Double Layer and Its Influence on the Rates of Electrode Reactions*, in *Advances in Electrochemistry and Electrochemical Engineering*, Vol. I, edited by P. DELAHAY, Interscience Publishers Inc., New York, 1961, Chapter 1.
11 E. S. HEDGES AND J. E. MYERS, *J. Chem. Soc.*, 125 (1924) 1282; 127 (1925) 1013.
12 E. S. HEDGES AND J. E. MYERS, *Nature*, 128 (1931) 398.
13 E. S. HEDGES AND J. E. MYERS, *The Problem of Physico-Chemical Periodicity*, Longman-Green, Inc., New York, 1926.
14 W. C. SCHUMB, C. N. SATTERFIELD AND R. L. WENTWORTH, *Hydrogen Peroxide*, Reinhold Publishing Co., New Uork, 1955, p. 499.
15 R. P. BUCK AND L. R. GRIFFITH, *J. Electrochem. Soc.*, 109 (1962) 1005.
16 J. J. LINGANE AND P. J. LINGANE, *J. Electroanal. Chem.*, 5 (1963) 411.
17 D. T. SAWYER AND E. T. SEO, *ibid.*, 5 (1963) 23.
18 A. J. KOLK, JR., *M. S. Thesis*, Case Institute of Technology, Cleveland, Ohio, 1953.
19 T. O. PAVELA, *Ann. Acad. Sci. Fennicae*, Ser. A II, No. 59 (1954) 1.
20 M. THALINGER AND M. VOLMER, *Z. Physik. Chem. (Leipzig)*, 150 (1930) 401.
21 J. A. V. BUTLER AND G. ARMSTRONG, *Nature*, 129 (1932) 613.
22 G. ARMSTRONG AND J. A. V. BUTLER, *Discussions Faraday Soc.*, 1 (1948) 122.
23 M. J. JONICICH AND N. HACKERMAN, *J. Phys. Chem.*, 57 (1953) 674.
24 J. A. V. BUTLER, *Electrical Phenomena at Interfaces*, Macmillan Co., New York, 1951, p. 209.
25 C. D. ALLEY, *Ph. D. Thesis*, University of Tennessee, [Univ. Microfilms, Inc., Ann Arbor, Mich.; Mic. 59–6890 (1959)].
26 J. OSTERWALD AND H. FELLER, *J. Electrochem. Soc.*, 107 (1960) 473.
27 J. J. LINGANE, *Electroanalytical Chemistry*, 2nd edn., Interscience, Publishers Inc., New York, 1958, Chapter XXII.
28 F. C. ANSON, *Anal. Chem.*, 33 (1961) 939.
29 F. C. ANSON, *ibid.*, 33 (1961) 1498.
30 J. J. LINGANE, *J. Electrochem. Soc.*, 1 (1960) 379.
31 F. C. ANSON AND J. J. LINGANE, *J. Am. Chem. Soc.*, 79 (1957) 1015.
32 F. C. ANSON AND J. J. LINGANE, *ibid.*, 79 (1957) 4901.
33 J. J. LINGANE, *J. Electroanal. Chem.*, 2 (1961) 296.
34 I. M. KOLTHOFF AND I. K. MILLER, *J. Am. Chem. Soc.*, 73 (1951) 3055.
35 M. TSAO AND W. K. WILMARTH, *Discussions Faraday Soc.*, 29 (1960) 137; *J. Phys. Chem.*, 63 (1959) 346.
36 L. J. CSÁNYI, *ibid.*, 29 (1960) 146.
37 D. T. SAWYER AND L. V. INTERRANTE, *J. Electroanal. Chem.*, 2 (1961) 310.
38 F. C. ANSON AND D. M. KING, *Anal. Chem.*, 34 (1962) 362.
39 D. G. DAVIS, JR., *Talanta*, 3 (1960) 335.

THE EFFECT OF THE CONCENTRATION OF LIGAND ON THE POLAROGRAPHIC REDUCTION WAVES OF PALLADIUM

ROBERT J. MAGEE AND WILLIAM H. DOUGLAS

Department of Chemistry, Queen's University, Belfast (N. Ireland)

(Received April 18th, 1963)

INTRODUCTION

One of the problems in the polarographic determination of the platinum metals is that the reduction peaks are often very close together[1] but this difficulty can be overcome if the analyst can find a means of controlling the position of a reduction peak. It is well known that the $E_{\frac{1}{2}}$ of the reduction peak of a platinum metal becomes more positive as the concentration of ligand is increased and quantitative investigation of the effect of the ligand concentration was therefore considered to be worthwhile.

The platinum metal and ligand chosen, were palladium and pyridine, respectively. There were a number of reasons for this choice. The palladium–pyridine complex gives a good reduction wave[2]; pyridine is probably the best complexing agent for the polarographic reduction of palladium. Further, reductions of organic compounds (steroids) are often carried out in a pyridine medium using a palladium catalyst; it is of value to the organic chemist to know the nature of the attacking species. Finally, it was found that no data are available for the palladium–pyridine complex in tables of equilibrium constants[3].

THEORY

DE FORD AND HUME[4] devised a method of correlating the shift in $E_{\frac{1}{2}}$ with the formation constants of complexes in solution; $E_{\frac{1}{2}}$ is measured in varying concentrations of ligand, and the results substituted in the relevant equation. This equation, refined by Irving[5] may be stated as follows:

$$\text{antilog}_{10} \frac{0.4343\, nF}{RT} \Delta E_{\frac{1}{2}}^{i} + \log_{10} \frac{I_s}{I_c} = \sum_{0}^{N} \frac{(B_j X^j)}{\gamma M X_j} \qquad (1)$$

where I_s and I_c are the values of I_{exp} for the simple ion and a mixture of complexes respectively. The expression on the right hand side is a function of X and is given the symbol $F^{\circ}(X)$. It may be expanded in the following way:

$$F^{\circ}(X) = 1 + \beta_1(X) + \beta_2(X)^2, + \ldots \qquad (2)$$

If the ionic strength is not affected by complexing, the activities remain constant. Such a situation would obtain where the ligand has no charge and for this reason pyridine was chosen[5].

The simplest way to solve eqn. (2) is graphically as shown by DE FORD AND HUME[4].

If C_M denotes the total amount of metal present in solution, and $[M]$ the concentration of simple metal ions, then

$$C_M = [M] + [MX] + [MX_2] \ldots [MX_n]$$

$[M]/C_M = 1/F^\circ(X)$ = fraction present as simple metal ion[5].
Similarly, $[MX_j]/C_M = \beta_j(X)/F^\circ(X)$ = fraction present as the complex MX_j[5].
Using this approach it is possible to determine cumulative formation constants of the reducible species in solution, and hence the effect of the concentration of the ligand. Before following this approach experimentally, however, it is important to consider the case where the ligand has basic or acidic properties, *e.g.*,

$$X + H^+ \rightarrow XH^+, \text{ where } X \text{ is a ligand.}$$

which means that the amount of complexing agent initially dissolved (apparent concentration L), and the amount remaining in solution are different (the difference being equal to XH^+).

If the acid dissociation constant of XH^+ equals K, then

$$X \text{ (true ligand concentration)} = \frac{L}{10^{-pH} \times 10^{-pK} + 1}$$

Thus, knowing the pH of the solution, and the acid dissociation constant, the activity of the complexing agent in the solution can be determined.

EXPERIMENTAL

All the work in this paper was carried out on an oscillographic polarograph in which the independent variable is varied periodically, and the cathode ray oscilloscope is used as the measuring instrument because of its low response time. In this method the potential applied to the cell is allowed to rise linearly, but more rapidly than in conventional d.c. polarography. This voltage sweep commences at a pre-determined time in the life of a mercury drop. With a drop time of 7 sec, for example, the voltage sweep takes place during the last 2 sec of the life of the drop, *i.e.*, when the change in surface area is negligible. Variations in cell current during the voltage sweep are shown on the screen of the cathode ray tube. For a depolariser the method produces a polarographic wave with a maximum, E_p (peak potential), which is different from that in conventional polarography. Resolution is such that it allows measurements of peaks differing by 0.1 V; a derivative circuit incorporated in the instrument reduces this limit to 0.04 V.

Ten 25-ml volumetric flasks were prepared, and varying amounts of pyridine ranging from 0.01–1.84 ml were placed in each. A fixed amount of $Pd(NO_3)_2$ was dissolved in water and made up to 20 ml with water. One ml of this solution was pipetted into each of the 25-ml flasks which were then made 1 M with Na_2SO_4 as base electrolyte (Table 1).

The pH of each solution was measured taking the pK of PyH^+ as 5.21[3]; (X) was calculated for each solution. Finally, each solution was polarographed at 25° and the values of E_p, $E_{\frac{1}{2}}$ and I_p determined.

The value of $E_{\frac{1}{2}}$ at zero pyridine concentration cannot be obtained experimentally, since it is masked by the current due to dissolution of mercury. The extrapolated value was, therefore, used. This method has been successfully used by other workers[6].

TABLE 1

No. of soln.	*Ml of pyridine added*	*Apparent molarity of pyridine (L)*	*pH of each solution*	*True molarity (X)*	$E_{\frac{1}{4}}$ *(S.C.E.)*	$E_{\frac{1}{4}c} - E_{\frac{1}{4}s}$
1	1.84	0.9139	8.88	0.9137	−0.361	+ 0.164
2	1.25	0.6208	8.77	0.6206	−0.34	+ 0.143
3	0.9	0.4470	8.70	0.4468	−0.318	+ 0.121
4	0.7	0.3477	8.65	0.3476	−0.301	+ 0.104
5	0.55	0.2732	8.45	0.2730	−0.289	+ 0.092
6	0.3	0.1490	8.22	0.1488	−0.261	+ 0.064
7	0.2	0.0993	8.09	0.0992	−0.253	+ 0.056
8	0.101	0.05016	7.75	0.050	−0.239	+ 0.042
9	0.05	0.0248	7.23	0.0246	−0.222	+ 0.025
10					−0.197*	

* extrapolation value

RESULTS

The recorded results were substituted into eqn. (1) (see Table 2) and the graphical solution obtained; the pertinent graphs of $(F^j(X), j = 1 \ldots 4)$ as ordinate, and $[X]$ as abscissa are shown in Figs. 1, 2, 3 and 4. From the curves, the following values for β_j are obtained:

$$\beta_1 = 221; \quad \beta_2 = 5{,}200 \quad \beta_3 = 4{,}000; \quad \beta_4 = 260{,}000$$

TABLE 2

Soln. No.	$\frac{0.4343NF}{RT} \cdot \Delta E_{\frac{1}{4}}$	I_s/I_c	F_0X	$F_1(X)$	$F_2(X)$	$F_3(X)$	$F_4(X)$
1	5.206	1.18	188,800	206,631	225,905	241,550	260,000
2	4.834	1.16	78,380	121,295	203,148	335,075	533,475
3	4.09	1.13	13,820	30,928	68,726	142,179	309,263
4	3.51	1.16	3,765	10,828	30,514	22,825	
5	3.11	1.11	1,413	5,172	18,135	47,380	
6	2.16	1.07	156	1,043	5,524		
7	1.89	1.03	80	796.3	5,799		
8	1.42	1.02	26.9	518	5,940		
9	0.845	1.00	7	243.9			

Experimental errors in the determination of $E_{\frac{1}{4}}$ are magnified in successive calculations of the $F^j(X)$ functions, especially for low concentrations. Fortunately, however, as has been pointed out by DE FORD AND HUME[4], the accumulated errors are in one direction and it is not too difficult to see the points which have deviated from the smooth curve. Further, at this juncture a knowledge of the initial slope of one graph indicates the intercept of the following graph. This is very useful in deciding which points must be ignored.

An anomaly was noticed in connection with the plot of $F_3(X)$. The appropriate equation

$$F_3(X) = \frac{F_{(2)}X - \beta_2}{(X)} = \beta_3 + \beta_4(X)$$

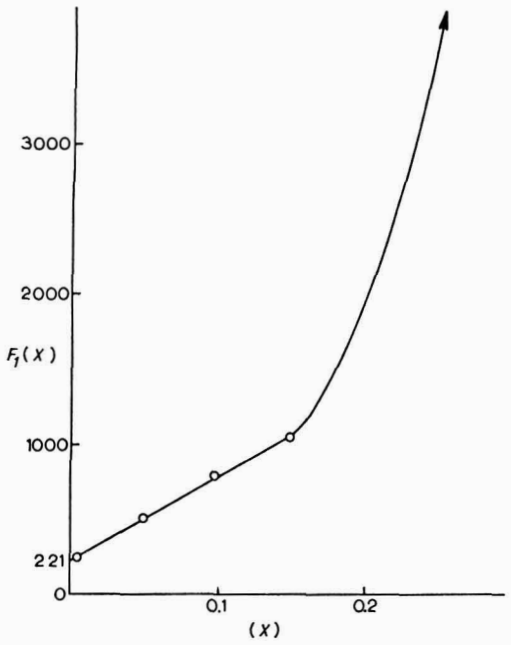

Fig. 1. Graphical solution for formation constant$_1$.

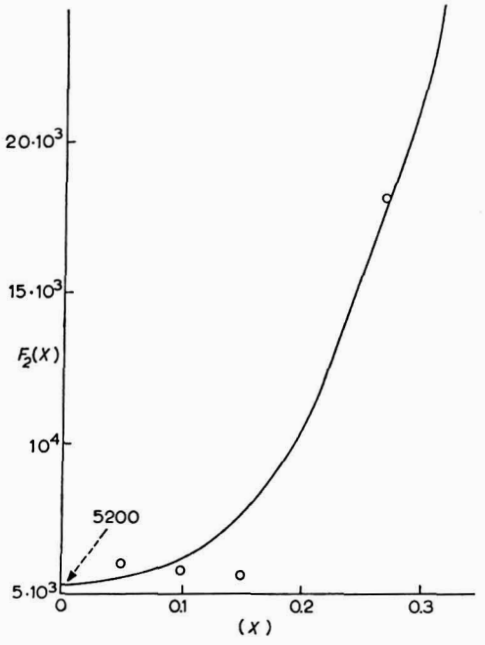

Fig. 2. Graphical solution for formation constant$_2$.

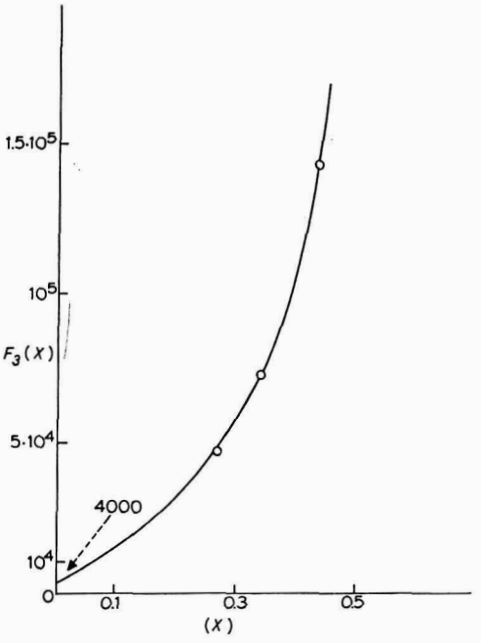

Fig. 3. Graphical solution for formation constant$_3$.

indicates a straight line relationship, whereas in practice a shallow curve was obtained. However, the deviation from the true cannot be great, since the limiting slope is approximately of the same order of magnitude as the β_4 constant, *i.e.*, 10^5.

Using eqns. (4) and (5) the percentage of the total metal present as the different

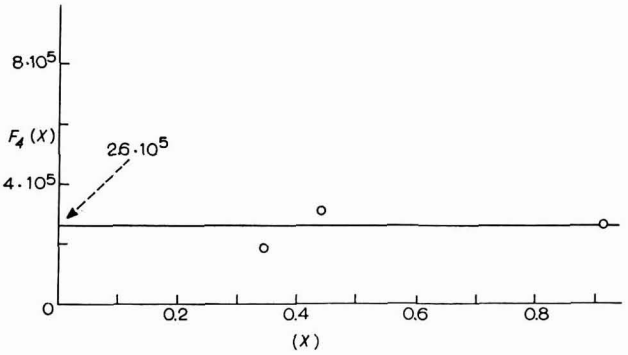

Fig. 4. Graphical solution for formation constant$_4$.

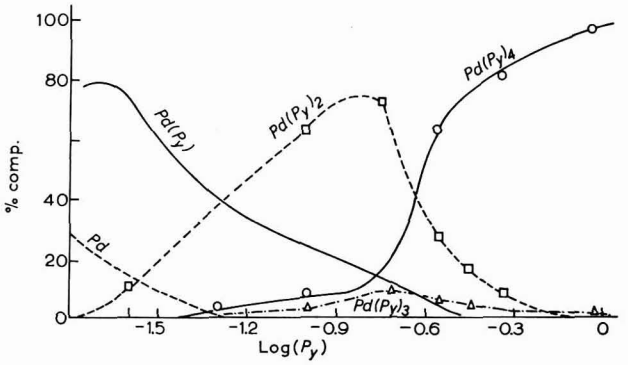

Fig. 5. Percentages of various complexes present at different pyridine concns.

complexes was calculated. These results are given in graphical form in Fig. 5. Most of the results for the highest complex were unreliable, due to the accummulation of errors, as already pointed out. In such cases, indirect results can be calculated by subtracting the sum of the percentages of the lower complexes from 100.

DISCUSSION

The relation between the cumulative formation constant and the stepwise constant K is given by $\beta_4 = K_1 \times K_2 \times K_3 \times K_4$ and $\beta_3 = K_1 \times K_2 \times K_3$. The following values for the stepwise constants were obtained:

$$K_1 = 221; \quad K_2 = 23.2; \quad K_3 = 0.77; \quad K_4 = 65.$$

The first three constants display the usual feature, in that they progressively decrease in magnitude. They may be explained on statistical considerations, *viz.*, the complex $Pd(Py)^{2+}$ has three vacant ligand positions and is, therefore more likely to *catch* a further ligand than $Pd(Py)_2^{2+}$ which has only two vacant positions. The constant K_4 indicates however, that the complex $Pd(Py)_4^{2+}$ is much more stable than its predecessor $Pd(Py)_3^{2+}$ which is never in excess of 10% of total metal present (Fig. 5). The implication is that statistical considerations are of minor importance and the stability is determined by the symmetry of the ion and by the greater splitting in the d-level electrons due to the increased complexation of the ion $Pd(Py)_4^{2+}$. Therefore, once the complex $Pd(Py)_3^{2+}$ has formed, there is a strong tendency *to catch* another pyridine molecule and make a completed co-ordination number of 4. COZZI AND PANTANI[7] determined some cumulative constants for rhodium chloro-complexes. If the stepwise constants are calculated from these, it will be observed that there is an increase at $RhCl_4$ in agreement with the results above, although the constants of the complexes $RhCl_5$ and $RhCl_8$ begin to the decrease again.

CONCLUSION

From the analytical point of view there are two implications in the investigation above. The first is that where a metal is spontaneously reduced, it may be possible, by the addition of a complexing agent, to endue the ion with sufficient stability to the extent of obtaining a reduction wave. The above work has clearly outlined the significance of this in a quantitative way. The second point is that it is possible to exercise in a limited way, control over the position of the reduction wave by varying the concentration of ligand. This is important in the situation where there is interference from other waves which are not affected by the concentration of ligand.

SUMMARY

The effect of the ligand concentration on the polarographic reduction waves of the platinum metals has been studied using pyridine as the ligand and palladium as a representative of the platinum metals. The shift in the reduction peak with increase in ligand concentration is used to calculate formation constants of the complexes formed in solution. The results obtained are discussed on the basis of statistical, symmetry- and d-level splitting-considerations.

REFERENCES

1 R. SIMPSON, R. EVANS AND H. SAROFF, *J. Am. Chem. Soc.*, 77 (1955) 1438.
2 R. J. MAGEE AND W. H. DOUGLAS, *J. Electroanal. Chem.*, 5 (1963) 171.
3 *Stability Constants*, The Chemical Society, London, 1958.
4 D. D. DE FORD AND D. N. HUME, *J. Am. Chem. Soc.*, 73 (1951) 5321.
5 H. IRVING, *Advances in Polarography*, Vol. 1, Pergamon Press, London, 1960, p. 42.
6 C. TANFORD AND S. WAWZONEK, *Ann. Rev. Phys. Chem.*, 3 (1952) 247.
7 D. COZZI AND F. PANTANI, *J. Inorg. & Nucl. Chem.*, 8 (1958) 391.

CARACTÉRISTIQUES ET PROPRIÉTÉS DE L'ÉLECTRODE DE PLATINE À BARBOTAGE. I

DANILO COZZI, GIORGIO RASPI ET LAMBERTO NUCCI

Institut de Chimie Analytique de l'Université de Pise (Italie)

(Reçu le 2 juillet, 1963)

Lors d'un travail précédent[1] ont été mises en évidence les possibilités d'emploi de l'électrode de platine à barbotage dans l'étude de systèmes oxydo-réducteurs à haut potentiel d'oxydo-réduction, principalement en vertu de sa passivité et de la caractéristique appréciable d'émettre un courant à impulsions facilement mesurable grâce aux mêmes moyens que la polarographie classique.

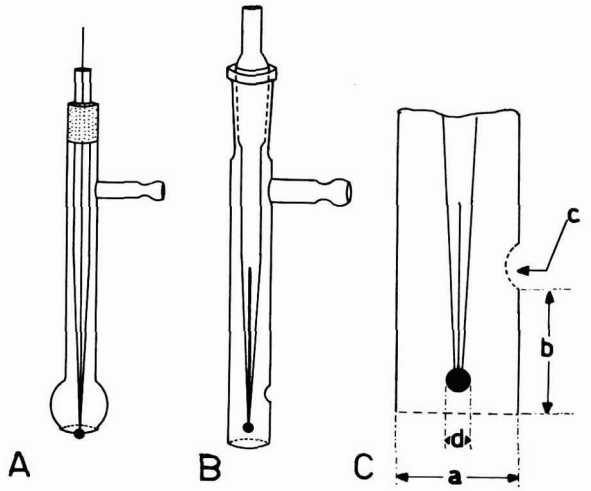

Fig. 1. (A), L'électrode de platine à barbotage telle qu'elle apparaissait dans l'étude précédente. (B) et (C), L'électrode de platine à barbotage utilisée dans la présente étude.

Après avoir effectué quelques modifications du modèle originel (Fig. 1) uniquement en vue de rendre plus constante la période entre l'expulsion d'une bulle et l'autre, et plus précis le réglage de la position de l'électrode par rapport au niveau minimum de la solution à l'intérieur du tube au cours des diverses phases qui accompagnent le barbotage, il a été possible de vérifier que les processus oxydo-réducteurs qui se déroulent sur cette électrode, même si la solution est périodiquement renouveleé à la surface de celle-ci, sont substantiellement contrôlés par la diffusion.

Dans ce but, on a employé une solution de NaOH 0.1 N contenant ferrocyanure et ferricyanure de potassium selon des rapports divers, et des concentrations diverses, à 25° ± 0.1°. On a constaté (Fig. 2) la constance du potentiel de demi-vague dans les polarogrammes obtenus dans la réduction de solutions contenant seulement du ferri-

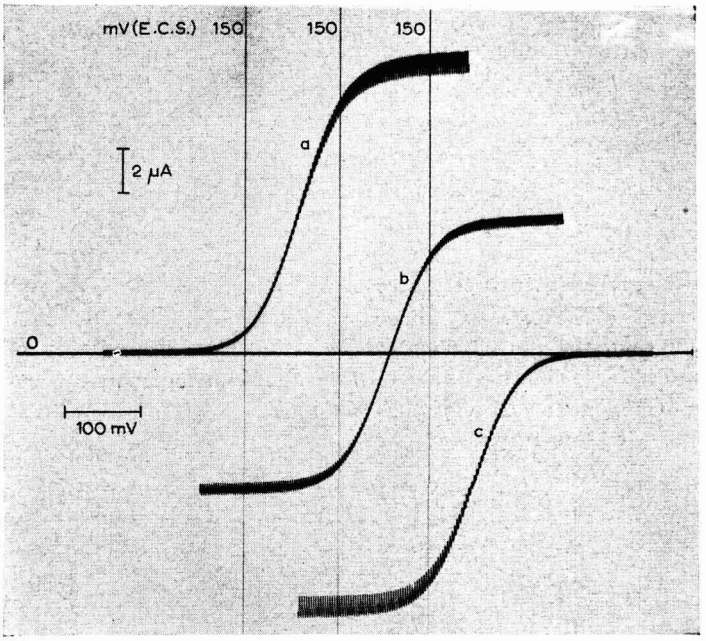

Fig. 2. Ondes polarographiques de $[Fe(CN)_6]^{4-}$ et $[Fe(CN)_6]^{3-}$ dans NaOH 0.1 N à 25° ± 0.1°: (a), $1 \cdot 10^{-3}$ M $[Fe(CN)_6]^{3-}$; (b), $5 \cdot 10^{-4}$ M $[Fe(CN)_6]^{3-}$, $5 \cdot 10^{-4}$ M $[Fe(CN)_6]^{4-}$; (c) $1 \cdot 10^{-3}$ M $[Fe(CN)_6]^{4-}$.

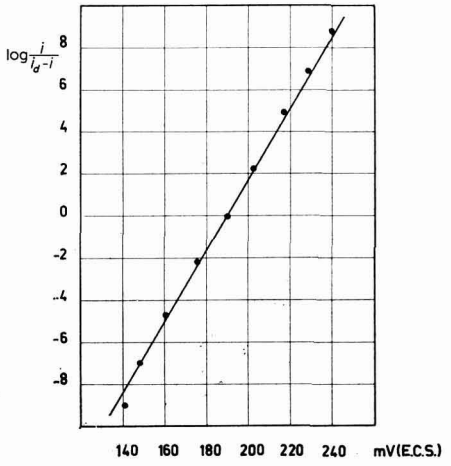

Fig. 3. Analyse mathématique de l'onde polarographique obtenue avec $1 \cdot 10^{-3}$ M $[Fe(CN)_6]^{4-}$ dans NaOH 0.1 N à 25° ± 0.1°.

cyanure (a), ou bien dans l'oxydo-réduction d'un mélange de ferri-et ferrocyanure (b), ou bien dans l'oxydation de ferrocyanure (c); on a constaté que le courant limite est proportionnel à la concentration et à la température de la solution et l'on a prouvé (Fig. 3) l'exacte coïncidence des données expérimentales avec celles calculées au moyen de:

$$E = 0.059 \log \frac{i}{i_d - i} \qquad (1)$$

Étant données ces prémisses de caractère expérimental, l'électrode de platine à barbotage se révèle caractérisée par des propriétés dignes d'être mises en relief. Pour cette raison, nous avons voulu étudier son fonctionnement, sa parfaite connaissance pouvant confirmer et expliquer des résultats d'un certain interêt, soit dans le domaine de la recherche, soit dans celui de l'application.

La recherche s'est effectuée en employant des électrodes qui, pendant les phases de barbotage, permettent de faire varier avec continuité la position de la sphère de platine par rapport au niveau minimum de la solution. Les divers types (Fig. 1C: diamètre *a* compri entre 5 et 10 mm; distance *b* comprise entre 8 et 15 mm; trou *c* de section comprise entre 5 et 15 mm^2; petite boule de diamètre *d* compris entre 1 et 2.5 mm) montrent entre eux des analogies notables. Par conséquent nous ne croyons pas nécessaire de relater le comportement de toutes les électrodes expérimentées, car nous nous exposerions à de très nombreuses répétitions; nous pensons plutôt qu'il suffit de considérer pour l'instant les résultats obtenus avec une série d'électrodes qui toutes dérivent d'une unique électrode de type moyen, et de relater le comportement de celle-ci, certains d'englober les propriétés générales de toutes les autres. L'électrode, choisie comme modèle représentatif, ayant les dimensions: *a* 9 mm, *b* 13 mm, *c* 10 mm^2, *d* 1.67 mm, a été expérimentée selon les procédés suivants:

(i) La petite sphère de platine pendant le barbotage demeure constamment plongée dans la solution. La position est telle que la calotte supérieure reste à 4 mm sous le niveau minimum de la solution. L'oscillation totale de celui-ci est de 8 mm.

(ii) La petite sphère de platine demeure constamment immergée, toutefois sa hauteur par rapport au trou *c* est telle qu'elle effleure la surface de la solution lorsque cette dernière atteint son niveau minimum. Les oscillations de ce dernier sont encore de 8 mm.

(iii) La petite sphère de platine demeure plongée dans la solution pendant 75/100 du temps de barbotage et émerge pendant 25/100 sans se détacher de la solution. L'oscillation du niveau de la solution est de 8 mm.

(iv) La petite sphère de platine demeure dans la solution pendant 64/100 du temps de barbotage, émerge pendant 32/100 sans se détacher de la solution, se détache de la solution pendant 4/100. L'oscillation du niveau de la solution est de 8 mm.

Dans les quatre procédés, les variations du courant en fonction du temps à partir du détachement d'une bulle, sont représentées par la Fig. 4. La solution employée est 0.1 *N* dans NaOH et $1 \cdot 10^{-3}$ *M* dans $K_4Fe(CN)_6$. Les mesures ont été effectuées à 25° ± 0.1°. L'électrode fonctionne en tant qu'anode, polarisée à + 0.450 V (E.C.S.).

L'oscillogramme (a) correspondant au procédé (i) révèle que le courant présente un minimum immédiatement avant et un maximum immédiatement après la formation d'une bulle. L'intensité du courant pendant l'intervalle de temps séparant une bulle de l'autre décroit d'une façon caractéristique, qui devrait être régie par les lois de la dif-

fusion sphérique. L'hypothèse se trouve justifiée par le fait qu'entre la formation d'une bulle et l'autre l'électrode se trouve plongée dans une solution qui peut être considérée stationnaire, en ce sens que le léger mouvement de celle-ci, de haut en bas, n'a pas une action perturbatrice sensible sur la couche de diffusion existant sur l'électrode, du moins tant que son épaisseur demeure relativement mince.

Analysant la courbe (a) de la Fig. 4 nous devrions donc noter une étroite dépendance

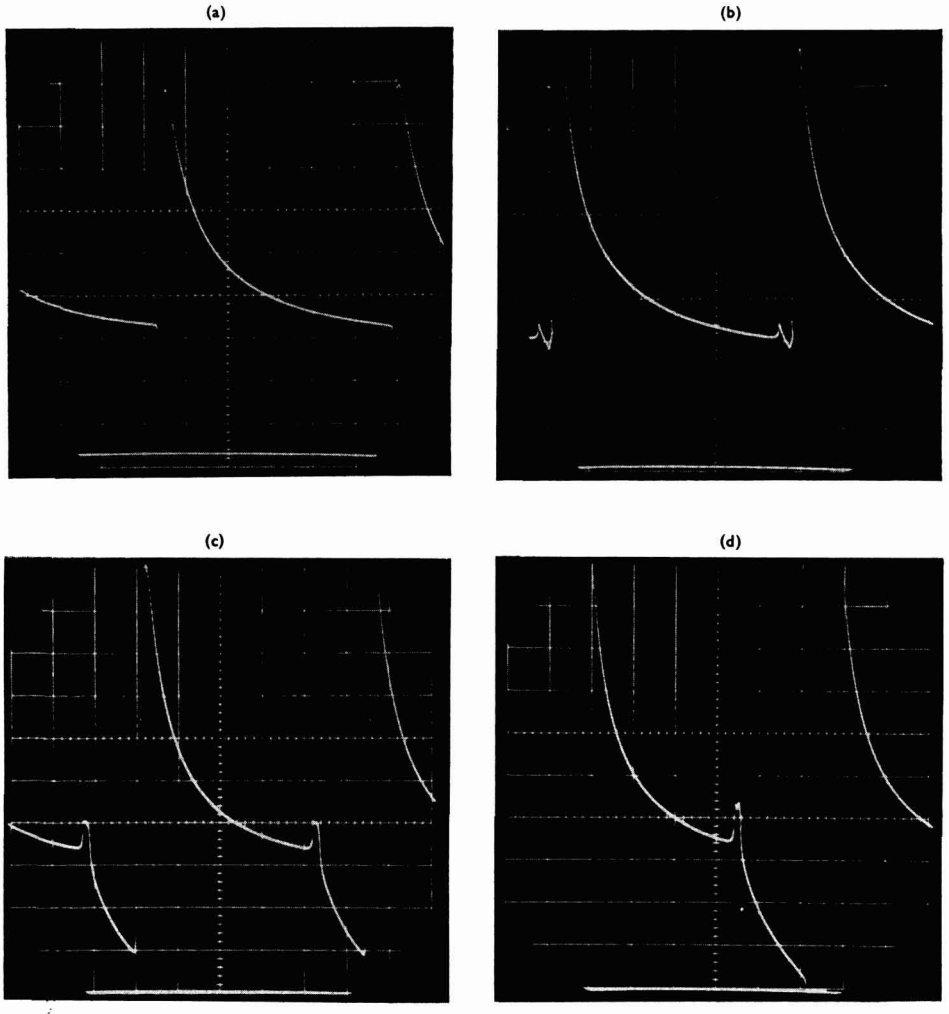

Fig. 4. Oscillogrammes de $1 \cdot 10^{-3}$ M $[Fe(CN)_6]^{-4}$ dans NaOH 0.1 N à 25° ± 0.1° obtenus avec électrode de platine à barbotage polarisée à + 0.450 V (E.C.S.): (a), La petite sphère de platine est constamment plongée dans la solution, procédé (i); (b), La petite sphère de platine effleure la surface de la solution lorsque celle-ci atteint son niveau minimum, procédé (ii); (c), La petite sphère de platine émerge partiellement de la solution pendant 25/100 du temps total de barbotage, procédé (iii); (d), La petite sphère de platine se détache de la solution pendant 4/100 du temps total de barbotage, procédé (iv). En abscisse sont reportés les temps (1 sec par division) et en ordonnée les intensités de courant (2 μA par division). La valeur $i = 0$ est représentée par la ligne en trait appuyé, au bas de chaque figure.

du courant i_t du temps t, mesuré à partir du moment où se produit l'expulsion d'une bulle, selon l'équation:

$$i_t = nFADC\left(\frac{1}{r} + \frac{1}{\sqrt{\pi Dt}}\right) \qquad (2)$$

où

i_t courant instantané, au temps t, exprimé en μA,

n nombre de Faradays d'électricité consommés par la réaction à l'électrode par mole,

F Faraday (96500 coulombs),

A aire de l'électrode en cm^2,

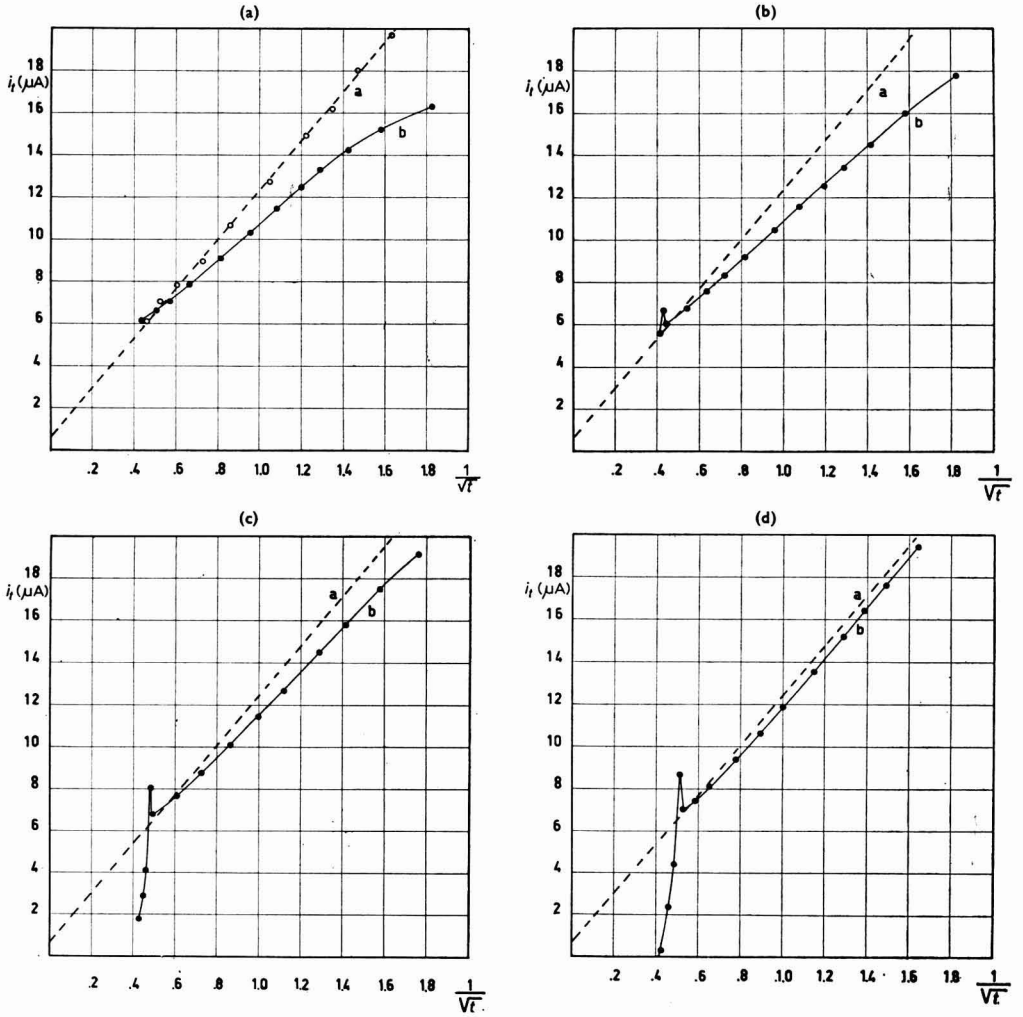

Fig. 5. Variations de i_t en fonction de $1/\sqrt{t}$: (a), ● valeurs expérimentales correspondant au procédé (i), ○ valeurs expérimentales correspondant au procédé (i) immédiatement après polarisation de l'électrode; (b), ● valeurs expérimentales correspondant au procédé (ii); (c), ● valeurs expérimentals correspondant au procédé (iii); (d), ● valeurs expérimentales correspondant au procédé (iv). La courbe en pointillé est calculée grâce à l'éqn. (2).

C concentration exprimée en moles/ml,
D coefficient de diffusion en cm^2sec^{-1},
r rayon de la petite sphère de platine en cm,
t temps en sec.

Dans la Fig. 5a sont reportées les variations théoriques de i_t, selon l'éqn. (2), en fonction de $1/\sqrt{t}$ (courbe a) et les variations de i_t expérimentales (courbe b) d'après la courbe (a) de la Fig. 4. La confrontation révèle que les intensités de courant expérimentales, les hypothèses évoquées ci-dessus restant valides, sont de valeur nettement inférieure à celle calculée. Le fait peut être attribué à l'existence d'un *défaut de renouvellement* de la solution dû à un renouvellement incomplet de l'électrolyte à la surface de l'électrode au moment de l'expulsion de la bulle. Cette explication a été confirmée par l'étude des variations du courant immédiatement après polarisation de l'électrode.

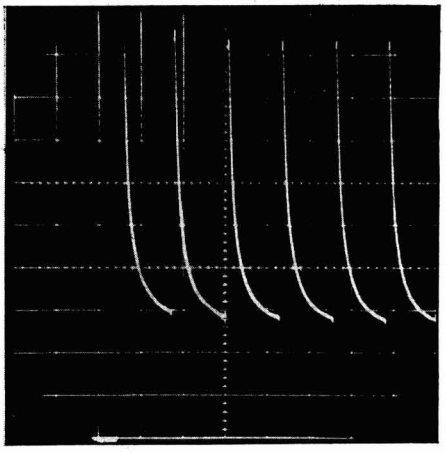

Fig. 6. Oscillogramme de $1 \cdot 10^{-3}$ M $[Fe(CN)_6]^{4-}$ dans NaOH 0.1 N à 25° ± 0.1° immédiatement après polarisation de l'électrode. Chaque division, en absisse = 5 sec; chaque division, en ordonnée = 2 μA.

Dans la Fig. 6 on remarque que le courant, durant la période précédant la formation de la première bulle, à égalité de temps t, est plus intense que celui relevé durant les périodes où a lieu la formation de la seconde bulle. Au bout de la 3ème ou 4ème période, on atteint la stabilisation. Les intensités de courant, enregistrées aussitôt après insertion de la différence de potentiel entre cathode et anode, sont reportées en fonction de $1/\sqrt{t}$ sur la Fig. 5a. Dans ces conditions de fonctionnement de l'électrode, les valeurs du courant de diffusion trouvées et calculées selon l'éqn. (2) sont bien en accord.

L'oscillogramme (b) de la Fig. 4, correspondant au procédé (ii), révèle un comportement analogue au procédé (i) exceptée une augmentation sensible de l'intensité du courant et l'existence d'un petit pic peu avant le détachement de la bulle ($1/\sqrt{t} = 0.43$). Le pic, qui se manifeste au moment où la petite sphère de platine affleure à la surface de la solution, est la conséquence de l'action de perturbation exercée sur la couche de diffusion par le liquide fuyant la zone d'affleurement. Cette action de perturbation,

suivie de la destruction de la couche de diffusion, est également la cause de l'amélioration de la réponse de l'électrode pendant le temps où celle-ci se trouve totalement immergée (Fig. 5b, courbe b, expérimentale; courbe a, théorique).

Sur l'oscillogramme (c) de la Fig. 4, correspondant au procédé (iii), on relève une notable exaltation des effets signalés lors du cas précédent: plus proches des niveaux calculés les variations du courant dans l'intervalle qui précède l'affleurement ($1/\sqrt{t} > 0.48$), bien évident le pic au moment de l'affleurement de l'électrode ($1/\sqrt{t} = 0.48$). Après le pic ($1/\sqrt{t} < 0.48$) est nettement visible la forte chute du courant à la suite de l'émersion partielle de la petite sphère.

Le rapprochement des intensités du courant, des valeurs calculées durant la période où l'électrode se trouve complètement immergée (Fig. 5c, courbe b, expérimentale; courbe a, calculée) analoguement à ce qui a été évoqué lors du procédé (ii), est dû à un renouvellement meilleur de la solution sur la surface de l'électrode après l'émersion partielle de la petite sphère.

Une amélioration ultérieure de la réponse de l'électrode, en se limitant à la période durant laquelle la petite sphère de platine est complètement immergée, a lieu dans le procédé (iv), oscillogramme (d). Dans ces conditions, le renouvellement de la solution est encore meilleur. Pendant la période où la sphère est complètement immergée se manifeste seulement un *défaut de renouvellement* négligeable et les résultats expérimentaux sont bien en accord avec les valeurs calculées (Fig. 5d). D'après l'examen des résultats expérimentaux, on peut déduire que l'électrode de platine à barbotage peut présenter trois phases. La première phase, qui correspond à la période pendant laquelle l'électrode fonctionne complètement immergée dans la solution, est présente dans chacun des quatre procédés expérimentaux décrits. Elle représente 100% du premier, 94% du second et respectivement 75.2 et 63.5% du troisième et du quatrième (Tableau 1). C'est la phase la plus intéressante du fonctionnement de l'électrode, car les courants, au cours de sa durée, sont dûs exclusivement à la diffusion et sont calculables grâce à une formule simple. Les quantités d'électricité qui traversent la cellule au cours de cette première phase sont très élevées, et, dans tous les cas, supérieures à 90% de la quantité totale. Ceci se vérifie également dans le procédé (iv) où la première phase

TABLEAU 1

	μ Coulombs totaux	Temps de barbotage (sec)	Première phase		Seconde phase		Troisième phase	
			μ Coulombs %	t%	μ Coulombs %	t%	μ Coulombs %	t%
Procédé (i)	47,142	5.6	100	100	—	—	—	—
Procédé (ii)	48,220	5.65	98.2	94	1.8	6.0	—	—
Procédé (iii)	45,819	5.45	91.3	75.2	8.70	24.8	—	—
Procédé (iv)	42,636	5.75	90.34	63.5	9.66	32.2	0	4.3

occupe seulement 63.5% de la durée. La seconde phase, qui correspond à l'intervalle de temps pendant lequel l'électrode affleure et émerge partiellement de la solution, est présente dans le second procédé pendant 6% de la durée totale, dans le troisième et le quatrième respectivement pendant 24.8% et 32.2%. Elle se manifeste par un accroissement initial rapide du courant (dû à l'action de perturbation et à la rupture de la couche de diffusion sur la sphère de platine) et par une rapide chute du courant

ensuite. Au cours de cette phase la cellule est traversée par des quantités de courant qui ne dépassent pas 10% du total. Les intensités de courant ne sont pas aisément calculables car elles résultent de la somme d'un courant de pure diffusion et d'un courant de convection, relatifs aux surfaces de la petite sphère (respectivement immergée et affleurant) variant avec rapidité.

La troisième phase, présente seulement dans le procédé (iv) pendant 4.3% de la période, est caractérisée par le détachement de la petite sphère de la solution. Pendant toute la durée de cette phase le courant d'électrolyse est zéro.

L'électrode de platine à barbotage, en conclusion, fonctionne exclusivement sur deux phases. La première est fondamentale. Les courants observés au cours de cette phase sont soumis à un *défaut de renouvellement* qui les rend considérablement inférieurs à ceux qui sont calculés en considérant les processus à l'électrode regis par la diffusion.

Cet effet, maximum lorsque la petite sphère de platine demeure constamment immergée dans la solution, procédé (i), s'atténue en présence de la seconde phase de façon d'autant plus évidente que la durée de celle-ci est plus longue.

Pour obtenir les meilleurs résultats, il semblerait donc préférable d'employer des électrodes où la seconde phase soit présente au maximum de sa durée. Effectivement, dans ces conditions, 90% de la quantité d'électricité traverse la cellule avec des intensités très proches de celles qui ont été calculées.

On ne peut cependant négliger le fait que l'amélioration remarquable de la réponse de l'électrode, apportée par la présence de la seconde phase, est atteinte par l'introduction d'actions de perturbation de forte importance qui intéressent 10% de la quantité d'électricité totale. Ainsi, même si les données expérimentales ne sont pas aussi bonnes que celles obtenues dans le procédé (iv), nous pensons préférable aux autres procédés, le procédé (i) où est présente seulement la première phase. *Le défaut de renouvellement*, étant donnée la simplicité de fonctionnement de l'électrode, peut être, à notre avis, facilement évalué ou mieux encore éliminé, en apportant à l'électrode quelques légères modifications.

REMERCIEMENTS

Ce travail a été effectué avec l'aide du C.N.R.

RÉSUMÉ

On a étudié les intensités instantanées des courants relevées au cours du fonctionnement de l'électrode de platine à barbotage comme anode dans une solution de $K_4Fe(CN)_6$ 10^{-3} *M* en NaOH 0.1 *N*.

Il a été possible de relever que pendant le temps d'immersion totale l'électrode produit des courants qui sont dûs exclusivement à la diffusion. Pendant le temps où elle affleure et émerge de la solution, aux courants de diffusion s'associent des courants dûs à des mouvements de convection qui se localisent dans les zones d'affleurement.

On a confronté les résultats atteints dans différentes conditions de fonctionnement, et on a démontré que seuls les courants s'obtenant avec électrode totalement immergée peuvent être calculés quand on connaît l'aire de la petite sphère de platine en contact avec la solution.

BIBLIOGRAPHIE

1 D. Cozzi et P. G. Desideri, *J. Electroanal. Chem.*, 4 (1960) 301.

CARACTÉRISTIQUES ET PROPRIÉTÉS DE L'ÉLECTRODE DE PLATINE À BARBOTAGE. II

DANILO COZZI, GIORGIO RASPI ET LAMBERTO NUCCI

Institut de Chimie Analytique de l'Université de Pise (Italie)

(Reçu le 20 juillet, 1963)

Dans deux travaux précédents[1,2] on a déjà attiré l'attention des chercheurs sur les caractéristiques et les propriétés de l'électrode de platine à barbotage qui tout en présentant un comportement identique à celui de l'électrode à goutte de mercure offre sur cette dernière l'avantage de permettre la recherche sur les systèmes à hauts potentiels d'oxydo-réduction.

Dans le premier de ces travaux, l'électrode employée était constituée par une petite sphère de platine alternativement immergée dans la solution ou partiellement émergée durant le fonctionnement. Dans le deuxième travail, on a examiné le comportement de l'électrode en fonction de la position donnée à la sphère de platine par rapport à la surface de la solution durant son fonctionnement. On ne rapportera pas ici les considérations déjà exposées et l'on se bornera à rappeler la conclusion de la recherche poursuivie alors: il est nécessaire que la petite sphère de l'électrode soit immergée de façon permanente dans la solution durant le fonctionnement pour que l'on enregistre des intensités de courant limite dues exclusivement à la diffusion sans actions perturbatrices provenant de l'agitation. Ces intensités sont toutefois inférieures aux valeurs théoriques par suite du renouvellement insuffisant de l'électrolyte sur la surface de l'électrode au moment de l'expulsion de la bulle de gaz ("défaut de renouvellement"). Afin d'atténuer ce défaut et de définir les conditions expérimentales garantissant la réponse la plus satisfaisante de la part de l'électrode par rapport au comportement théorique valable pour la diffusion sphérique, on a voulu examiner le comportement d'un type d'électrode fonctionnant dans des conditions d'immersion totale et permanente de la sphère et présentant quelques légères modifications de construction par rapport aux modèles précédents. L'hémisphère supérieur de la boule de platine a en effet été recouvert d'une couche de verre de sorte que le tube qui porte soudée à son extrémité inférieure la petite sphère se contracture en elle sans brusques variations de diamètre et que seul l'hémisphère inférieur, ou une partie de celui-ci, demeure en contact avec la solution. Cette modification a été apportée dans le but d'éliminer les zones de la sphère qui se trouvent moins exposées, durant le fonctionnement de l'électrode, au lavage de la solution au moment où sort la bulle de gaz. On a en outre fixé à l'extrémité inférieure du tube trois petits obstacles afin de favoriser l'homogénéisation de la solution. Dans la Fig. 1, on a reporté en (A) la zone terminale

des électrodes sphériques utilisées aux cours des recherches précédentes et en (B) et (C) celle des électrodes hémisphériques utilisées au cours du présent travail.

Pour simplifier l'exposition et offrir une vue d'ensemble des résultats obtenus avec la série des électrodes expérimentées, dont la surface est comprise entre 0.02 et 0.08

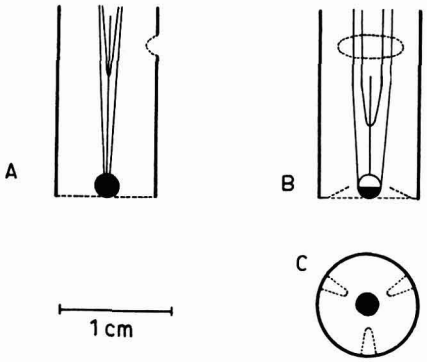

Fig. 1. (A), partie terminale de l'électrode sphérique de platine à barbotage utilisée dans le travail précédent[2]. (B) et (C), partie terminale de l'électrode hémisphérique de platine à barbotage utilisée dans la présente étude.

cm^2, nous rapporterons les résultats obtenus avec une électrode ayant une surface utile de platine égale à 0.049 $cm^2 \pm 0.001$ cm^2. Les caractéristiques du fonctionnement ont été maintenues constantes pour toutes les électrodes: diamètre intérieur du tube, 9 mm; oscillation totale du liquide, 8 mm; section du trou latéral, 9.4 mm^2; extrémité inférieure de l'hémisphère tangente au centre du cercle de base du tube extérieur; électrode polarisée à +0.450 V (E.C.S.) dans une solution $1 \cdot 10^{-3}$ M de $K_4Fe(CN)_6$ en NaOH 0.1 N, à $25° \pm 0.1°$.

Les intensités de courant i_t de chacune des oscillations ont été confrontées avec les i_t calculées suivant l'équation:

$$i_t = nFADC\left(\frac{1}{r} + \frac{1}{\sqrt{\pi Dt}}\right) \qquad (1)$$

où:

i_t: courant limite instantané au temps t, exprimé en μA;
n: nombre de Faraday d'électricité consommés dans la réaction à l'électrode pour chaque mole;
F: Faraday (96500 C);
A: surface de l'électrode exprimée en cm^2 (0.049);
C: concentration exprimée en moles/ml ($1 \cdot 10^{-6}$);
D: coefficient de diffusion (0.74×10^{-5} cm^2 sec^{-1});
r: rayon de la petite sphère de platine exprimée en cm (0.1);
t: temps en sec;

où t est mesuré à partir du moment même où se produit l'expulsion d'une bulle.

Dans la Fig. 2 sont reportées: les variations théoriques (ligne a) de la i_t pour l'électrode hémisphérique, obtenues grâce à l'éqn. (1), en fonction de $1/\sqrt{t}$; les i_t expérimentales pour des temps de barbotage de 9.72, 6.12 et 3.00 secondes, auxquelles on com-

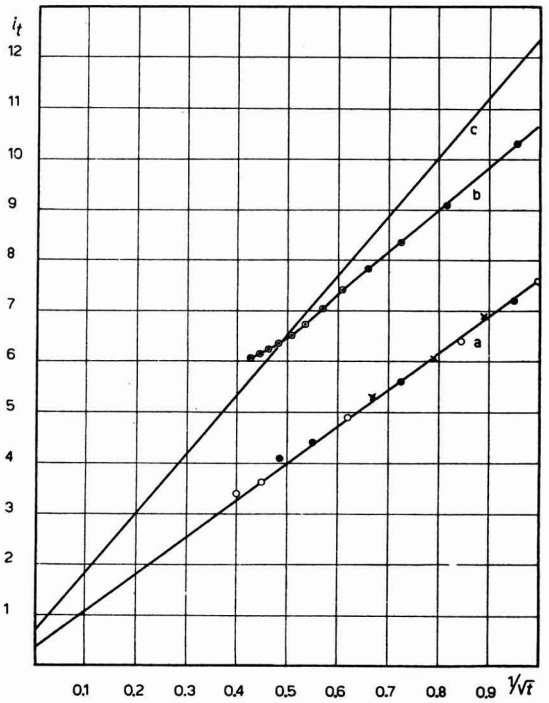

Fig. 2. i_t en fonction de $1/\sqrt{t}$ obtenues avec l'électrode hémisphérique et l'électrode sphérique dans l'intervalle $0 \leqslant 1/\sqrt{t} \leqslant 1$. Électrode hémisphérique. Ligne (a) calculée au moyen de l'éqn. (1); valeurs expérimentales correspondant à $t_{tot.}$ 9.72 sec (○); 6.12 sec (●); 3.00 sec (×). Électrode sphérique. Ligne (c) calculée au moyen de l'éqn. (1); valeurs expérimentales correspondant à $t_{tot.} = 5.60$ sec (⊙).

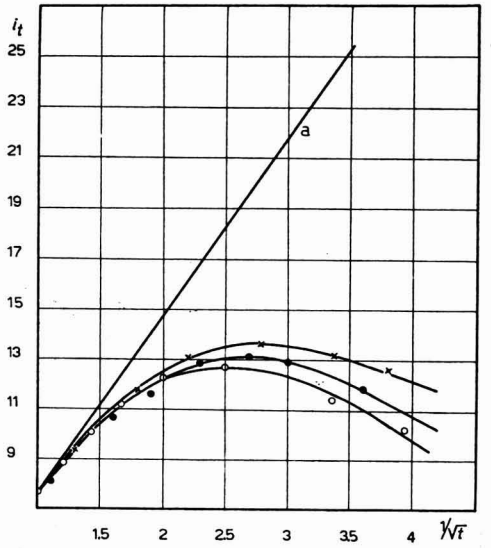

Fig. 3. i_t en fonction de $1/\sqrt{t}$ obtenues avec l'électrode hémisphérique dans l'intervalle $1 \leqslant 1/\sqrt{t} \leqslant 4$. Ligne (a) calculée au moyen de l'éqn. (1); valeurs expérimentales correspondant à $t_{tot.}$ 9.72 sec (○); 6.12 sec (●); 3.00 sec (×).

pare les variations des i_t expérimentales en fonction de $1/\sqrt{t}$ pour un temps de barbotage de 5.6 sec (courbe b) obtenues avec la même électrode avant l'isolement de l'hémisphère supérieur de la petite boule de platine. On peut remarquer que les i_t expérimentales obtenues en utilisant l'électrode sphérique présentent une valeur nettement inférieure à la valeur calculée (ligne c), ceci à cause de la présence d'un important "défaut de renouvellement". Les i_t obtenues avec l'électrode hémisphérique sont égales aux valeurs calculées. Lorsque le rapport $1/\sqrt{t}$ augmente (Fig. 3) les valeurs expérimentales,

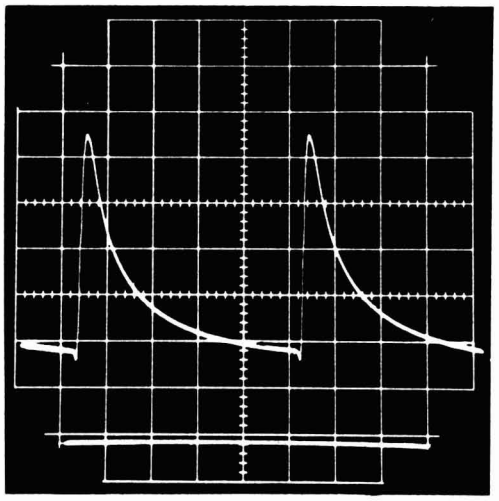

a

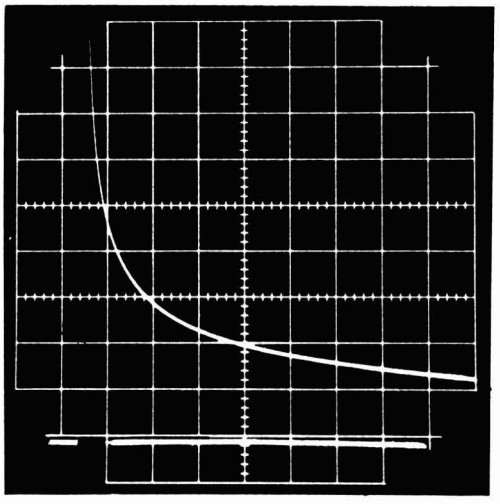

b

Fig. 4. (a), oscillogramme de $1 \cdot 10^{-3}$ M $[Fe(CN)_6]^{4-}$ en NaOH 0.1 N à 25° ± 0.1° obtenu avec l'électrode hémisphérique de platine à barbotage ($t_{tot.}$ = 5.1 sec) polarisée à + 0.450 V (E.C.S.). En abscisses les temps (1 sec/division) et en ordonnées les intensités de courant (2 μA/division). La valeur i = 0 est représentée par la ligne en trait appuyé au bas de la figure. (b), oscillogramme obtenu avec la même électrode, stationnaire dans la solution, dans les mêmes conditions.

même dans le cas de l'électrode hémisphérique, s'éloignent des valeurs calculées (ligne a). Ceci est expliqué par l'examen oscillographique de chacune des pulsations.

Dans la Fig. 4(a) on a reporté la courbe oscillographique de l'électrode hémisphérique fonctionnant avec un temps de barbotage de 5.1 sec; dans la Fig. 4(b) la courbe oscillographique de la même électrode stationnaire dans la solution.

L'intensité du courant expérimental au temps zéro, c'est-à-dire à l'instant où la bulle de gaz sort par le trou latéral, est définie par l'épaisseur de la couche diffuse qui s'est formée sur l'électrode durant la période qui précède la formation de la bulle. La bulle une fois détachée, le liquide effectue une soudaine remontée; on a l'amincissement de la couche diffuse et l'intensité du courant varie de ce fait vers des valeurs plus élevées atteignant un maximum après une fraction de seconde ($t_{max.}$). La variation du courant à proximité du maximum peut être plus aisément observée dans l'agrandissement de la Fig. 5. Une fois le maximum atteint, le courant décroît en se maintenant à

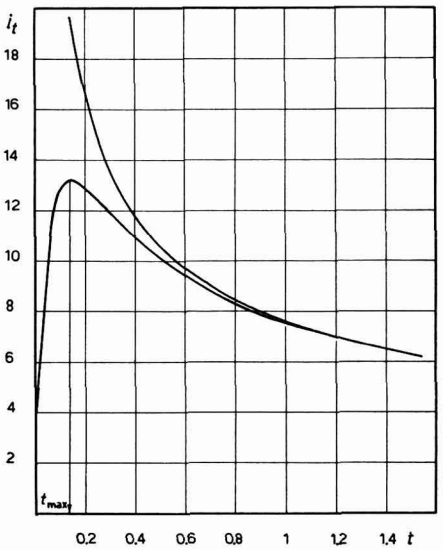

Fig. 5. Agrandissement des Figs. 4 (a) et 4 (b) dans l'intervalle de t compris entre 0 et 1.6 sec.

un niveau bas par rapport au niveau théorique pendant une durée d'une seconde. Au delà d'une seconde, le courant décroît avec une variation très proche de la variation théorique, c'est-à-dire très proche de la variation du courant de l'électrode stationnaire.

La quantité d'électricité traversant la cellule durant la période comprise entre la formation d'une bulle et celle de la suivante est égale à l'aire comprise entre la courbe de la Fig. 4(a) et l'axe des temps et s'établit comme suit:

$$Q_{exp.} = I_{exp.} t_{tot.} \tag{2}$$

où:

$I_{exp.}$ valeur de l'intensité moyenne du courant, égale au courant limite de diffusion i_d, mesuré avec les méthodes de la polarographie traditionnelle, corrigé du courant résidu;

$t_{tot.}$ temps de barbotage.

La quantité d'électricité théorique est représentée par:

$$Q_{\text{th.}} = I_{\text{th.}} t_{\text{tot.}} \tag{3}$$

où $I_{\text{th.}}$ est plus grand que $I_{\text{exp.}}$ puisque l'aire délimitée par la courbe de la Fig. 4(b) est plus grande que celle délimitée par la courbe de la Fig. 4(a).

En effet, si l'on applique à l'éqn. (1) la relation:

$$Q_{\text{th.}} = \int_0^{t_{\text{tot.}}} i_t \mathrm{d}t$$

on obtient:

$$Q_{\text{th.}} = \frac{nFADC}{r} t_{\text{tot.}} + \frac{nFADC}{\sqrt{\pi D}} 2\sqrt{t_{\text{tot.}}} \tag{4}$$

En substituant dans l'éqn. (4) les termes connus pour l'électrode, fonctionnant avec $t_{\text{tot.}} = 5.1$ sec, et en combinant avec l'éqn. (3) on obtient la valuer de $I_{\text{th.}}$ égale à 6.77 μA. La valeur expérimentale est $I_{\text{exp.}} = 5.72$ μA.

Le rapport entre l'intensité moyenne du courant expérimental et l'intensité moyenne du courant théorique, c'est-à-dire le rapport $I_{\text{exp.}} : I_{\text{th.}}$, n'est pas constant: il croît et se rapproche d'autant plus de 1 que la période de barbotage est plus longue (Tableau 1).

TABLEAU 1

$t_{tot.}$ (sec)	$Q_{th.}$ (μC)	$Q_{exp.}$ (μC)	$I_{th.}$ (μA)	$I_{exp.}/I_{th.}$	$I_{exp.}$ (μA)	$I_{calc.}$ (μA)	$t_{max.}$ (sec)
9.72	48.7	42.8	5.02	0.88	4.40	4.42	0.16
8.42	45.1	39.4	5.36	0.87	4.68	4.67	0.16
7.23	41.6	35.8	5.76	0.86	4.95	4.98	0.15
6.12	38.1	32.2	6.23	0.85	5.27	5.34	0.14
5.10	34.5	29.2	6.77	0.84	5.72	5.70	0.14
3.80	29.6	24.2	7.79	0.82	6.38	6.40	0.13
3.00	26.2	20.8	8.73	0.80	6.93	6.97	0.13
1.96	21.0	16.0	10.72	0.76	8.18	8.13	0.12
1.32	17.1	12.3	12.95	0.72	9.30	9.45	0.10

A la suite de ces observations, il a été possible de déduire que la quantité d'électricité traversant la cellule durant la période qui précède la formation d'une bulle ne peut pas être celle calculée à partir de l'éqn (4), puisque la couche diffuse n'est jamais entièrement détruite. Si l'on ouvre le circuit à l'instant même où la solution commence sa rapide montée ($t = 0$) et si on le referme à l'instant où débute sa lente redescente ($t = t_0$) on remarque que les intensités de courant mesurées sur la courbe satisfont l'éqn. (1) à condition que les temps soient calculés à partir du moment où s'effectue l'ouverture du circuit et non au moment de sa fermeture. Ce fait prouve que l'électrode à barbotage révèle, au moment de la fermeture du circuit, un courant limite de diffusion égal à celui que présenterait une électrode stationnaire non pas au moment de la fermeture du circuit, mais après un temps égal à t_0. La quantité d'électricité qui traverse la cellule durant la période de formation de la bulle peut être calculée en intégrant l'éqn. (1) entre les limites t_0 et $t_{\text{tot.}}$:

$$Q_{\text{calc.}} = at_{\text{tot.}} + 2b\sqrt{t_{\text{tot.}}} - at_0 - 2b\sqrt{t_0} \tag{5}$$

où

$$a = \frac{nFADC}{r}, \qquad b = \frac{nFADC}{\sqrt{\pi D}}.$$

L'intensité moyenne du courant dans la même période est:

$$I_{\text{calc.}} = a + \frac{2b}{\sqrt{t_{\text{tot.}}}} - \frac{at_0}{t_{\text{tot.}}} - \frac{2b\sqrt{t_0}}{t_{\text{tot.}}} \tag{6}$$

La courte période de temps t_0 est un terme caractéristique de l'électrode qui dépend de la façon dont l'électrode est lavée durant la remontée de la solution à la suite de la formation de la bulle. La valeur de t_0 est d'autant plus petite que le déplacement de la solution par rapport à la petite sphère de platine et sa vitesse sont plus grands. Durant le fonctionnement normal de l'électrode on ne constate aucune interruption du courant, mais celui-ci présente les variations caractéristiques déjà illustrées à la Fig 4(a). La quantité d'électricité

$$Q_{\text{th.}} - Q_{\text{exp.}} = \int_0^{t_0} i_t \mathrm{d}t$$

est représentée sur le graphique par l'aire délimitée par la courbe de l'électrode stationnaire et celle de l'électrode hémisphérique à barbotage.

Le temps t_0 s'identifie avec une bonne approximation au temps t_{max}. Si l'on introduit dans l'éqn. (6), à la place de t_0, les temps auxquels apparaît le maximum du courant mesuré oscillographiquement, on obtient les résultats reportés au Tableau 1. L'accord des intensités du courant limite de diffusion mesurées avec les méthodes de la polarographie traditionnelle et des intensités moyennes calculées peut être considéré comme satisfaisant.

REMERCIEMENTS

Ce travail a été effectué avec l'aide du C.N.R.

RÉSUMÉ

On a expérimenté le comportement d'une série d'électrodes hémisphériques de platine, caractérisées par des surfaces comprises entre 0.02 et 0.08 cm², à différents temps de barbotage. On relate le comportement d'une électrode ayant une surface de 0.049 cm². Il résulte de l'expérience que la variation de l'intensité de courant instantané en fonction de $1/\sqrt{t}$ concorde assez bien avec la variation théorique calculée sur la base de l'équation valable pour la diffusion sphérique.

On a confronté les variations des courants limites de diffusion et les variations théoriques et on a défini un temps t_0, caractéristique pour chaque électrode, capable d'exprimer la différence du comportement expérimental par rapport au comportement théorique.

SUMMARY

We have investigated the behaviour of hemispherical bubbling platinum electrodes of surface areas 0.02–0.08 cm² at different rates of bubble formation. Results are given for an electrode of surface area 0.049 cm². It was found that the relationship between

the value of the instantaneous current and $i/\sqrt{t}$ was in approximate agreement with the theoretical relationship calculated on the basis of the equation governing spherical diffusion. We have calculated from experimental and theoretical values of the limiting diffusion currents, a value t_0 for each electrode. This value expresses the difference between experimental and theoretical behaviour.

BIBLIOGRAPHIE

[1] D. Cozzi et P. G. Desideri, *J. Electroanal. Chem.*, 4 (1960) 301.
[2] D. Cozzi, G. Raspi et L. Nucci, *J. Electroanal. Chem.*, 4 (1963) 267.

THE CHRONOPOTENTIOMETRIC REDUCTION OF OXYGEN AT GOLD ELECTRODES

DENNIS H. EVANS AND JAMES J. LINGANE

Department of Chemistry, Harvard University, Cambridge 38, Mass. (U.S.A.)

(Received July 5th, 1963)

The chronopotentiometric reduction of oxygen has been studied at mercury[1], platinum[2] and palladium[3] electrodes. The products and mechanism of the reaction depend on the metal used and on the electrolytic history of the electrode. In particular the formation and reduction of oxide films on platinum and palladium electrodes are found to have a profound effect on the characteristics of chronopotentiograms subsequently obtained. Although several aspects of oxygen reduction at gold have been investigated[4,5,6], little attention has been directed to the effect of electrode pretreatment on the nature of the reaction. In this communication a systematic study of the chronopotentiometric reduction of oxygen at gold electrodes in various media is reported.

EXPERIMENTAL

The electrical circuit was the same as that used in a previous study[7]. Measurements of transition time were made with a Dumont 304-H cathode ray oscilloscope. In the *manual method* the electrolysis was interrupted when the oscilloscopic trace had reached a pre-determined transition potential. The transition time was then read directly from a Model S-10 electric stop-clock (Standard Electric Time Co.) which operated when the electrolysis circuit was closed. In the *photographic method*[8] the complete oscilloscopic trace was photographed and the transition times were measured from the photographs. All chronopotentiograms presented in this paper were recorded with a Sargent Model MR strip-chart recording potentiometer whose full scale response time was one second.

The electrolysis cell has already been described, see ref. 7, p. 380, Fig. 2. Gold wire working electrodes were constructed from pure gold wire (Eastern Smelting and Refining Co., Boston) of radius 0.0255 cm. All but a 1–3 cm portion of the gold wire was covered with a layer of Tygon paint (Type K-63, U.S. Stoneware Co.) thus exposing a cylindrical surface to the solution. An electrode sealed in glass with Varno-Cement (Varniton Company, Los Angeles) covered with paraffin gave results indistinguishable from those obtained with a Tygon-coated electrode. All experiments were carried out with the cell in a water thermostat with a temperature controlled to $\pm$ 0.05°.

Chemicals for supporting electrolytes were of reagent quality. Distilled water of specific conductance less than $2 \cdot 10^{-6}\ \Omega^{-1}\ cm^{-1}$ was used to prepare all solutions. The

oxygen was supplied by the Air Reduction Company and was guaranteed to be 99.5% pure, the major impurities being argon and nitrogen.

OXYGEN REDUCTION IN SODIUM HYDROXIDE SOLUTIONS

Characteristics of oxygen chronopotentiograms

Figure 1 shows a series of chronopotentiograms for the reduction of oxygen at a gold wire electrode in oxygen-saturated 1.0 *M* sodium hydroxide. Three minutes before curve 1, Fig. 1, the electrode had been anodized to oxygen evolution, forming a gold oxide film on the electrode. The first wave in curve 1 corresponds to the reduction of this gold oxide film, and the next two waves are due to reduction of oxygen. Anodization to oxygen evolution followed by a cathodization, producing a chronopotentiogram identical to curve 1, constituted the standard electrode pre-treatment used throughout this investigation. Curves 2–5 of Fig. 1 were recorded after curve 1 with successively longer intervals of time between trials.

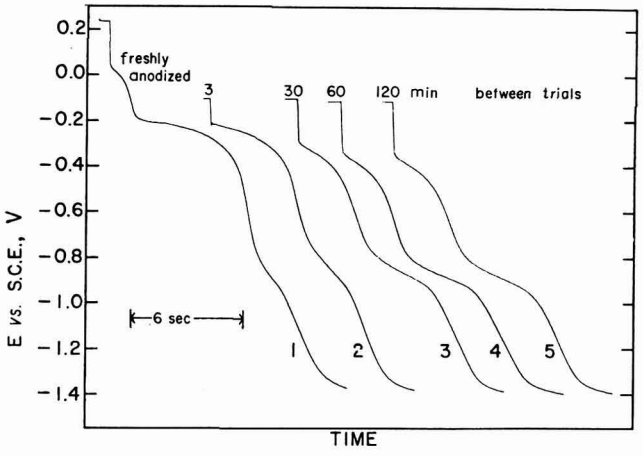

Fig. 1. Typical oxygen reduction chronopotentiograms in 1.0 *M* NaOH; $i = 104.6\ \mu A$, electrode area = 0.168 cm^2, temp. = 25.00°.

In Fig. 1 it can be seen that the first transition time is somewhat longer at an electrode which has been recently pre-treated (curve 2) than it is at an electrode which has been in contact with the solution for a longer period of time after pre-treatment. It will be shown later that the first transition time at a recently pre-treated electrode is too long to correspond to the diffusion-controlled 2-electron reduction of oxygen to hydrogen peroxide. However, as the time after pre-treatment increases, the first transition time becomes shorter approaching the value corresponding to the 2-electron reduction. When the electrode was again pre-treated after curve 5, Fig. 1, and 3 min was allowed to elapse, a chronopotentiogram identical to curve 2 was obtained. The enhancement of the first transition time observed immediately after electrode pre-treatment (anodization followed by cathodization) will be designated the *activation* effect. The subsequent decrease of the first transition time and the concomitant increase in the over-potential of the first wave will be called the *aging* effect.

The second characteristic of the oxygen chronopotentiograms is that the total transition time (measured from the beginning of electrolysis to the inflection in the second wave) remains constant and is independent of the history of the electrode. This demonstrates that the overall electrochemical reaction of oxygen is always the same.

The overall electrochemical reaction was identified by studying the variation of the total transition time with the current density. The theoretical expression relating the transition time to current density for chronopotentiometry with cylindrical electrodes has been derived by PETERS AND LINGANE[8].

$$\frac{i\tau^{1/2}}{AC^{\circ}} = \frac{\pi^{1/2} n F D^{1/2}}{2}\left[\frac{1}{1 - \frac{\pi^{1/2} D^{1/2}\tau^{1/2}}{4r_o} + \frac{D\tau}{4r_o^2} - \frac{3\pi^{1/2} D^{3/2}\tau^{3/2}}{32r_o^3} + \ldots}\right] \quad (1)$$

where i is the current (amp.), τ is the transition time (sec), A is the electrode area (cm^2), C° is the concentration of the electroactive species (moles/cm^3), n is the number of Faradays of electricity per mole of reaction, F is the Faraday constant (96493 C), D is the diffusion coefficient of the electro-active species (cm^2/sec), and r_o is the radius of the electrode (cm). Additional terms in the denominator on the right-hand side of eqn. (1) have been derived[9,10] and are used in all calculations reported.

The results of measurements of the total transition time in 1.0 M sodium hydroxide over a wide range of current densities are presented in Table 1. The chronopotentiograms were recorded at 15 min intervals with no pre-treatment between trials since pre-treatment does not affect the total transition time. Theoretical values of $i(\tau_1 + \tau_2)^{1/2}/AC^{\circ}$ were calculated from eqn. (1) using $1.79 \cdot 10^{-5}$ cm^2/sec for the diffusion coefficient of oxygen[2]. The solubility of oxygen in 1 M sodium hydroxide at 25° is $8.45 \cdot 10^{-4} M$ at one atmosphere[11]. The atmospheric pressure during the experiment was slightly less than one atmosphere and the oxygen contained 0.5% inert gases. When corrections were made for these factors, the concentration of oxygen in the solution was calculated to be $8.38 \cdot 10^{-4}$ M. The value of n in eqn. (1) was assumed to be four to correspond to the overall reaction in alkaline solution

$$O_2 + 2\,H_2O + 4\,e = 4\,OH^- \quad (2)$$

In Fig. 2, the data of Table 1 are plotted *vs.* transition time. The solid curve labelled $n = 4$ is the theoretical curve.

The good agreement between the experimental results and the theoretical predictions based on an independent measurement of the diffusion coefficient and the assumption that n is four, demonstrates unambiguously that the total transition time for oxygen reduction represents the 4-electron, diffusion-controlled reduction to hydroxide ion.

Although the total transition time is invariant, the first transition time varies extensively. The effect of electrode pre-treatment was investigated in a series of experiments carried out in 1.0 M sodium hydroxide. The electrode was subjected to an anodic-cathodic pre-treatment for a given time before a chronopotentiogram was recorded. The first transition time was found to be reproducible provided the time elapsing after the pre-treatment was carefully duplicated. In this case the oxygen

concentration was $8.43 \cdot 10^{-4}$ M. The results of these experiments are summarized in Tables 2 and 3. The data in Table 2 were obtained with 15-sec stirring and a 45-sec unstirred period following the pre-treatment. In Table 3 the time elapsing after pre-treatment was 10 min (9 min stirring, 1 min quiet).

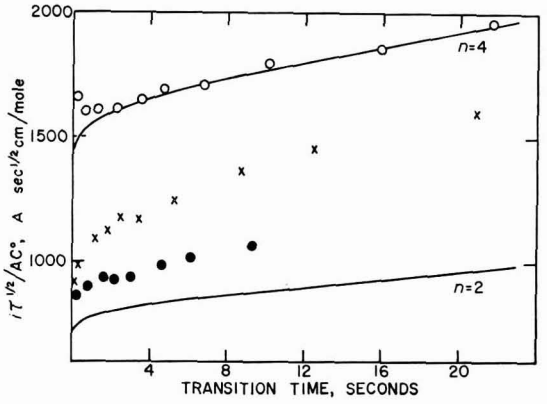

Fig. 2. $i\tau^{1/2}/AC^\circ$ as a function of transition time in 1.0 M NaOH. Open circles, data for total transition time (Table 1); crosses, data for first transition time 1 min after pre-treatment (Table 2); solid circles, data for first transition time 10 min after pre-treatment (Table 3). Solid curves are theoretical curves for 2- and 4-electron processes.

TABLE 1

CHRONOPOTENTIOMETRY OF OXYGEN AT A GOLD CATHODE IN 1 M SODIUM HYDROXIDE (TOTAL TRANSITION TIME)

Transition times measured by the photographic method, 15 min between trials. Times given are averages of three trials. Average deviation given in parentheses. Temp. = 25.00 ± 0.05°. Concn. of oxygen = $8.38 \cdot 10^{-4}$ M. Area of electrode = 0.485 cm^2. Theoretical values of $i(\tau_1 + \tau_2)^{1/2}/AC^\circ$ calculated from eqn. (1) and assumption that $n = 4$.

i (μA)	$\tau_1 + \tau_2$ (sec)	$i(\tau_1 + \tau_2)^{1/2}/AC^\circ$ (A sec$^{1/2}$ cm/mole)	
		obs.	theor.
1422	0.255 (±0.002)	1660	1497
808.6	0.648 (±0.002)	1602	1531
577.0	1.28 (±0.01)	1607	1565
435.1	2.27 (±0.01)	1613	1603
356.6	3.53 (±0.06)	1649	1641
316.5	4.71 (±0.05)	1690	1670
266.6	6.79 (±0.04)	1710	1713
229.1	10.12 (±0.04)	1794	1772
188.8	15.90 (±0.07)	1853	1861
170.8	21.70 (±0.41)	1958	1949

The currents in Tables 2 and 3 have been corrected for the simultaneous charging of the electrical double-layer and the reduction of any spontaneously formed oxide film by means of the relation proposed and tested earlier[7,8].

$$i_{corr.} = i_{obs.} - Q/\tau \qquad (3)$$

TABLE 2

CHRONOPOTENTIOMETRY OF OXYGEN AT A GOLD CATHODE IN 1 *M* SODIUM HYDROXIDE (FIRST TRANSITION TIME)

Transition times were measured by the photographic method *one minute* (15 sec stirring, 45 sec quiet) after electrode pre-treatment. Times given are averages of two trials. Average deviation given in parentheses. Temp. = 25.00 ± 0.05°. Concn. of oxygen = $8.43 \cdot 10^{-4}$ *M*. Area of electrode = 0.477 cm^2.

$i_{corr.} = i_{obs.} - 21/\tau_1$ (see text)

$i_{obs.}$ (μA)	τ_1 (*sec*)	$i_{corr.}$ (μA)	$i\tau_1^{1/2}/AC^\circ$ (*A* $sec^{1/2}$ *cm/mole*)	
			obs.	*corr.*
1408	0.96 (±0.002)	1190	1081	913
789.4	0.305*	720	1080	985
425.9	1.16 (±0.06)	408	1136	1089
350.0	1.79 (±0.13)	338	1160	1120
310.4	2.47 (±0.01)	301.9	1209	1176
260.8	3.42 (±0.28)	254.7	1195	1167
222.7	5.28 (±0.22)	218.7	1268	1245
188.5	8.72 (±0.14)	186.1	1379	1361
167.8	12.44 (±0.06)	166.1	1466	1451
142.3	20.88 (±0.20)	141.3	1610	1599

* One trial only

TABLE 3

CHRONOPOTENTIOMETRY OF OXYGEN AT A GOLD CATHODE IN 1 *M* SODIUM HYDROXIDE (FIRST TRANSITION TIME)

Transition times measured by the photographic method *ten minutes* (9 min stirring, 1 min quiet) after electrode pre-treatment. Times given are averages of two trials. Average deviation given in parentheses. Temp. = 25.00 ± 0.05°. Concn. of oxygen = $8.43 \cdot 10^{-4}$ *M*. Area of electrode = 0.477 cm^2.

$i_{corr.} = i_{obs.} - 21/\tau_1$ (see text)

$i_{obs.}$ (μA)	τ_1 (*sec*)	$i_{corr.}$ (μA)	$i\tau_1^{1/2}/AC^\circ$ (*A* $sec^{1/2}$ *cm/mole*)	
			obs.	*corr.*
1407	0.086 (±0.006)	1170	1021	850
794.6	0.241 (±0.005)	708	966	861
564.5	0.470 (±0.035)	519	958	881
431.7	0.80 (±0.02)	406	956	899
352.8	1.18 (±0.03)	335	949	901
312.3	1.59 (±0.02)	299	975	934
263.7	2.17 (±0.00)	254.0	962	926
224.2	3.03 (±0.02)	217.3	967	937
189.1	4.62 (±0.06)	184.6	1006	982
168.6	6.14 (±0.06)	165.2	1034	1013
143.0	9.32 (±0.16)	140.7	1082	1063

where Q is the quantity of electricity consumed in any process other than the reduction of oxygen. In this case, the quantity Q was evaluated by exposing the pre-cathodized electrode to the oxygen-saturated 1.0 *M* sodium hydroxide for 15 min. The electrode

was then removed and placed in oxygen-free 1.0 M sodium hydroxide for 15 min and then cathodized. It was found that 21 μC was required to polarize the electrode (0.477 cm^2) to the first transition potential. In 0.10 M sodium hydroxide Q was 17 μC. The currents of Tables 2 and 3 have all been corrected *via* eqn. (3) with Q set equal to 21 μC. For the sake of comparison both the corrected and uncorrected values of $i\tau_1^{1/2}/AC^\circ$ have been included.

Similar corrections should undoubtedly be applied to the data obtained for the total transition time (Table 1). However, no reliable results for Q corresponding to the total transition time could be obtained because the second transition potential was too close to the hydrogen evolution potential.

In Fig. 2 the values of $i\tau_1^{1/2}/AC^\circ$ are plotted *vs.* transition time. The crosses represent data from Table 2 and the solid circles represent data from Table 3. The solid line labelled $n = 2$ is the theoretical curve for the 2-electron reduction. The experimental data fall considerably above the theoretical curve, *i.e.*, the first transition time is greater than the $n = 2$ value. Furthermore, the data taken 10 min after pre-treatment are much closer to the theoretical curve than the data taken 1 min after pre-treatment. This is simply another manifestation of the aging effect illustrated in Fig. 1.

The enhancement of the first transition time above the $n = 2$ value at a recently pre-treated electrode undoubtedly is due to the disproportionation of hydrogen peroxide at the electrode surface. Oxygen is first reduced to hydrogen peroxide which in very alkaline solutions is present mainly as HO_2^- ($H_2O_2 + OH^- = HO_2^- + H_2O$, $K = 180$)[12]

$$O_2 + H_2O + 2\,e = HO_2^- + OH^- \qquad (4)$$

The hydrogen peroxide anion can then disproportionate at the electrode surface

$$2\,HO_2^- \overset{k_h}{\rightleftharpoons} O_2 + 2\,OH^- \qquad (5)$$

where k_h is the heterogeneous rate constant for the disproportionation process. The oxygen formed by reaction (5) can then be reduced *via* reaction (4), thus lengthening the time required for the oxygen concentration to decrease to zero at the electrode surface, *i.e.*, the first transition time. After the first transition time, the remaining HO_2^- formed in the first step is further reduced to hydroxide ion,

$$HO_2^- + H_2O + 2\,e = 3\,OH^- \qquad (6)$$

and oxygen continuing to diffuse to the electrode or being formed by reaction (5) is directly reduced to hydroxide ion by reaction (2).

The relative enhancement of the first transition time depends upon the rate of reaction (5). If $k_h = 0$, no oxygen would be regenerated and the first transition time would correspond exactly to the 2-electron reduction of oxygen. For larger and larger finite values of k_h, the first transition time becomes longer until it finally fuses into the second and the resulting chronopotentiogram then has but one wave for the 4-electron reduction of oxygen.

Evidence that the enhancement of the first transition time is due to a kinetically controlled process was obtained from the effect of temperature on the chronopotentio-

grams. Chronopotentiograms obtained at three different temperatures in 1.0 M sodium hydroxide are presented in Fig. 3. Each chronopotentiogram was recorded 3 min after an anodic-cathodic pre-treatment. The relative enhancement of the first transition time with increasing temperature reflects the positive temperature coefficient of k_h.

The effect of sodium hydroxide concentration on the reduction of oxygen at a gold wire electrode was also investigated. A series of chronopotentiograms recorded in oxygen-saturated 0.10 M sodium hydroxide is shown in Fig. 4. Three minutes before curve 1 was recorded, the electrode was anodized just to oxygen evolution. The first wave in curve 1 is due to the reduction of the gold oxide film formed in the previous

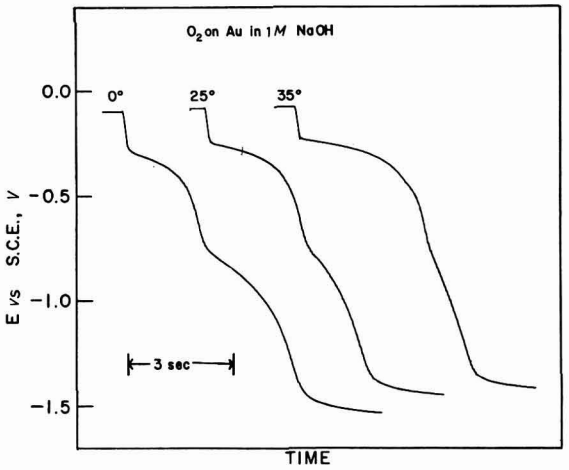

Fig. 3. Effect of temp. on enhancement of first transition time; i = 185 μA, electrode area = 0.268 cm^2. Chronopotentiograms recorded 3 min after electrode pre-treatment.

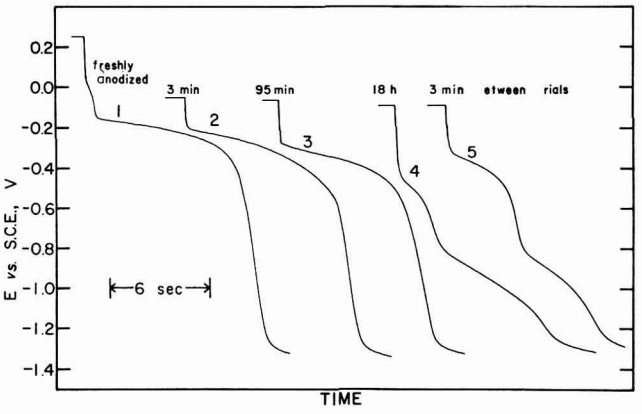

Fig. 4. Typical oxygen reduction chronopotentiograms in 0.10 M NaOH; i = 134.3 μA, electrode area = 0.168 cm^2, temp. = 25.00°.

anodization. This is followed by a single chronopotentiometric wave for the reduction of oxygen. Curves 2–5 were recorded after various intervals of time had elapsed after curve 1. The electrode was not pre-treated between trials.

In contrast to the behavior in 1 M sodium hydroxide, a recently pre-treated electrode in 0.1 M sodium hydroxide was so active with respect to disproportionation of hydrogen peroxide that only a single 4-electron chronopotentiometric wave was observed. Furthermore, the aging of the electrode was much slower than in 1.0 M sodium hydroxide, many hours being required before a two-wave chronopotentiogram was observed. It was again found that the total transition time remained constant as the electrode aged. Cathodization also tended to activate the electrode. The first transition time of curve 5 in Fig. 4 is considerably greater than in curve 4 although the electrode was not pre-treated between these trials. Additional cathodizations continued to increase the enhancement of the first transition time although the activity manifested in curves 2 or 3 of Fig. 4 was never attained. In 1.0 M sodium hydroxide, too, cathodizations tend to reactivate the electrode though the effect is not so large as it is in 0.10 M sodium hydroxide.

The dependence of transition time on current density was also studied for oxygen reduction in 0.10 M sodium hydroxide and it was found that the observed values of $i(\tau_1 + \tau_2)^{1/2}/AC^\circ$ agreed to within 1% of the theoretical values for transition times between 0.4 and 25 sec. The theoretical values were calculated from eqn. (1) assuming $n = 4$. The diffusion coefficient used ($2.16 \cdot 10^{-5}$ cm^2/sec) was the value for 1.0 M sodium hydroxide corrected for the difference in viscosities between 1.0 and 0.10 M sodium hydroxide by means of the STOKES–EINSTEIN equation[13]. The solubility of oxygen in 0.10 M sodium hydroxide is $1.23 \cdot 10^{-3}$ M [11]. The good agreement between experiment and theory again demonstrates that the overall electrochemical reaction is the diffusion-controlled 4-electron reduction to hydroxide ion.

The aging effect

It was found that the rate of aging observed with solutions that had been stored prior to use was much greater than with freshly prepared solutions. For example, the

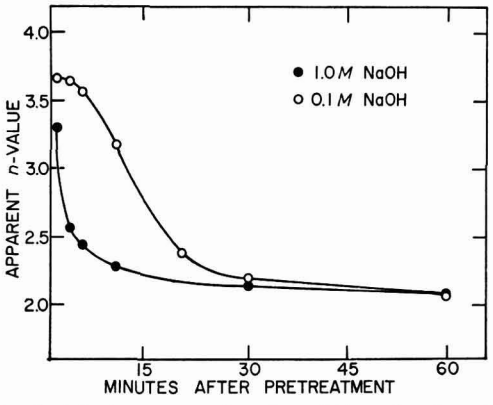

Fig. 5. "Apparent n-value" of first wave as a function of time elapsing after pre-treatment. Data taken from Tables 4 and 5.

data in Tables 4 and 5 were obtained with solutions that had been stored in polyethylene bottles for two weeks. The "apparent n-values" were calculated from eqn. (1) from the observed or known values of τ_1, i, A, C°, D and r_o. In Fig. 5 these "apparent n-values" are presented as a function of time elapsing after electrode pre-treatment. It can be seen that the first transition time corresponds to the 2-electron reduction after an hour has elapsed since pre-treatment. The "apparent n-value" never becomes less than two but approaches two as a limit. With freshly prepared solutions (see Figs. 1 and 4) the aging is much slower, but finally just as complete if sufficient time is allowed to pass. With aged electrodes there can be no doubt that the two waves of the chronopotentiogram correspond to the step-wise reduction of oxygen first to hydrogen peroxide and then to hydroxide ion.

The *aging* effect is due to a decrease in the rate of disproportionation of hydrogen peroxide as the electrode is allowed to stand in contact with the test solution. Accord-

TABLE 4

FIRST TRANSITION TIME; AGING EFFECT IN 1 M SODIUM HYDROXIDE

Transition times measured by the photographic method at various times after electrode pre-treatment. Temp. = 25.00 ± 0.05°. Area of electrode = 0.477 cm². Electrode radius = 0.0255 cm. Concn. of oxygen = $8.43 \cdot 10^{-4}$ M. Theoretical values of $i\tau_1^{1/2}/AC^\circ$ calculated from eqn. (1) with $n = 2$. Soln. stored in polyethylene bottle. $i_{obs.} = 312.3$ μA. $i_{corr.} = i_{obs.} - 21/\tau_1$ (see text)

Time after pretreatment (min)	τ_1 *(sec)*	$i_{corr.}$ *(μA)*	$i\tau_1^{1/2}/AC^\circ$ *(A sec$^{1/2}$ cm/mole)*		*"Apparent n-value"*
			corr.	*theor.*	
1	3.10	305.5	1338	814	3.29
3	1.83	300.8	1012	793	2.56
5	1.68	299.8	966	790	2.45
10	1.47	298.0	898	787	2.28
30	1.30	296.2	840	783	2.14
60	1.22	295.1	811	781	2.08
180	1.21	294.9	807	780	2.07

TABLE 5

FIRST TRANSITION TIME; AGING EFFECT IN 0.10 M SODIUM HYDROXIDE

Transition times measured by the photographic method at various times after electrode pre-treatment. Temp. = 25.00 ± 0.05°. Area of electrode = 0.477 cm². Electrode radius = 0.0255 cm. Concn. of oxygen = $1.23 \cdot 10^{-3}$ M. Theoretical values of $i\tau_1^{1/2}/AC^\circ$ calculated from eqn. (1) with $n = 2$. Soln. stored in polyethylene bottle. $i_{obs.} = 556.3$ μA. $i_{corr.} = i_{obs.} - 17/\tau_1$ (see text)

Time after pre-treatment (min)	τ_1 *(sec)*	$i_{corr.}$ *(μA)*	$i\tau_1^{1/2}/AC^\circ$ *(A sec$^{1/2}$ cm/mole)*		*"Apparent n-value"*
			corr.	*theor.*	
1	3.10	550.8	1653	904	3.66
3	3.08	550.8	1648	904	3.65
5	2.91	550.5	1601	901	3.56
10	2.25	548.7	1403	884	3.18
20	1.23	542.5	1025	864	2.38
30	1.06	540.3	948	859	2.21
60	0.92	537.8	879	854	2.06

ing to the theory developed by BLACKBURN AND LINGANE[3], the catalytic agent for the disproportionation is finely divided metal on the electrode surface which is formed when the oxide film is cathodically reduced during the pre-treatment process. The *aging* effect is attributed to the oxidation of the finely divided metal by dissolved oxygen followed by the dissolution of the metal oxide thus formed. The electrode can be reactivated by anodizing it to form an oxide film and cathodically reducing the oxide to form a layer of finely divided metal.

An alternative explanation is that the *aging* effect is due to the accumulation of impurities on the electrode surface either by adsorption or chemical interaction. These materials render the surface inactive toward the disproportionation of hydrogen peroxide. The activation of the electrode by an anodic-cathodic pre-treatment is due to the removal of impurities by the anodization and cathodization processes.

The fact that the rate of aging with solutions which had been stored for some time, was much greater than when freshly prepared solutions were used, favors the latter interpretation. Additional impurities could have dissolved in the solutions from the walls of the storage containers. In addition the rate of aging in freshly prepared 0.10 *M* sodium hydroxide was much slower than in freshly prepared 1.0 *M* sodium hydroxide. Impurities whose origin is in the sodium hydroxide would be at a 10-fold lower level in the former.

It was also found that the activity of an aged electrode could be restored by procedures which do not form freshly deposited gold on the surface. In one experiment the first transition time in 1.0 *M* sodium hydroxide decreased from 5.52 sec two minutes after pre-treatment to 3.24 sec thirty minutes later. The electrode was again pre-treated and allowed to stand in contact with the solution for 30 min. It was then removed, washed in 1 *M* hydrochloric acid and water, returned to the cell, and a chronopotentiogram was recorded. The first transition time was 4.53 sec instead of the 3.24 sec observed previously *i.e.*, the rinsing process partially reactivated the electrode. Furthermore, when a gold oxide film is removed by dissolving in 1 *M* hydrochloric acid, an activated electrode is obtained. An electrode aged in 1.0 *M* sodium hydroxide was anodized to oxygen evolution. The electrode was removed and exposed to the hydrochloric acid stripping solution for 2 min, a procedure which is known to remove the oxide film quantitatively[14]. When the electrode was returned to the cell and a chronopotentiogram was recorded, the first transition time was as large as it was immediately after an anodic-cathodic pre-treatment. In other words, freshly deposited gold is not a necessary condition for an activated electrode.

It was also found that the presence of a large quantity of finely divided gold was not sufficient in itself to cause the electrode to be active. The same electrode used for the chronopotentiograms in Fig. 1 was cathodically polarized at 8.3 mA/cm^2 for 100 sec in a solution $1.6 \cdot 10^{-2}$ *M* in gold chloride and 2 *M* in nitric acid. The electrode became dark brown in color. The electrode was rinsed and soaked in water for 20 min. It was then placed in oxygen-saturated 1.0 *M* sodium hydroxide and curve 1, Fig. 6, was recorded. The enhancement of the first transition time is about the same as it is after a single anodic-cathodic pre-treatment (see curve 2, Fig. 1) The electrode was then anodized to oxygen evolution and then curve 2, Fig. 6, was recorded showing a rather extended wave for the reduction of the oxide film and two waves for oxygen reduction the first of which is greatly enhanced. Curve 3 was recorded 3 min after curve 2. This chronopotentiogram shows that the pre-treatment has generated a very

active electrode. However, even when a large quantity of freshly deposited finely divided gold is on the surface, an anodic-cathodic pre-treatment is necessary to realize the full catalytic power of the surface.

On the other hand, the addition of surface active materials to the solution produced results which support the freshly deposited metal theory. Substances which might be expected to be strongly adsorbed on the gold surface and thus decrease the rate of disproportionation of hydrogen peroxide had no effect on the relative enhancement of the first transition time. These included *n*-amyl alcohol (1%), methyl red (0.001%)

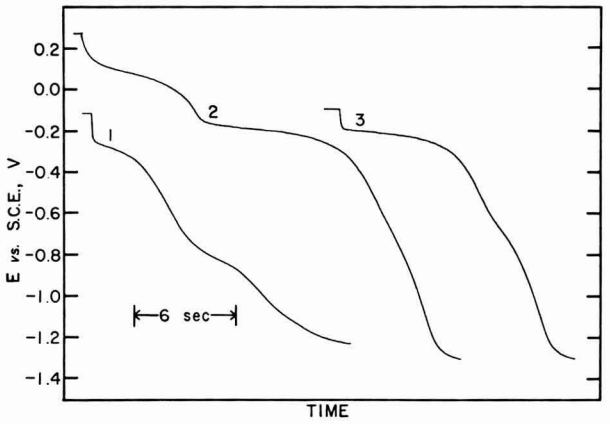

Fig. 6. Oxygen reduction chronopotentiograms with an electrode covered by a layer of finely divided gold. 1.0 *M* NaOH saturated with oxygen at 1 atm. and 25.00°. Gold wire electrode (0.168 cm^2) cathodized 100 sec at 8.3 mA/cm^2 in $1.6 \cdot 10^{-2}$ *M* gold chloride in 2 *M* HNO_3; electrode was dark brown in color. Curve 1, cathodization. Curve 2, cathodization after electrode was anodized to oxygen evolution. Magnitude of oxide reduction wave is larger than curve 1, Fig. 1, since real surface area has increased. Curve 3, 3 min after curve 2. $i = 87.14\ \mu A$.

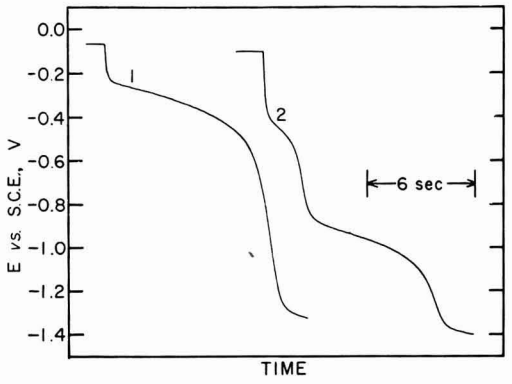

Fig. 7. Effect of cyanide ion on the enhancement of the first transition time. 0.10 *M* NaOH saturated with oxygen at 1 atm. and 25.00°. Curve 1, cathodization 3 min after electrode pre-treatment. Curve 2, cathodization 3 min after pre-treatment except solution made 10^{-5} *M* in NaCN (added after pre-treatment). Area of electrode = 0.168 cm^2, $i = 134.3\ \mu A$.

and Triton X-100 (Rohm and Haas Co.) detergent (3%). However, materials which could aid in the dissolution of freshly deposited gold *via* oxidation by dissolved oxygen and complexation had a profound effect on the first transition time. As little as $10^{-7}M$ sodium cyanide or sodium iodide, in 0.10 M sodium hydroxide caused the normal single wave (curve 2, Fig. 4) to split into two waves. Higher concentrations caused the two waves to assume the correct ratio for the step-wise reduction of oxygen. This is shown in Fig. 7. Curve 1 is the normal oxygen chronopotentiogram in 0.10 M sodium hydroxide 3 min after pre-treatment. Curve 2 was recorded under conditions identical to those in curve 1 except that immediately after the pre-treatment the solution was made 10^{-5} M in sodium cyanide. The "apparent n-value" for the first transition time in curve 2 is 2.09, demonstrating that the presence of sodium cyanide completely removes the catalytic activity of the electrode.

Identification of hydrogen peroxide as intermediate

In addition to the evidence presented that the "apparent n-value" for the first transition time at an aged electrode is 2, it was also found that when hydrogen peroxide was added to an oxygen-saturated 1.0 M sodium hydroxide solution, the second wave of the oxygen chronopotentiogram was lengthened to an extent directly dependent upon the hydrogen peroxide concentration. This demonstrates that the intermediate formed in the reduction of oxygen is reduced at the same potential as hydrogen peroxide.

Further evidence that hydrogen peroxide is the first stable product in oxygen reduction at gold electrodes in alkaline media, and that this hydrogen peroxide is partially consumed by disproportionation, is provided by current-reversal chronopotentiometry. If the product of an electrochemical reduction can be reoxidized at the electrode in question, it will show a discrete chronopotentiometric wave if the polarity of the working electrode is reversed sometime prior to the first transition time. The rela-

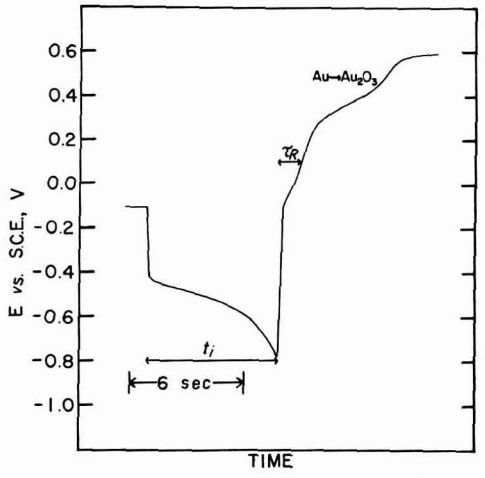

Fig. 8. Oxygen reduction chronopotentiogram with current reversal. 1.0 M NaOH saturated with oxygen at 1 atm. and 25.00°, i = 55.37 μA. Cathodization time (t_1) = 6.96 sec. Time from current reversal to first anodic transition time, τ_R = 1.29 sec. Second anodic wave is due to oxide film formation. Electrode area = 0.168 cm².

tionship between the electrolysis time before current reversal and the reverse transition time for cylindrical diffusion has been derived by MURRAY AND REILLEY[15].

A typical current-reversal chronopotentiogram for oxygen at a partially aged electrode in 1.0 *M* sodium hydroxide is shown in Fig. 8. The cathodic branch of the chronopotentiogram (t_1) lasted 6.96 sec and then the current was reversed. The first oxidation wave occurs at the same potential as the wave for hydrogen peroxide oxidation in the same medium[14]. The second oxidation wave is due to the formation of a gold oxide film on the electrode. The observed reverse transition time for hydrogen peroxide oxidation was 1.29 sec compared to 1.92 sec calculated from the MURRAY AND REILLEY relation with the diffusion coefficient of hydrogen peroxide set equal to $1.00 \cdot 10^{-5}$ cm^2/sec[14]. In other words, an appreciable fraction of the hydrogen peroxide formed in the cathodic electrolysis had disproportionated and could not contribute to the anodic current between t_1 and $t_1 + \tau_R$, causing τ_R to be shorter than the theoretically predicted value.

With a freshly pre-treated electrode only a very short reverse-current chronopotentiometric wave for hydrogen peroxide oxidation can be detected since most of the hydrogen peroxide has decomposed. However, in the presence of 10^{-5} *M* sodium cyanide the reverse transition time is within 4% of the theoretical value since the sodium cyanide removes the catalytic activity of the electrode surface (see above).

OXYGEN REDUCTION IN SULFURIC ACID SOLUTIONS

Typical chronopotentiograms for oxygen reduction in 1 *M* sulfuric acid are shown in Fig. 9. Curve 1 was recorded after an oxide film had been formed by a previous anodization. The first wave represents the reduction of the gold oxide film and the second beginning at *ca.* 0.0 V *vs.* S.C.E. is due to the reduction of oxygen. The other curves in

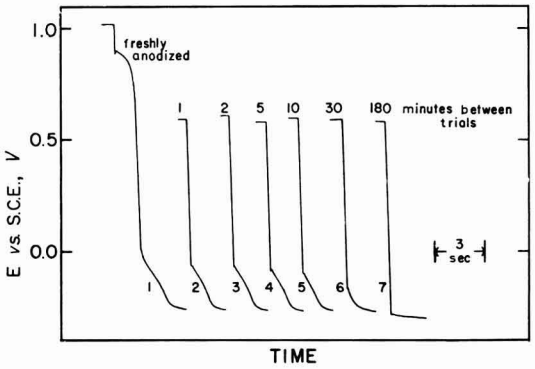

Fig. 9. Typical oxygen reduction chronopotentiograms in 1 *M* H_2SO_4. $i = 134.3\,\mu A$, electrode area $= 0.168\ cm^2$.

Fig. 9 were recorded at various intervals of time after curve 1. As the electrode is allowed to stand in contact with the test solution, the oxygen reduction wave becomes shorter and the over-potential for the process increases until in curve 7 no chronopotentiometric wave at all is observed. The "apparent *n*-value" calculated from eqn. (1) is 1.92 in curve 2. The solubility of oxygen is $1.05 \cdot 10^{-3}$ *M* [11] and its diffusion

coefficient is $2.02 \cdot 10^{-5}$ cm^2/sec^2. If the electrode is repeatedly anodized and cathodized, the transition time becomes longer and the potential at which the wave occurs becomes more oxidizing. The transition time can then correspond to an "apparent n-value" as large as 2.5.

The effect of current density on the transition time was also studied. The electrode had been anodized and cathodized several times after the curves in Fig. 9 were recorded and it was thus in a more active condition. To achieve reproducible results the electrode was pre-treated 3 min before each trial. The data are presented in Table 6. No attempt was made to correct the data for the simultaneous occurrence of processes other than the reduction of oxygen. The theoretical values of $i\tau_1^{1/2}/AC^\circ$ were calculated from eqn. (1) assuming $n = 2$. The data of Table 6 are also presented in Fig. 10. The solid curve is the theoretical $n = 2$ curve. The transition times are obviously too great for a simple 2-electron process. We conclude that the disproportionation of hydrogen peroxide, though slower in acid media, causes the first transition time to be greater than the $n = 2$ value. In sulfuric acid two processes are responsible for the

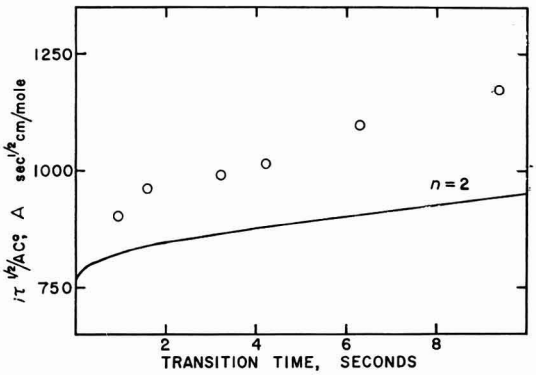

Fig. 10. $i\tau^{1/2}/AC^\circ$ as a function of transition time for oxygen reduction in 1 M H_2SO_4. Open circles, data from Table 6; solid curve is theoretical curve for 2-electron process.

TABLE 6

CHRONOPOTENTIOMETRY OF OXYGEN AT A GOLD CATHODE IN 1 M SULFURIC ACID

Transition times measured by the manual method 3 min after electrode pre-treatment. Transition potential = −0.10 V *vs.* S.C.E. Times given are averages of two trials. Average deviation given in parentheses. Temp. = 25.00 ± 0.05°. Theoretical values of $i\tau^{1/2}/AC^\circ$ calculated from eqn. (1) and assumption that $n = 2$.

i (μA)	τ (sec)	$i\tau^{1/2}/AC^\circ$ (A sec$^{1/2}$ cm/mole)	
		obs.	theor.
164.1	0.94 (±0.02)	902	825
134.3	1.60 (±0.02)	963	843
97.44	3.22 (±0.04)	991	873
87.14	4.23 (±0.08)	1016	888
77.25	6.30 (±0.12)	1099	913
67.54	9.38 (±0.06)	1173	945

decay of the wave: (i) as the electrode ages its catalytic activity toward the disproportionation of hydrogen peroxide decreases and the "apparent n-value" approaches two, and (ii) simultaneously the over-potential for oxygen reduction increases causing the wave to merge into the final potential halt until it completely disappears. It is this second process which causes the "apparent n-value" to become less than two and finally approach zero in the limit.

OXYGEN REDUCTION IN OTHER MEDIA

Figure 11 summarizes typical chronopotentiograms obtained in nine different media. The current density varies slightly from one solution to another, and the solubility and diffusion coefficient of oxygen undoubtedly vary, so the exact magnitudes of the transition times cannot be quantitatively compared. However, the chronopotentiograms do provide important clues concerning the nature of the oxygen reduction reaction in each solution.

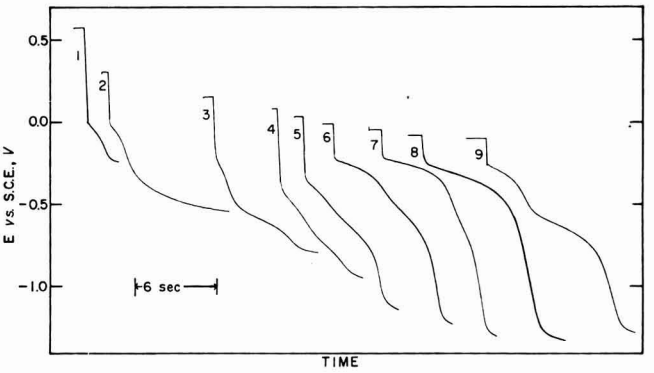

Fig. 11. Chronopotentiograms for oxygen reduction in various media; current density in $\mu A/cm^2$ in parentheses: curve 1, 1 M H_2SO_4 (800); curve 2, phosphate buffer pH = 1.6 (450); curve 3, acetate buffer pH = 4.7 (693); curve 4, phosphate buffer pH = 6.7 (693); curve 5, carbonate buffer (776); curve 6, phosphate buffer pH = 11 (693); curve 7, phosphate buffer pH = 12 (693); curve 8, 0.10 M NaOH with 0.30 M Na_2SO_4 (691); curve 9, 1.0 M NaOH (519); Temp. = 25.00°, ionic strength = 1.0.

Curve 1 was obtained in 1 M sulfuric acid. Curve 2 represents oxygen reduction in phosphate buffer pH = 1.6. No wave is observed with an aged electrode. Before curve 2 was recorded, the electrode was subjected to five anodic-cathodic cycles. Curve 3 was obtained in acetate buffer pH = 4.7 after ten anodic-cathodic cycles. Two distinct waves are observed. The over-potential for each increases as the electrode ages but the waves never disappear entirely. Curve 4 is a typical curve obtained in phosphate buffer pH = 6.7 three minutes after a single anodic-cathodic cycle. Two waves are observed though they are not well differentiated. As the electrode ages the first wave becomes shorter. Curve 5 was obtained in carbonate buffer pH = 9.7 3 min after an anodic-cathodic pre-treatment. Oxygen reduction is obviously a two-step process in this medium also. As the electrode ages the separation between the two waves increases.

Curve 6 (phosphate buffer pH = 11), and curve 7 (phosphate buffer pH = 12), were also recorded 3 min after a single pre-treatment. The chronopotentiograms are very similar to those observed in sodium hydroxide solutions. There are two waves the first of which is too long for a 2-electron reduction. The length of the first wave decreases and the over-potential of each wave increases as the electrode is allowed to stand in contact with the oxygen-saturated solution. The aging does not affect the total transition time. The main difference between curves 6 and 7 is that the relative enhancement is somewhat greater in the latter. Curve 8 is a chronopotentiogram recorded 3 min after pre-treatment in 0.10 *M* sodium hydroxide adjusted to an ionic strength of one with sodium sulfate. Curve 9 was obtained in 1.0 *M* sodium hydroxide 3 min after pre-treatment. Note that the relative enhancement of the first transition time is maximal at a hydroxide ion concentration of 0.10 (curve 8) and that it is less at either lower (curves 6 and 7) or higher (curve 9) hydroxide ion concentrations. This is in qualitative agreement with the observation of BREDIG AND REINDERS[16] that the rate of disproportionation of hydrogen peroxide catalyzed by gold sols was greatest at a hydroxide ion concentration between 0.01 and 0.1 *M* and was smaller at either higher or lower concentrations.

It is also interesting to note that in acidic solutions the potential at which the first wave occurs is about 0.4 V more reducing than the reversible oxygen–hydrogen-peroxide potential, $0.440 - 0.059 \times$ pH V *vs.* S.C.E.[17] (curves 1–4, Fig. 11). In alkaline solution, however, the over-potential of the process decreases until at pH > 12 (curves 7–9) the quarter-wave potential of the first wave is equal to the reversible oxygen–hydrogen-peroxide potential. Similar behavior has been observed with the oxygen–hydrogen peroxide system at the dropping mercury electrode[18] where the system is essentially reversible above pH = 10.

This survey of the chronopotentiometric reduction of oxygen at gold cathodes provides several general conclusions: (i) in all solutions studied the first wave in the chronopotentiogram corresponds to the reduction of oxygen to hydrogen peroxide; (ii) in all but the most acidic solutions the hydrogen peroxide is further reduced in a second wave; (iii) it is generally more difficult to obtain a well-developed chronopotentiogram in acidic solutions, often repeated anodizations and cathodizations are required; (iv) in most solutions the first transition time at a pre-treated electrode is too long for the simple 2-electron reduction of oxygen — this is due to the regeneration of oxygen *via* the disproportionation of hydrogen peroxide; (v) if the electrode is allowed to stand in contact with the oxygen-saturated solution, two *aging* phenomena are observed — the length of the first transition time decreases and the overpotential for the process increases — in the two most acidic solutions, where the wave is very close to the hydrogen evolution potential, the increase in overpotential eventually causes the wave to disappear completely.

ACKNOWLEDGEMENT

Appreciation is expressed to the National Institutes of Health and the Danforth Foundation for fellowship support of one of us (D.H.E.).

SUMMARY

Oxygen reduction at gold cathodes was studied chronopotentiometrically. In sodium hydroxide solutions two waves are observed. The first of these, due to the reduction of

oxygen to hydrogen peroxide, is longer than the 2-electron value due to the surface-catalyzed disproportionation of hydrogen peroxide which regenerates more oxygen. This effect is most pronounced at an electrode which has been recently anodized and cathodized (pre-treated). The effect diminishes as the electrode is allowed to stand in contact with the test solution. The total transition time for the two waves is unaffected by electrode treatment. In sulfuric acid a single wave due to the 2-electron reduction is observed at a pre-treated electrode. In other media of pH between 1.6 and 12, two oxygen reduction waves are observed.

REFERENCES

1 T. BERZINS AND P. DELAHAY, *J. Am. Chem. Soc.*, 75 (1953) 4205.
2 J. J. LINGANE, *J. Electroanal. Chem.*, 2 (1961) 296.
3 T. R. BLACKBURN AND J. J. LINGANE, *ibid.*, 5 (1963) 216.
4 I. M. KOLTHOFF AND J. JORDAN, *J. Am. Chem. Soc.*, 74 (1952) 4801.
5 D. T. SAWYER AND L. V. INTERRANTE, *J. Electroanal. Chem.*, 2 (1961) 310.
6 K. I. ROZENTAL' AND V. I. VELOVSKII, *Zh. Fiz. Khim.*, 35 (1961) 2481.
7 J. J. LINGANE, *J. Electroanal. Chem.*, 1 (1960) 379.
8 D. G. PETERS AND J. J. LINGANE, *ibid.*, 2 (1961) 1.
9 J. J. LINGANE, *ibid.*, 2 (1961) 46.
10 D. H. EVANS AND J. E. PRICE, *ibid.*, 5 (1963) 77.
11 A. SEIDELL, *Solubilities of Inorganic and Metal Organic Compounds*, Vol. 1, Van Nostrand Co., Inc., New York, 1940, 3rd ed., p. 1355.
12 M. G. EVANS AND N. URI, *Trans. Faraday Soc.*, 45 (1949) 224.
13 I. M. KOLTHOFF AND J. J. LINGANE, *Polarography*, Vol. 1, Interscience Publishers, Inc., New York, 2nd ed., 1952, p. 57.
14 D. H. EVANS, unpublished data.
15 R. W. MURRAY AND C. N. REILLEY, *J. Electroanal. Chem.*, 3 (1962) 182.
16 G. BREDIG AND W. REINDERS, *Z. Physik. Chem.* (Leipzig), 37 (1901) 323.
17 W. M. LATIMER, *Oxidation Potentials*, Prentice-Hall, Inc., Englewood Cliffs, N.J., 2nd ed., 1952, p. 43.
18 D. M. H. KERN, *J. Am. Chem. Soc.*, 76 (1954) 4208.

THE EFFECT OF ELECTRICAL MIGRATION ON THE CHRONOPOTENTIOMETRIC TRANSITION TIME

MICHAEL D. MORRIS AND JAMES J. LINGANE

Department of Chemistry, Harvard University, Cambridge 38, Mass. (U.S.A.)

(Received July 1st, 1963)

Chronopotentiometry has received considerable attention in recent years because of its promise as an analytical technique and its usefulness in the study of electrode processes. Although much attention has been paid to the effect of such factors as electrode material, electrode geometry and the influence of kinetic factors on the chronopotentiometric wave, the study of the effects of electrical migration has been neglected. We have investigated the influence of electrical migration on the transition time in plane electrode chronopotentiometry, derived equations describing the effect of electrical migration on the transition time, and obtained experimental evidence in support of these equations.

There has been little previous work on the effect of electrical migration on the chronopotentiometric transition time. SAND[1] first noted that for the reduction of cupric ion, the transition time is enhanced in the absence of supporting electrolyte. He assumed that in the absence of supporting electrolyte, the flux, f, in moles/cm^2/sec of the cation *at the electrode surface* is given by

$$f = \frac{i(1 - T_1)}{n_1 A F} \tag{1}$$

where i is the current (amp), T_1 is the transference number of the reducible cation, n_1 is the number of electrons in the electrode reaction, A is the electrode area (cm^2), and F is the Faraday constant (C/equiv.). Equation (1) rests on the assumption that the solution is homogeneous throughout and that the ohmic potential gradient causing migration is constant and given by the derivative with respect to distance of the product of the constant current and the solution resistance. SAND also used Fick's second law as the expression for the time rate of change of depolarizer concentration. These assumptions lead to the following expression for the chronopotentiometric constant in the absence of supporting electrolyte:

$$\frac{i(\tau)^{1/2}}{AC_1} = \frac{n_1(\pi)^{1/2} F D^{1/2}}{2(1 - T_1)} \tag{2}$$

where τ is the transition time (sec), C_1 is the bulk concentration of the reducible ion (moles/cm^3), and D its diffusion coefficient (cm^2/sec).

If D is taken to be the diffusion coefficient of the salt (to be defined below), rather than the diffusion coefficient of the reducible ion, eqn. (2) is valid despite the fact that it rests on erroneous assumptions. In particular, the solution is not homogenous, but is less concentrated in the diffusion layer than further away from the electrode. The potential gradient is not constant in the diffusion layer, but increases with decreasing distance from the electrode. Furthermore, Fick's second law must be modified to include the effect of the potential gradient (see eqn. (6), below).

Equation (2) may be derived without recourse to the approximations used by SAND. It is necessary, however, to assume ideal ionic behavior, in order that the diffusion coefficient and equivalent conductance of an ion may be simply related. That is, the following eqn. (3) must be assumed to hold in the concentration region of interest, although it is strictly valid only at infinite dilution[2]:

$$D_i = \frac{RT\lambda_i}{|z_i| F^2} \tag{3}$$

where λ_i is the equivalent conductance of the i_{th} ion ($\Omega^{-1}\text{cm}^2$), z_i is the charge on the i_{th} ion, including sign ($z = -1$ for Cl^-), and R and T are the gas constant and absolute temperature, respectively.

We shall use the subscript (1) denote the reducible cation and the subscript (3) to denote its counter-ion. A supporting electrolyte having the same anion will be assigned subscripts (2) and (3). It is assumed that the cation is reduced to an uncharged species. The x co-ordinate is taken to be possitive away from the electrode surface.

The fluxes f_1 and f_3 of the cation and anion in the presence of diffusive and migrational forces are given by:

$$f_1 = D_1\left(\frac{\partial C_1}{\partial x} + z_1 C_1 \frac{F}{RT}\frac{\partial \phi}{\partial x}\right) \tag{4}$$

$$f_3 = D_3\left(\frac{\partial C_3}{\partial x} + z_3 C_3 \frac{F}{RT}\frac{\partial \phi}{\partial x}\right) \tag{5}$$

where $\partial\phi/\partial x$ is the potential gradient to which the ions are subjected. The time rate of change of each ion concentration is given by:

$$\frac{\partial C_1}{\partial t} = D_1\left(\frac{\partial^2 C_1}{\partial x^2} + z_1 \frac{F}{RT}\frac{\partial C_1}{\partial x}\frac{\partial \phi}{\partial x} + z_1 C_1 \frac{F}{RT}\frac{\partial^2 \phi}{\partial x^2}\right) \tag{6}$$

$$\frac{\partial C_3}{\partial t} = D_3\left(\frac{\partial^2 C_3}{\partial x^2} + z_3 \frac{F}{RT}\frac{\partial C_3}{\partial x}\frac{\partial \phi}{\partial x} + z_3 C_3 \frac{F}{RT}\frac{\partial^2 \phi}{\partial x^2}\right) \tag{7}$$

Equations (4)–(7) are extensions of Fick's first and second laws to include the effect of electrical migration. For fundamental derivations of these equations the reader is referred to a recent paper by KIES[3] and to the monograph of KOLTHOFF AND LINGANE[2].

Since electro-neutrality must obtain throughout the solution (ignoring the region of the electrical double-layer), for a single electrolyte

$$z_1 C_1 = -z_3 C_3 \tag{8}$$

The electro-neutrality relationship may be used to transform eqn. (7) into an expression in C_1.

$$-\frac{\partial C_3}{\partial t} = \frac{z_1}{z_3}\frac{\partial C_1}{\partial t} = D_3\left[\frac{z_1}{z_3}\frac{\partial^2 C_1}{\partial x^2} + z_1\frac{F}{RT}\frac{\partial C_1}{\partial x}\frac{\partial \phi}{\partial x} + z_1 C_1\frac{F}{RT}\frac{\partial^2 \phi}{\partial x^2}\right] \tag{9}$$

The potential gradient terms may be eliminated by multiplying eqn. (9) by D_1 and subtracting the product from eqn. (6) multiplied by D_3.

$$\left(D_3 - D_1\frac{z_1}{z_3}\right)\frac{\partial C_1}{\partial t} = D_1 D_3\left(1 - \frac{z_1}{z_3}\right)\frac{\partial^2 C_1}{\partial x^2} \tag{10}$$

Rearrangement of terms in eqn. (10) yields eqn. (11).

$$\frac{\partial C_1}{\partial t} = \left[\frac{D_1 D_3(z_1 - z_3)}{z_1 D_1 - z_3 D_3}\right]\frac{\partial^2 C_1}{\partial x^2} \tag{11}$$

The diffusion coefficient of a salt, D_s, is defined by eqn. (12).

$$D_s = \frac{D_1 D_3(z_1 - z_3)}{z_1 D_1 - z_3 D_3} \tag{12}$$

Equation (11) may be written

$$\frac{\partial C_1}{\partial t} = D_s\frac{\partial^2 C_1}{\partial x^2} \tag{13}$$

For chronopotentiometry, the flux of the reducible species at the electrode surface is constant.

$$(f_1)_{x=0} = \frac{i}{n_1 FA} = D_1\left[\frac{\partial C_1}{\partial x} + z_1 C_1\frac{F}{RT}\frac{\partial \phi}{\partial x}\right]_{x=0} \tag{14}$$

Since the anion is not consumed at the electrode surface, its flux there is zero. From this fact and eqn. (5) we obtain

$$\left(\frac{\partial C_3}{\partial x}\right)_{x=0} = -z_3 C_3\frac{F}{RT}\left(\frac{\partial \phi}{\partial x}\right)_{x=0} \tag{15}$$

The electro-neutrality relation may be introduced into eqn. (15) to obtain an expression in C_1.

$$\left(\frac{\partial C_3}{\partial x}\right)_{x=0} = -\frac{z_1}{z_3}\left(\frac{\partial C_1}{\partial x}\right)_{x=0} = z_1 C_1\frac{F}{RT}\left(\frac{\partial \phi}{\partial x}\right)_{x=0} \tag{16}$$

Equations (14) and (16) may be combined to eliminate the potential gradient terms.

$$\frac{i}{n_1 FA} = D_1\left[\frac{\partial C_1}{\partial x} - \frac{z_1}{z_3}\frac{\partial C_1}{\partial x}\right]_{x=0} \tag{17}$$

$$\frac{i}{n_1 FA} = D_1\left(1 - \frac{z_1}{z_3}\right)\left(\frac{\partial C_1}{\partial x}\right)_{x=0} \tag{18}$$

The other chronopotentiometric conditions are, that for C_1, the initial bulk concentration of the reducible cation

$$C_1(x,t) = C_1, \text{ for all } x, \text{ when } t = 0 \tag{19}$$

$$C_1(x,t) = C_1, \; x \to \infty, \text{ for all } t \tag{20}$$

The solution of a system of equations of this form has been given by SAND[1]. It is

$$C_1(x,t) = C_1 - \frac{iD_s^{1/2}}{An_1\pi^{1/2}FD_1\left(1 - \frac{z_1}{z_3}\right)}\int_0^t \frac{1}{t^{1/2}} \exp\left(-\frac{x^2}{4D_s t}\right)dt \tag{21}$$

At the electrode surface, $x = 0$ and

$$C_1(0,t) = C_1 - \frac{2iD_s^{1/2}t^{1/2}}{An_1\pi^{1/2}FD_1\left(1 - \frac{z_1}{z_3}\right)} \tag{22}$$

Or

$$C_1(0,t) = C_1 - \frac{2iD_s t^{1/2}}{An_1\pi^{1/2}FD_1 D_s^{1/2}\left(1 - \frac{z_1}{z_3}\right)} \tag{23}$$

Writing D_s in the numerator of the fraction according to eqn. (12) we obtain

$$C_1(0,t) = C_1 - \frac{2it^{1/2}}{An_1\pi^{1/2}FD_s^{1/2}}\left[\frac{-z_3D_3}{z_1D_1 - z_3D_3}\right] \tag{24}$$

From eqn. (3) and from the definition of the transference number, given by eqn. (25)

$$T_3 = \frac{\lambda_3}{\lambda_1 + \lambda_3} = 1 - T_1 \tag{25}$$

we find

$$C_1(0,t) = C_1 - \frac{2it^{1/2}(1 - T_1)}{n_1A\pi^{1/2}FD_s^{1/2}} \tag{26}$$

But at $t = \tau$ (the transition time), $C_1(0,\tau) = 0$ and eqn. (27) is obtained.

$$\frac{i\tau^{1/2}}{AC_1} = \frac{n_1\pi^{1/2}FD_s^{1/2}}{2(1 - T_1)} \tag{27}$$

Equation (27) is seen to be identical with eqn. (2).

A generalization of the treatment given above to cover any amount of supporting electrolyte would be extremely difficult. The electro-neutrality expression for more than two ions does not allow all ionic concentrations to be expressed as multiples of the concentration of one ion, and it is impossible to eliminate all terms in the concentration of non-reducible ions. An approximate treatment of the polarographic system has been made by OKADA *et al.*[4] for a supporting electrolyte and a reducible electrolyte with a common anion. Their expression was obtained by numerical methods and is extremely cumbersome.

MAMANTOV AND DELAHAY[5] have derived an expression for the transition time for processes controlled partly by diffusion and partly by migration in a constant potential gradient. They assume that mass transfer is controlled primarily by diffusion. Their result is

$$\frac{i\tau^{1/2}}{AC_1} = \frac{n_1\pi^{1/2}FD_1^{1/2}}{2\left(1 - \frac{n_1}{z_1}T_1\right)} - \frac{\left(\frac{i}{A}\tau^{1/2}\right)^2\lambda_1\pi^{1/2}}{4D_1^{1/2}\varkappa F} - \frac{\left(\frac{i}{A}\tau^{1/2}\right)^3\lambda_1^2}{8D_1\varkappa F^2C_1} \tag{28}$$

where $\varkappa$ is the specific conductance of the solution in $\Omega^{-1}\text{cm}^{-1}$ The second and third terms of the right-hand side are negligible in magnitude and the first term is similar to a semi-empirical relation which we shall present below.

A semi-empirical extension of eqn. (29) is easily obtained if one assumes that the form of the equation will remain unchanged in the general case. This seems a reasonable assumption in view of the fact that eqn. (27) is of the same form as the ordinary SAND equation, the limiting case for a large amount of supporting electrolyte, if D_s is replaced by D_1 and $T_1 = 0$. If we limit ourselves to the case where the counter-ion of the reducible species is the same as the anion of the supporting electrolyte, we can generalize the definitions of diffusion coefficient and transference number.

For this case, the transference number of the reducible cation is given by[6]

$$T_1 = \frac{z_1C_1^*\lambda_1}{z_1C_1^*\lambda_1 + z_2C_2^*\lambda_2 - z_3C_3^*\lambda_3} \tag{29}$$

where C_i^* is the concentration of the i_{th} ion in gram-ions/cm^3. The minus sign before z_3 accounts for the fact that z_3 is a negative number. The transference number approaches zero as the amount of supporting electrolyte is made large (C_2, $C_3 \gg C_1$).

To generalize the concept of the diffusion coefficient of a salt we must consider the problem of the electrostatic coupling of ionic flows in the diffusion layer in the presence of small amounts of supporting electrolyte. If one electrolyte is allowed to diffuse *through* another, a concentration gradient of the initially homogeneous electrolyte is built up and then decays as the solution approaches equilibrium. This phenomenon, electrostatic coupling, occurs chiefly because the various ions have different mobilities and all of the ions contribute to the maintainance of electro-neutrality. It is maximal when small amounts of supporting electrolyte are present.

The system in which the common and diffusing electrolyte have one ion in common has been treated by GOSTING[7]. He has shown that the ionic diffusion coefficient should be replaced by another diffusion coefficient, D_{11} which is defined by eqn. (30).

$$D_{11} = D_1\left[1 - \frac{z_1^2C_1(D_1 - D_3)}{z_1(z_1D_1 - z_3D_3)C_1 + z_2(z_2D_2 - z_3D_3)C_2}\right] \tag{30}$$

For the system Tl_2SO_4, K_2SO_4 treated in this paper, thallous ion is reduced at the electrode and K_2SO_4 may be regarded as the initially homogeneous electrolyte. Thus $D_1 = D_{Tl^+}$, $D_2 = D_{K^+}$, $D_3 = D_{SO_4^{2-}}$, and D_{11} for Tl^+ is as defined above for particular initial concentrations of Tl_2SO_4 and K_2SO_4. It is to be noted that if C_2, the concentration of the supporting electrolyte, is zero, $D_{11} = D_s$ and if $C_2 \gg C_1$, $D_{11} = D_1$.

If D_s in eqn. (27) is replaced by D_{11} and T_1 is defined by eqn. (29), a good fit of the data to this equation is obtained. With these substitutions, eqn. (27) becomes

$$\frac{i\tau^{1/2}}{AC_1} = \frac{n_1\pi^{1/2}D_{11}^{1/2}F}{2(1 - T_1)} \tag{31}$$

Equations (27) and (31) have been used to evaluate chronopotentiometric data for the reduction of thallous and cupric ions in the presence of various amounts of supporting electrolyte.

Because the mathematical treatment of diffusion-migration problems is simplified by the elimination of potential gradient terms from the equations under consideration, little attention has been paid to the nature of the potential gradient in these problems. A detailed examination of this gradient is possible for the case where there is no supporting electrolyte, where the mathematical manipulations are simple.

The current in a conductor is the same at any point in the conductor and so may be a function of time but not distance. We may write the current in terms of the flux of each ion for a solution of a single binary electrolyte according to

$$\frac{i_t}{AF} = z_1f_1 + z_3f_3 \tag{32}$$

where i_t is the current as a function of time. The fluxes may be written according to eqns. (4) and (5) to obtain

$$\frac{i_t}{AF} = z_1D_1\left[\frac{\partial C_1}{\partial x} + z_1C_1\frac{F}{RT}\frac{\partial\phi}{\partial x}\right] + z_3D_3\left[\frac{\partial C_3}{\partial x} + z_3C_3\frac{F}{RT}\frac{\partial\phi}{\partial x}\right] \tag{33}$$

Terms in C_3 may be eliminated by the use of the electro-neutrality relation, $z_1C_1 = -z_3C_3$. The resulting equation may be rearranged to give eqn. (24), an exact expression for the potential gradient at any point in the solution.

$$\frac{\partial\phi}{\partial x} = \frac{RT}{F^2}\frac{i_t/A}{z_1C_1(z_1D_1 - z_3D_3)} - \frac{RT}{F}\frac{(D_1 - D_3)}{C_1(z_1D_1 - z_3D_3)}\frac{\partial C_1}{\partial x} \tag{34}$$

The two terms on the right-hand side of eqn. (34) are readily shown to be the contributions from the ohmic potential gradient and the diffusion (liquid junction) potential gradient.

The first term on the right-hand side of eqn. (34), *viz.*,

$$\frac{RT}{F^2}\frac{i_t}{Az_1C_1(z_1D_1 - z_3D_3)} = \frac{i_t}{Az_1C_1(\lambda_1 + \lambda_3)} = \left(\frac{\partial\phi}{\partial x}\right)_{\text{ohmic}} \tag{35}$$

is nothing more than the ohmic potential gradient in an electrolyte solution of molar concentration C_1. This term represents the contribution of the ohmic resistance of the solution to the potential gradient. This ohmic contribution is, of course, a function of distance because the electrolyte concentration itself is a function of distance.

The second term on the right-hand side of eqn. (34) is a form of the expression for the gradient of the liquid junction potential between solutions of the same electrolyte at different concentrations. This point is made clearer if the term is put in the more

familiar integrated form, as has been done in eqn. (37).

$$-\frac{RT}{F}\frac{(D_1 - D_3)}{C_1(z_1 D_1 - z_3 D_3)}\frac{\partial C_1}{\partial x} = \left(\frac{\partial \phi}{\partial x}\right)_{\text{diffusion}} \tag{36}$$

$$\Delta\phi_{\text{diffusion}} = -\frac{RT}{F}\frac{(D_1 - D_3)}{(z_1 D_1 - z_3 D_3)}\Delta \ln C_1 = -\frac{RT}{z_1 F}\left(1 + \frac{(z_1 - z_3)}{z_3}\right)T_3 \Delta \ln C_1 \tag{37}$$

The diffusion potential gradient arises because of the inhomogeneity of the solution. The diffusion potential gradient may enhance or oppose the ohmic potential gradient as D_1 is less than or greater than D_3. It vanishes altogether if $D_1 = D_3$.

Similar arguments can be made about the nature of the potential gradient in a solution containing two or more electrolytes. In these cases the equations are much more involved. Diffusion potential terms, in particular, become rather complicated because of the interdependence of the concentration gradients.

Because the above arguments are not limited to the case of constant current, the description of the potential gradient applies equally well to polarography and other voltammetric techniques in the absence of supporting electrolyte.

EXPERIMENTAL PROCEDURE

Five times recrystallized thallous sulfate was used as the source of thallous ion. Reagent grade copper sulfate pentahydrate, recrystallized from hot water and stored over a saturated sodium chloride solution was used as the source of cupric ion. All other chemicals were of analytical reagent grade and were used as received.

Distilled water, having a specific conductance of $1.1 \cdot 10^{-6}$ $\Omega^{-1}\text{cm}^{-1}$ or less was used to prepare solutions containing no supporting electrolyte, or containing a supporting electrolyte at a concentration equivalent to or less than that of the reducible substance. All other solutions were prepared with distilled water having a specific conductance of $2.0 \cdot 10^{-6}$ $\Omega^{-1}\text{cm}^{-1}$ or less.

The electrolysis circuit has been described in detail in ref. 8.

The potential change during electrolysis was followed on a Leeds and Northrup # 7664 pH Indicator. The output of this meter was fed into a Sargent model MR recorder, whose full-scale response was one second. The pen-recorder trace was used as permanent record of the chronopotentiogram and as a means of estimating the transition potential.

The transition time was taken as the inflection point of the potential break of the chronopotentiogram. Transition times were measured by interrupting the electrolysis current as the transition potential was reached and noting the elapsed time on a stop clock.

The cell employed (Figs. 1 and 2) was similar in design to that of ROUSE[9]. The body of the cell was constructed from a Pyrex inside-ground 45/50 standard taper joint. The cell top and bottom were machined of Nylon. A copper disc used to back the platinum foil cathode prevented distortion of the foil by the irregular surface of the bolt and insured that the foil pressed uniformly against the edges of the cathode cavity. The cylindrical platinum auxiliary electrode was immersed in the same solution as the cathode. The cell was thermostatted in a water bath maintained at $25.0 \pm 0.1°$.

Stirring and deaeration were accomplished simultaneously by passing two streams of nitrogen through the cell. One stream flushed out the cathode cavity while both agitated and deaerated the liquid.

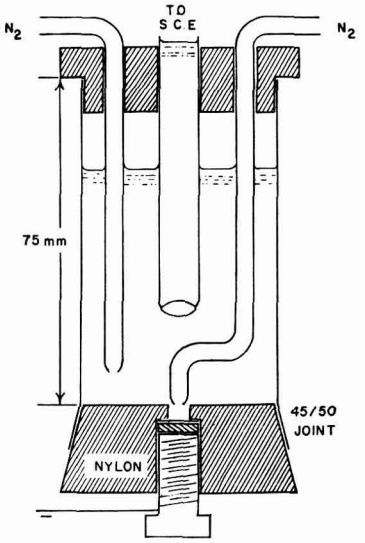

Fig. 1. Chronopotentiometric cell. The auxiliary electrode dips directly into the cathode compartment. For clarity, the auxiliary electrode has been omitted. The top and bottom of the cell are made of Nylon and the bottom is machined to fit a 45/50 standard taper joint.

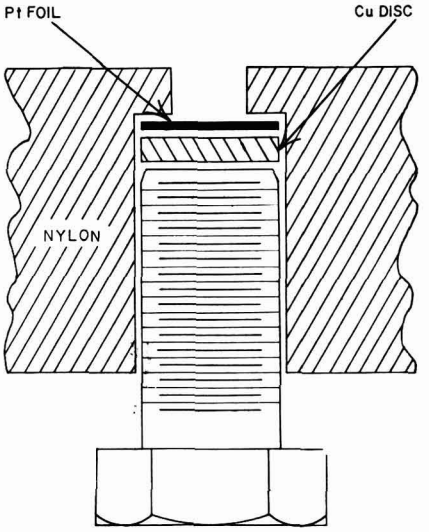

Fig. 2. Detail of chronopotentiometric cell, showing construction of working electrode cavity. The platinum foil cathode is supported by a thick (*ca.* 5 mm) copper disc to prevent mechanical distortion of the foil by the steel bolt. The protruding end of the bolt is painted with Tygon paint to prevent corrosion. Electrical contact is made by a Tygon-covered wire (not shown) soldered to the head of the bolt.

Contact between the working electrode and the reference electrode was made by a high resistance cracked-glass-seal salt bridge filled with 0.1 M potassium chloride. Conductance tests showed that the rate of leakage from the bridge was less than $4 \cdot 10^{-6}$ M potassium chloride/h, the approximate duration of a set of measurements. No precipitates were observed when solutions exposed to this salt bridge for an hour or more were treated with 0.1 M silver nitrate. Furthermore, with all of the solutions, the transition time at a given current density did not depend upon the length of time for which the salt bridge had been immersed. Thus, it is safe to conclude that the use of this potassium chloride-filled salt bridge does not contaminate the solutions.

THE EFFECT OF SUPPORTING ELECTROLYTE ON CATHODIC TRANSITION TIMES

Cupric and thallous ion reductions

The effect of electrical migration on the chronopotentiometric reduction of a cation is to lengthen the transition time for the reduction relative to that which would be observed at the same cation concentration and current density in the presence of excess supporting electrolyte. The product of current density and the square root of transition time remains independent of current density over the range of transition times measured, 3–30 sec. The data in Tables 1, 2 and 3 illustrate this.

TABLE 1

THE EFFECT OF POTASSIUM SULFATE ON THE TRANSITION TIME OF $5.06 \cdot 10^{-3}$ M THALLOUS ION (AS THALLOUS SULFATE)

(area of electrode = 0.201 cm²; temp. = 25.0 ± 0.1°)

i (μA)	τ (sec)	$i\tau^{1/2}/AC$ ($A\ sec^{1/2}\ cm/mole$)
A. No potassium sulfate ($5.01 \cdot 10^{-3}$ M Tl^+), $D_{Tl} = 1.56 \cdot 10^{-5}$ cm²/sec, $T_{Tl^+} = 0.481$.		
133.4 ± 0.2	23.5 ± 0.3	652 ± 10
189.2 ± 0.05	12.6 ± 0.1	669 ± 2
251.6 ± 0.05	6.62 ± 0.01	643 ± 0.5
303.5 ± 1.4	4.61 ± 0.01	648 ± 4
Average = 654 ± 10; theory = 654		
B. $1.25 \cdot 10^{-3}$ M potassium sulfate, $D_{Tl} = 1.70 \cdot 10^{-5}$ cm²/sec, $T_{Tl^+} = 0.323$.		
96.0 ± 0.01	25.6 ± 0.05	479 ± 0.5
123.3 ± 0.01	16.1 ± 0.2	486 ± 1
253.4 ± 0.2	4.12 ± 0.05	506 ± 0.5
Average = 490 ± 11; theory = 520		
C. $2.50 \cdot 10^{-3}$ M potassium sulfate, $D_{Tl} = 1.78 \cdot 10^{-5}$ cm²/sec $T_{Tl^+} = 0.243$.		
86.8 ± 0.05	28.4 ± 0.05	454 ± 1
96.3 ± 0.05	22.9 ± 0.02	453 ± 0.1
135.2 ± 0.1	12.3 ± 0.3	467 ± 1
191.1 ± 0.01	5.96 ± 0.04	459 ± 2
Average = 457 ± 3; theory = 477		
D. 0.250 M potassium sulfate, $D_{Tl} = D_{ion} = 1.79 \cdot 10^{-5}$ cm²/sec; diffusion control.		
75.0	23.8[a]	360
96.1	13.8[a]	352
135.0	7.46[a]	363
191.1 ± 0.01	3.80 ± 0.05	366 ± 0.05
Average 362 ± 5; theory = 362		

[a] Single measurement only.

TABLE 2

THE EFFECT OF THALLOUS ION CONCENTRATION ON THE CATHODIC TRANSITION TIME OF THALLOUS SULFATE IN THE ABSENCE OF SUPPORTING ELECTROLYTE

(area of electrode = 0.201 cm^2; temp. = 25.0 ± 0.1°)

i (μA)	τ (sec)	$i\tau^{1/2}/AC$ ($A\ sec^{1/2}\ cm/mole$)
A. 1.99 · 10^{-3} M thallous ion		
47.0 ± 0.01	32.0 ± 0.1	662 ± 0.5
62.7 ± 0.01	18.5 ± 0.4	674 ± 7
94.8 ± 0.01	7.56 ± 0.06	650 ± 2.5
133.3 ± 0.01	4.01 ± 0.02	666 ± 1
Average 663 ± 7		
B. 5.01 · 10^{-3} M thallous ion, for details see Table 1. Average 654 ± 10		
C. 10.4 · 10^{-3} M thallous ion		
251.4 ± 0.05	31.0 ± 0.5	671 ± 5
304.5 ± 0.2	20.9 ± 0.2	667 ± 3
591.0 ± 0.2	5.60 ± 0.8	670 ± 5
Average 669 ± 4		

TABLE 3

THE EFFECT OF POTASSIUM SULFATE ON THE TRANSITION TIME OF 2.45 · 10^{-3} M CUPRIC ION (AS COPPER SULFATE)

(area of electrode = 0.201 cm^2; temp. = 25.0 ± 0.1°)

i (μA)	τ (sec)	$i\tau^{1/2}/AC$ ($A\ sec^{1/2}\ cm/mole$)
A. No potassium sulfate, D_{11} = 0.865 · 10^{-5} cm^2/sec, $T_{Cu^{2+}}$ = 0.395.		
63.3 ± 0.01	36.1 ± 0.06	777 ± 3
95.5 ± 0.3	15.8 ± 0.05	775 ± 4
123.3 ± 0.2	9.34 ± 0.06	767 ± 2
190.0 ± 0.01	3.99 ± 0.01	779 ± 1
Average 775 ± 5; theory = 832		
B. 1.00 · 10^{-3} M potassium sulfate, D_{11} = 0.810 · 10^{-5} cm^2/sec, $T_{Cu^{2+}}$ = 0.272.		
47.6 ± 0.2	29.1 ± 0.3	523 ± 3
63.5 ± 0.01	16.3 ± 0.05	522 ± 0.05
96.1 ± 0.1	7.17 ± 0.07	524 ± 3
135.3 ± 0.2	3.65 ± 0.05	528 ± 1
Average = 524 ± 2.5; theory = 669		
C. 2.50 · 10^{-3} M potassium sulfate D_{11} = 0.786 · 10^{-3} cm^2/sec, $T_{Cu^{2+}}$ = 0.183.		
47.6 ± 0.01	24.6 ± 0.05	482 ± 0.5
63.6 ± 0.05	14.2 ± 0.05	487 ± 1
96.2 ± 0.01	6.21 ± 0.09	489 ± 4
123.7 ± 0.01	3.73 ± 0.03	486 ± 2
Average = 486 ± 3; theory = 587		
D. 0.200 M potassium sulfate, D_{11} = D_{ion} = 0.72 · 10^{-5} cm^2/sec.		
38.0 ± 0.05	27.2 ± 0.7	445 ± 8
63.6 ± 0.04	10.07 ± 0.27	447 ± 6
96.3 ± 0.05	4.41 ± 0.01	449 ± 2
124.0 ± 0.2	2.73 ± 0.03	453 ± 2
Average = 448 ± 6; theory = 459		

The plot of $i\tau^{1/2}/AC$ as a function of thallous ion transference number for the reduction of $5.06 \cdot 10^{-3}$ M thallous ion (as thallous sulfate) in various potassium sulfate solutions (Fig. 3) shows that eqn. (31) is obeyed very well. The infinite dilution ionic

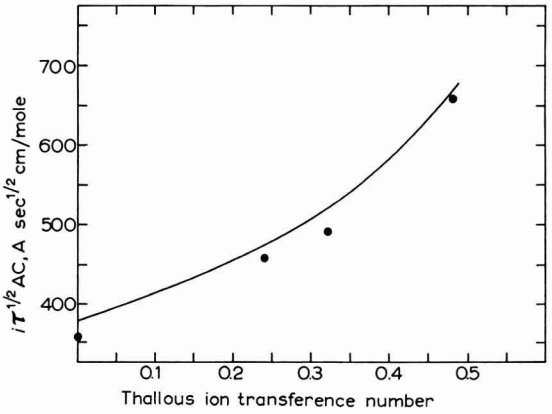

Fig. 3. A plot of $i\tau^{1/2}/AC$ *vs.* thallous ion transference number for the reduction of 5.01×10^{-3} M thallous ion (as Tl_2SO_4) in K_2SO_4 solns.

conductances and diffusion coefficients have been used to calculate transference numbers and thallous ion diffusion coefficients (D_{11}) for comparison with experimental results in this figure.

The chronopotentiometric constant obtained for the diffusion-controlled reduction of thallous ion, 362 A sec$^{1/2}$ cm/mole, is 5% below the value calculated from the infinite dilution diffusion coefficient of thallous ion. This value ($2.00 \cdot 10^{-5}$ cm^2/sec) is probably significantly higher than the actual value at this ionic strength. WANG AND POLESTRA[10] measured the diffusion coefficient of thallous ion in $2–5 \cdot 10^{-3}$ M thallous chloride in solutions containing $5–200 \cdot 10^{-3}$ M potassium chloride. They observed that in the presence of $200 \cdot 10^{-3}$ M potassium chloride the diffusion coefficient of thallous ion is only $1.79 \cdot 10^{-5}$ cm^2/sec. The value of the diffusion coefficient of thallous ion in $250 \cdot 10^{-3}$ M potassium sulfate is probably closer to $1.8 \cdot 10^{-5}$ cm^2/sec than to $2.0 \cdot 10^{-5}$. The use of $1.79 \cdot 10^{-5}$ cm^2/sec in the SAND equation gives a chronopotentiometric constant equal to that found experimentally.

The quantity $i\tau^{1/2}/AC$ for thallous ion reduction in the absence of supporting electrolyte varies only slightly with thallous ion concentration (Table 2). The magnitude of this variation is sufficiently small (about 3% of $i\tau^{1/2}/AC$) to fall within experimental error, and the quantity may be considered to be a constant.

Equations (27) and (31) predict that $i\tau^{1/2}/AC$ should be independent of thallous ion concentration.

Both the diffusion coefficient[11] of thallous sulfate and its cation transference number[12] decrease somewhat with increasing salt concentration, but the changes are small in the concentration ranges used in this study and would tend to compensate one another. Since the published data are insufficient to make a valid extrapolation to the concentration range of interest here, the infinite dilution values are used for comparison with the data. The observed values of $i\tau^{1/2}/AC$ are within 2% of the value calculated from eqn. (27) using infinite dilution parameters.

When intermediate amounts of supporting electrolyte are present, $i\tau^{1/2}/AC$ is found to be about 5–6% below the predicted value. This agreement is very good in view of the empirical nature of eqn. (31).

The enhancement of the transition time for the 2-electron reduction of cupric ion is significantly lower than is predicted by eqn. (31). Experimental results may be compared with theory in Table 3 or Fig. 4. The chronopotentiometric constant for the diffusion-controlled reduction is in good agreement with that calculated from the

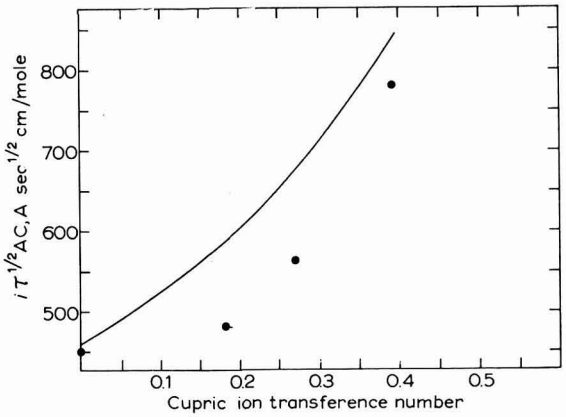

Fig. 4. A plot of $i\tau^{1/2}/AC$ *vs.* cupric ion transference number for the reduction of $2.45 \cdot 10^{-3}$ *M* cupric ion (as $CuSO_4$) in K_2SO_4 solns.

infinite dilution diffusion coefficient for copper. The expected values of $i\tau^{1/2}/AC$ for reduction of copper sulfate in the presence of small amounts of supporting electrolyte were calculated from the infinite dilution parameters. At $2.5 \cdot 10^{-3}$ *M* the transference number of cupric ion in copper sulfate is 0.395 as compared to 0.403 at infinite dilution[13]. The actual value was used. The diffusion coefficient of copper sulfate as a function of concentration is not available, but D_{salt} probably is not very different from its infinite dilution value at the ionic strength used.

The relatively poor agreement, then, is not due to uncertainties in the magnitude of the parameters, but must be ascribed to the approximate nature of our general treatment of migration.

Benzoquinone

If the observed enhancement of cathodic transition times with decreasing amounts of supporting electrolyte is really due to electrical migration, then one would except the transition time for the reduction of a non-polar compound to be unaffected by changes in the amount of supporting electrolyte. To test this prediction, $5 \cdot 10^{-3}$ *M* quinone was reduced chronopotentiometrically in the presence of $5 \cdot 10^{-3}$ *M* potassium chloride and $500 \cdot 10^{-3}$ *M* potassium chloride. The results are presented in Table 4. In both cases $i\tau^{1/2}/AC$ is approximately independent of current density. The value is about the same in both supporting electrolytes. The 3% increase (from 498 A sec$^{1/2}$ cm/mole to 516) with increase in potassium chloride concentration from $5 \cdot 10^{-3}$–$500 \cdot 10^{-3}$ *M*

probably due in part to the small decrease in viscosity (about 2%) of potassium chloride solutions in this concentration range. At any rate, the two values of the chronopotentiometric constant differ by a value only slightly greater than can be accounted for by experimental error and are in good agreement with the value of about 483 A $sec^{1/2}$ cm/mole found by PETERS AND LINGANE[14] on a platinum wire

TABLE 4

THE EFFECT OF POTASSIUM CHLORIDE CONCENTRATION ON THE CATHODIC TRANSITION TIME OF BENZOQUINONE

(area of electrode = 0.201 cm^2; temp. = 25.0 ± 0.1°)

i (μA)	τ (sec)	$i\tau^{1/2}/AC$ ($A\ sec^{1/2}\ cm/mole$)
A. $4.52 \cdot 10^{-3}$ M quinone in $4.98 \cdot 10^{-3}$ M potassium chloride.		
95.2 ± 0.01	21.3 ± 0.1	485 ± 2
133.4 ± 0.01	11.30 ± 0.13	495 ± 3
189.4 ± 0.1	5.91 ± 0.01	507 ± 2
198.7 ± 0.01	5.27 ± 0.01	503 ± 0.5
Average = 498 ± 8; theory = 500 ($D = 0.86 \cdot 10^{-5}$ cm^2/sec)		
B. $4.79 \cdot 10^{-3}$ M quinone in 0.498 M potassium chloride.		
95.4 ± 0.01	26.1 ± 0.05	506 ± 1
108.1 ± 0.01	20.8 ± 0.03	512 ± 0.5
133.7 ± 0.2	13.87 ± 0.01	517 ± 1
189.4 ± 0.01	7.07 ± 0.04	523 ± 2
221.7 ± 0.05	5.24 ± 0.04	526 ± 1
Average = 516 ± 4; theory = 500		

electrode in 1 M sulfuric acid. The small effect of supporting electrolyte concentration on the reduction of quinone supports the contention that the observed dependence of $i\tau^{1/2}/AC$ on supporting electrolyte concentration in the case of the reduction of cations is due to electrical migration. The increase of $i\tau^{1/2}/AC$ with current density may be due to pre-adsorption of quinone. At any rate, it is unaffected by supporting electrolyte concentration, and its presence in no way changes the conclusions about the effect of electrical migration.

ACKNOWLEDGEMENTS

We wish to thank Professor LUCIEN GIERST and Dr. CHARLES RUSSELL for helpful discussions and criticisms. We are indebted to the National Institutes of Health, Division of General Medical Sciences for a fellowship held by one of us (M.D.M.).

SUMMARY

Sand's theory of electro-migration in chronopotentiometry has been re-derived and extended. The theory, although approximate, satisfactorily describes the enhancement of cathodic transition times. The behaviour of thallous sulfate in the presence of little or no supporting electrolyte agrees well with that predicted by the equation $i\tau^{1/2}/AC = (n_1\pi^{1/2}FD_{11}^{1/2}/2(1 - T_1))$. The enhancement of the cupric ion transition time for the reduction of cupric sulfate in the presence of little or no supporting electrolyte is less than predicted by this equation. As expected, the transition time for the reduction of benzoquinone is little affected by the concentration of supporting electrolyte.

REFERENCES

1 H. J. S. SAND, *Phil. Mag.*, 1 (1901) 45.
2 I. M. KOLTHOFF AND J. J. LINGANE, *Polarography*, Interscience Publishers Inc., New York, 2nd ed., 1952.
3 H. L. KIES, *J. Electroanal. Chem.*, 4 (1962) 156.
4 S. OKADA, S. HOSHIZAWA, F. HINE AND K. SADA, *J. Electrochem. Soc. Japan*, 27 (1959) 140.
5 G. MAMANTOV AND P. DELAHAY, *J. Am. Chem. Soc.*, 76 (1954) 5342.
6 S. GLASSTONE, *Textbook of Physical Chemistry*, D. Van Nostrand Co., Inc., New York, 2nd ed., 1946.
7 L. J. GOSTING, in *Advances in Protein Chemistry*, Vol. XI, edited by M. L. ANSON, K. BAILEY AND J. T. EDSALL, Academic Press, Inc., New York, 1956.
8 J. J. LINGANE. *J. Electroanal. Chem.*, 1 (1960) 379.
9 T. O. ROUSE, *An Evaluation of Chronopotentiometry*, Ph.D. Thesis, University of Minnesota, 1961.
10 J. H. WANG AND F. M. POLESTRA, *J. Am. Chem., Soc.* 76 (1954) 1584.
11 J. M. CREETH AND B. E. PETER, *J. Phys. Chem.*, 64 (1960) 1502.
12 *International Critical Tables*, Vol. VI, edited by E. W. WASHBURN, McGraw-Hill Book Company, New York, 1929.
13 J. J. FRITZ AND C. R. FUGET, *J. Phys. Chem.*, 62 (1958) 303.
14 D. G. PETERS AND J. J. LINGANE, *J. Electroanal. Chem.*, 2 (1961) 1.

SOME APPLICATIONS OF ULTRA-VIOLET SPECTROPHOTOMETRY TO STUDIES OF ADSORPTION AT COPPER, NICKEL AND SILVER ELECTRODES

R. G. BARRADAS AND B. E. CONWAY

Department of Chemistry, University of Toronto, Toronto (Canada)
Department of Chemistry, University of Ottawa, Ottawa (Canada)

(Received 23rd June, 1963)

INTRODUCTION

Experimental investigations of electrochemical adsorption at the mercury–solution interface are based on unequivocal thermodynamic foundations and have been reported in the literature over many years. Earlier work was mainly concerned with inorganic additives but lately more active interest has been centred on the quantitative behaviour in organic systems[1–7], *e.g.*, with regard to the nature of the isotherm for adsorption of neutral organic molecules and related conjugate ions and the role of two-dimensional interaction effects[1,2,3,6,7]. Adsorption at solid electrodes has been somewhat neglected despite its greater practical importance in corrosion inhibition and electroplating, and currently available methods suffer from experimental limitations or some lack of thermodynamic rigour[8], *e.g.*, with regard to interpretation of capacity measurements[9] or maintenance of equilibrium at the interface[10]. The adsorption behaviour of organic adsorbates at solid electrodes is of interest in studies of corrosion inhibition[11] and electro-catalytic effects of organic additives[12] and in fuel-cell operation.

An u.v. spectrophotometric technique for the determination of the equilibrium adsorption of organic adsorbates at solid electrodes was first developed by CONWAY, BARRADAS AND ZAWIDZKI[13,14] and applied in an interesting way by NEWMILLER AND PONTIUS[15] to studies of adsorption of photographic developers on silver.

In the present work, we describe further applications of the method and also indicate some of its limitations. In particular we show that the method can be applied to establish the nature of the species, whether ionic or neutral, which adsorbs on the metal surface from solutions of some organic bases to which sufficient acid has been added to ensure, by protonation, the predominant existence of their conjugate ions in the bulk phase. The adsorption of N-methyl quaternised salts of the organic bases has also been examined for comparative purposes.

The thermodynamic functions for adsorption can in some cases be evaluated as a function of coverage to yield data for comparison with the previously published[1,2] adsorption behaviour of similar organic compounds at the mercury–aqueous solution interface.

EXPERIMENTAL

Materials and method

The method and apparatus used, and the technique for purification of the solutions and electrode surfaces were as previously described[13,14]. The method allows specifically the determination of the adsorption of the organic ion (in organic salt solutions), and is thus not complicated by difficulties which arise with more indirect thermodynamic approaches such as the electrocapillary method when protonation acid–base equilibria are involved[1,2,3]. Adsorption isotherms for acridine, quinoline, pyridine, 2,3-benzacridine, 1,2-benzacridine, 3,4-benzacridine, N-methylacridinium chloride and N-methylacridinium methosulphate, were determined on pure nickel, copper and silver (in the form of wire-gauze helices[13] 700 cm^2 in area) from aqueous solutions using conductance water ($\varkappa = 5 \cdot 10^{-7}$ mho cm^{-1}), methanol and acidic aqueous solutions (HCl and $HClO_4$) as solvents. Ultra-purification is unnecessary as shown previously[13].

Typical isotherms are shown in Fig. 1 (a, b, c, and d). For the evaluation of the

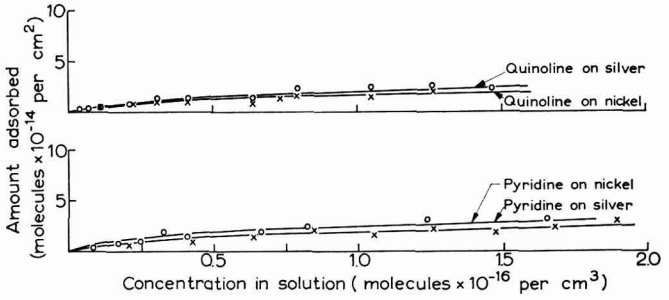

Fig. 1a

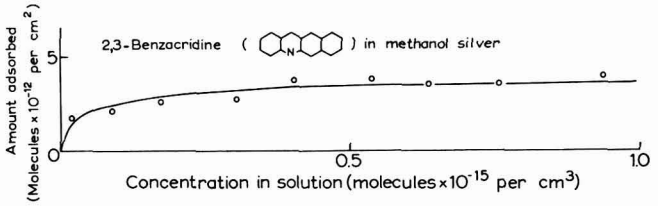

Fig. 1b

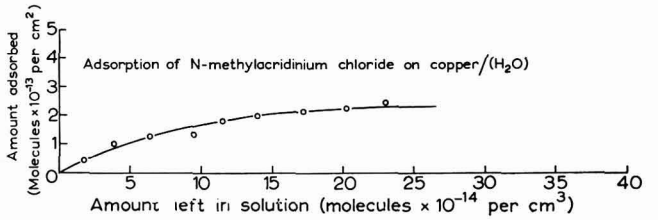

Fig. 1c

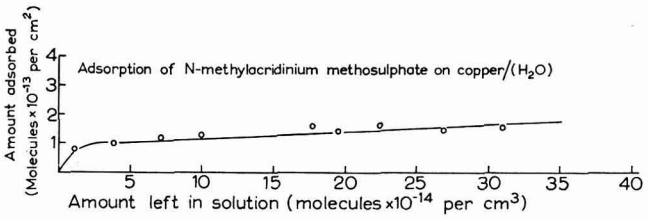

Fig. 1d

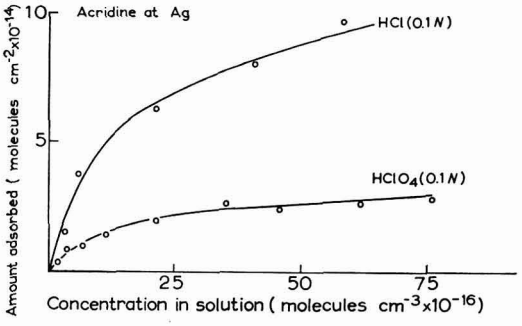

Fig. 1e

Fig. 1. (a), isotherms for adsorption of pyridine and quinoline on nickel and silver at 22° from aq. soln; (b), isotherms for adsorption of 2,3-benzacridine on silver at 22° from methanolic soln; (c), isotherms for adsorption of N-methyl acridinium chloride on copper at 22° from aq. soln.; (d), isotherms for adsorption of N-methyl acridinium methosulphate on copper at 22° from aq. soln.; (e), comparison of isotherms for adsorption of acridine on silver at 22° from 0.1 *N* HCl and 0.1 *N* $HClO_4$ aq. solns.

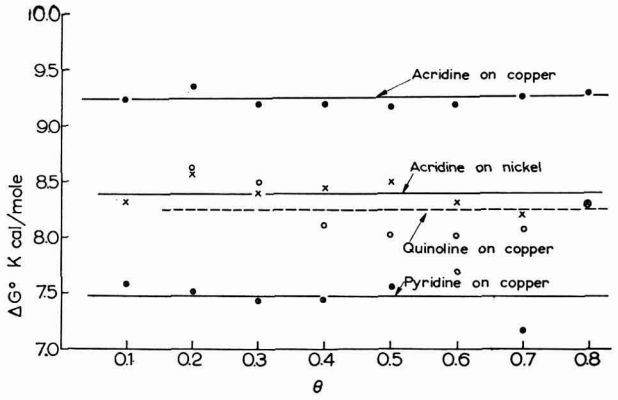

Fig. 2. Apparent standard free energies of adsorption of heterocyclic bases on copper and nickel at 22° as a function of fractional coverage θ.

thermodynamic functions, isotherms were obtained at 22° and 80° and a series of isotherms for acridine on silver, copper and nickel are shown in Fig. 2. Where not otherwise stated, all data reported have been obtained at 22°.

A number of unsuccessful attempts were made to obtain isotherms for 1,2,7,8-dibenzacridine, 1,2,6,7-dibenzacridine, 3,4,6,7-dibenzacridine, pyrrole, indole and carbazole and only where relevant, will brief mention of these results be made in the ensuing discussion. Difficulties arise on account of the low solubility of these additives.

Reagents and solutions

Pyridine (Baker Analyzed Reagent Grade) and quinoline (Refined Grade) were redistilled in nitrogen and *in vacuo*, respectively; acridine (Matheson, Coleman and Bell) was recrystallized from methanol and sublimed.

N-methylacridinium methosulphate[16] was prepared by adding acridine (2 g) to redistilled nitrobenzene (10 ml) at 160°, followed by freshly distilled dimethyl sulphate (2.2 g). The mixture was allowed to cool at once and poured into ether. After an hour, the mixture was filtered giving the methosulphate as yellow crystals in 95% yield. The salt was recrystallised from methanol and ether. N-methylacridinium chloride was prepared from the methosulphate by passing a concentrated aqueous solution of the methosulphate through several columns containing a strongly basic anion-exchange resin (Dowex 1-X8, Baker Chemical Co.) which had been previously converted to the chloride form and washed. The N-methylacridinium chloride was recrystallised from methanol and ether and the chloride content checked by volumetric titration with silver nitrate (Volhard's method). The salt was found to be almost quantitatively stoichiometric.

Hydrochloric and perchloric acids were of the Baker Analyzed Reagent Grade. The methanol used was the "acetone free" reagent grade purified from trace amounts of ethanol by standard procedures. Three isomers of benzacridine were obtained by courtesy of Professor ADRIEN ALBERT. These samples were allrecrystallised from methanol. Pyrrole was purifed by distillation *in vacuo*. Indole and carbazole were recrystallised from water and methanol, respectively.

Potentials

Electrode potentials were maintained near the reversible hydrogen potential for the given solution. Variation of electrode potentials from this region resulted in some dissolution of the metal, or electro-catalytic reduction of the adsorbate[13], which could be detected by direct observation of changes of shape and absorption maximum in the u.v. absorption envelope for the adsorbate examined.

RESULTS AND DISCUSSION

(i) *Characteristic difficulties*

Attempts were made to measure the adsorption of acridinium cations on copper, nickel and silver. Pyridinium and quinolinium ions were not used because of the relatively smaller amounts adsorbed as shown in earlier experiments with the corresponding neutral molecules[13]. In order to maintain the organic bases in their fully ionized state, with negligible hydrolysis, acidified solutions of the substrates must be used. However, the presence of excess acidity gives rise to a problem of a different and difficult nature, namely the dissolution of the adsorbent. The presence of traces of copper and nickel ions, and/or complexes formed between the metallic ions and the organic compounds tends to distort the u.v. absorption bands of the organic adsorbate, thus interfering with the spectrophotometric analytical determinations.

Copper is normally insoluble in completely oxygen-free acid solutions, but such ideal conditions can only be achieved experimentally with considerable difficulty. Acidic solutions of acridine, for example, were de-oxygenated by continuous bubbling with de-oxygenated nitrogen or hydrogen but complete exclusion of oxygen could not be attained. Very small traces of oxygen were sufficient to cause significant dissolution of copper which led to interference with the quantitative observation of the u.v. spectra of acridine and other organic substrates.

Satisfactory isotherms for the adsorption of acridinium chloride and, acridinium perchlorate on silver have already been reported[14].

(ii) *Standard electrochemical free energies of adsorption and the isotherm*

In order to investigate the form of the isotherm which could represent the results obtained in the present work, and to compare the behaviour of the adsorbates at solid metals with that previously observed at mercury, the apparent relative* standard free energies of adsorption $\Delta\bar{G}^{\circ}_{\text{ads.}}$ have been calculated from the following equation[1,3,7] for the standard state of half-coverage ($\theta = \frac{1}{2}$) by the organic adsorbate

$$\ln\left(\frac{\theta}{1-\theta}\cdot\frac{55{\cdot}5}{c}\right) = -\Delta\bar{G}^{\circ}_{\text{ads.}}/RT \qquad (1)$$

where c is the bulk concentration in moles/l. When lateral interactions in the interphase are important, the apparent values of $\Delta\bar{G}^{\circ}_{\text{ads.}}$ will vary with coverage[1,3], and in fact include the coverage dependent term $RT \ln f_\theta$ where f_θ is the activity coefficient for the species in the two-dimensional interphase at a coverage θ**.

The experimental values of the fractional coverage were obtained directly from the observed diminution of concentration of the organic adsorbate in the adsorption cell, the known apparent area of the electrode and the volume of solution used. The calculation of θ requires also an estimate of the surface concentration at full coverage. This was obtained by measuring the planar projected areas derived from space-filling scale atomic models (Courtauld type) and the following areas were derived: acridine 65 Å^2; quinoline 53 Å^2; pyridine 38 Å^2. The real to apparent area factor for copper was taken as 3.5[21] and this factor was assumed to apply to nickel and silver electrodes prepared with the same pre-treatment[10]. Accordingly, the maximum coverages by the heterocyclic bases were estimated to be 5.4×10^{14}, 6.7×10^{14} and 9.1×10^{14} molecules cm^{-1} for acridine, quinoline and pyridine, respectively.

The $\Delta\bar{G}^{\circ}_{\text{ads.}}$ plot for quinoline shown in Fig. 3 (dotted line) departs somewhat from linearity especially at low coverage (below 30%). This may possibly be due to some experimental uncertainty in the determination of the isotherm at low coverage. The best experimental results have always been obtained with acridine and Fig. 3 demonstrates quite clearly that $\Delta\bar{G}^{\circ}_{\text{ads.}}$ is independent of θ for nickel and copper as distinct from the case of polarised mercury surfaces where there is evidence of sharp changes in the slope of plots of θ (or $\theta^{3/2}$ when $\Delta\bar{G}^{\circ}_{\text{ads.}}$ varies with coverage due to

* The values calculated represent, of course, the *difference* between the energy of adsorption of the organic molecule and that of water at the interface.

** The true $\Delta\bar{G}^{\circ}_{\text{ads.}}$, which of course must be a constant independent of conditions (except the definition of the standard state), can be obtained by extrapolation of the θ-dependent apparent values to $\theta \rightarrow 0$.

dipole repulsion[1]) *vs.* $\Delta\bar{G}^{\circ}_{ads.}$ for several adsorbates, even at the potential of zero charge. The latter effect can be semi-quantitatively accounted for[1,2] by intermolecular repulsions arising from orientation of the dipoles in the double-layer at some critical concentration and electrode-solution field intensity. *Flat* orientation which occurs at mercury near the potential of zero charge and up to $\theta \doteqdot 0.75$, is maintained to appreciable anodic and cathodic potentials only with the least π-deficient molecules such as 2-aminopyridine or with two-ring systems like quinoline [1,8]. It is therefore tempting to attribute the constancy of $\Delta\bar{G}^{\circ}_{ads.}$ with coverage found in the present work, to a greater tendency for the heterocyclics to lie flat upon the metal with maximum overlap of π-orbitals with orbitals at the surface of the transition and neighboring metals (Cu, Ag, Ni), than occurs at mercury which has no vacant d-surface states (*e.g.*, copper, although at the end of the first transition series, has anomalous adsorption properties believed to be associated with vacant surface d-orbitals[24] arising by promotion). Benzene and toluene are adsorbed at mercury from the vapour phase[25] in the *flat* configuration, which is consistent with our observations here.

The independence of $\Delta\bar{G}^{\circ}_{ads.}$ upon θ shown in Fig. 3 indicates that the Langmuir isotherm is applicable over a surprising range of surface coverage. The tendency for the

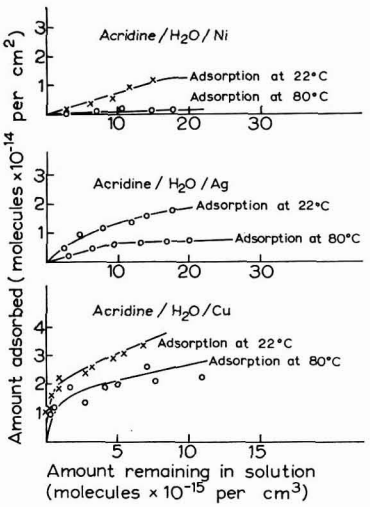

Fig. 3. Adsorption isotherms for acridine on nickel, silver and copper at two temperatures.

molecule to be adsorbed in the *flat configuration* will presumably be determined amongst other factors, by the π-orbital interaction with the metal discussed above, which is then possible. The flat orientation will give no net dipole interaction, since in two dimensions, the flat heterocyclic bases will tend to be oriented at random so that $\Delta\bar{G}^{\circ}_{ads.}$ will not tend to fall with coverage, due to repulsion effects.

It is still puzzling why under these conditions $\Delta\bar{G}^{\circ}_{ads.}$ does not numerically increase with θ on account of van der Waals interactions[3]. A possible explanation may be that as the surface concentration of organic molecules increases and that of water decre-

ases, the energy of displacement of the latter will tend to increase and compensate coincidentally the higher net energy of adsorption of the organic adsorbate with increasing coverage. Constancy of heat of adsorption with coverage θ can also arise if the surface sites have a distribution of adsorption energies but the film is immobile[26]. However, with the present relatively large adsorbate molecules, the van der Waals intermolecular attraction potential U_v will become significant beyond about $\theta \doteqdot 0.6$ and an approximate value, for example, for pyridine can be calculated using the following equation (*cf.* refs. 1,2,3),

$$U_v = -\tfrac{1}{2}NC\phi_v = -\tfrac{1}{2}NC\ 1190 \cdot \frac{zh\theta^3}{\varepsilon_0\pi^3 R^{3/2}} \qquad (2)$$

where ϕ_v is the nearest neighbour interaction potential[3] per pair of molecules in an array of nearest neighbour coordination number C, N is Avogrado's number, z the number of outer shell electrons in the molecule, ε_0 the dielectric constant of the surface layer and R the effective radius of the molecule related to the area ($A = \pi R^2$). $(U_v)_{\theta=0.75}$ for pyridine is obtained as approximately 5 kcal mole^{-1} using a value of[3] about 6 for ε_0. The latter value is rather uncertain and probably itself varies with coverage and molecular orientation[1].

(iii) *Adsorption of ionic adsorbates.* — Acridine is strongly adsorbed when it is in the protonated ionic form in aqueous solutions of excess acid. In such solutions, the acridinium ion is present in large excess over the neutral molecule and it could normally be presumed that the acridinium cation is the species adsorbed. In the case of aromatic and aliphatic amines, it has been suggested however, that the *neutral* molecule may, in fact, be the adsorbed species active in corrosion inhibition in acid solution[17-18]. With heterocyclic bases, where the N-atom is in a conjugated ring, this may not be the case.

The possible difference of behaviour may be explained in the following manner. In the case of heterocyclic bases, both the H^+ or N-methyl quaternary ions and the corresponding neutral bases could be adsorbed through the π-orbitals[1,2,22] at the N—C bonds so that little difference between their standard free enegies of adsorption might be expected, as is found in their adsorption on mercury[1,2] (see below). However, with aromatic or alicyclic bases no such π-orbital interaction at the N-centre is possible in the quaternary ions; in the neutral bases, on the other hand, the lone-pair orbital on the nitrogen atom is available for interaction with the metal, in fact, it has been argued[20] that in some cyclic amines, the hybrid character of the C—N and N—H bonding at the nitrogen centre approaches sp^3. The observation[18] that quaternised aromatic and aliphatic bases are less active as corrosion inhibitors than corresponding solutions of the same bases in acids, has led to the suggestion that in the acid solutions it is, in fact, the neutral molecule which is effective in modifying the kinetics of the partial reactions proceeding in the electrochemical corrosion of iron. In the present work, strong adsorption of the quaternary ion *N-methyl*acridinium (chloride or methosulphate) from neutral aqueous solutions was observed (see Fig. 1, (c) and (d)) and was as strong as that for acridine in HCl solution where the ionic species would be the protonated base. For the N-methyl quaternary ion there can be no ambiguity concerning the species adsorbed and it therefore appears that it is justifiable to regard the adsorption from acridine solutions in acids as involving the protonated ca-

tion*. It is of interest that the gegen-anion has a specific influence on the adsorption of the organic cation as shown in Fig. 1(e) where adsorption of the acridinium ion from 0.1 *N* HCl and $HClO_4$ is compared. The appreciable difference of adsorption in these solutions is probably due to a synergetic effect associated with specific adsorption of the Cl^- anion, an effect sometimes found with mixtures of cationic and anionic leveling agents in electro-plating.

Further evidence concerning the identity of species adsorbed from solutions of heterocyclic bases may be obtained from related studies at the mercury electrode. We have previously shown that the free energies of adsorption of various heterocyclic bases in neutral and protonated ionic forms were surprisingly similar[1,2]. This would be the case if the neutral molecules (or the ions) were adsorbed in both the neutral *and* the acidic solutions, despite the fact that in acid solutions the concentration of neutral molecules would be very small. From electrocapillary measurements on the adsorption on mercury of pyridine in HCl[1,2] and N-methylpyridinium chloride (MePyCl) in HCl[23], it is possible to make a direct comparison between the standard electrochemical free energies of adsorption, $\Delta\bar{G}^{\circ}_{ads.}$, of pyridine and MePyCl at the mercury electrode. The figures (for the indicated fractional coverage, θ, by the adsorbate) are shown in Table 1.

TABLE 1

APPARENT STANDARD FREE ENERGIES OF ADSORPTION AT THE MERCURY ELECTRODE IN kcal $mole^{-1}$

Absorbate	*At* $E_{cal} = -800$ *mV* $\theta = 0.25$	*At* $E_{cal} = -1000$ *mV*	
		$\theta = 0.25$	$\theta = 0.5$
Pyridine° (KCl)	−4.2	−4.8	−4.8
Pyridinium$^+$ (HCl)	−4.7	−4.7	−3.5
$MePy^+$ (HCl)	−4.2	−4.9	−4.7
(Estimated error)	±0.1	±0.1	±0.1

It is seen that at the given potentials, the values of $\Delta\bar{G}^{\circ}_{ads.}$ for pyridine are quite similar to those for MePyCl for which there can be no ambiguity concerning the identity of species adsorbed. This comparison is regarded as valid since the quaternary ion differs from the protonated ion only by one *methylene* group. It is therefore concluded that the species adsorbed on mercury from pyridine solutions in aqueous HCl, and those adsorbed on silver from acridine solutions in aqueous HCl or $HClO_4$, are predominantly the protonated pyridinium and acridinium ions, respectively, and that the comparison between the electrochemical free energies of adsorption of neutral and protonated ions is hence meaningful.

It may be noted that in a 10^{-2} *M* pyridine solution in 1 *N* HCl (typical concentrations used in the adsorption measurements), the ratio of the activity of the protonated

* Unfortunately, in this and other cases (*e.g.*, aniline) the ionic and neutral forms of the molecule have quantitatively similar absorption behaviour in the u.v. (below 320 mμ).

pyridinium ion to that of the neutral pyridine molecule will be about 1.5×10^5 ($pK_A = 5.2$). In order for the neutral molecule to be preferentially adsorbed, say by a factor of ten under these conditions, it is readily calculated that the difference between the standard free energy of adsorption of the neutral molecule and that of the conjugate ion must be at least 8.5 kcal mole^{-1}. The above observations and those given previously[1,2], indicate that the difference between the standard free energy of adsorption of the bases and their conjugate ions is much less than the limiting figure calculated above. The same conclusions apply to acridine ($pK_A = 4.5$) adsorption from acid solutions. In acid solutions, therefore, such molecules are to be regarded as predominantly adsorbed in the ionic protonated form.

(iv) *Heats and entropies of adsorption*

The spectrophotometric method was also applied to the estimation of isosteric heats of adsorption $\Delta H°$ of acridine at copper by obtaining the isotherms at different temperatures (Fig. 2) and applying an integrated form of the Clausius–Clapeyron equation. At half-coverage of the metal surface, the heat of adsorption may be calculated as about 5 kcal mole^{-1} (see Table 2).

TABLE 2

Function	*Coverage* θ				*Probable error*
	0.2	*0.3*	*0.4*	*0.5*	
$\Delta H°$ (Cu) (kcal mole^{-1})	−5.8	−5.1	−5.4	−4.9	±0.5
$\Delta S°$ (Cu) (e.u.)	11	14	13	14	±2
$\Delta H°$ (Ag) (kcal mole^{-1})	−3.8	−3.9	−4.1	—	±0.5
$\Delta S°$ (Ag) (e.u.)	14	14	14	—	±2

For the adsorption of acridine at silver or nickel, the isosteric heat of adsorption could not be calculated (see Fig. 2) since over the range of concentrations studied, comparable surface coverages were not obtained at the two temperatures examined and even at lower coverages the same problem remains for nickel. Values of $\Delta H°$ were estimated for acridine on copper and silver at lower surface coverage and the results are tabulated (Table 2) together with the corresponding $\Delta S°$ values derived from $\Delta H°$ and $\Delta G°$ values. The values of $\Delta H°$ are almost constant (within experimental error) with coverage and this is consistent with the observed constancy of the apparent standard free energy with coverage (Fig. 2) calculated by means of eqn. (2).

The main point of interest in the values of the standard entropies of adsorption is that they are positive, while in the case of adsorption from the gas phase, entropy changes are usually negative on account of loss of degrees of freedom of the adsorbate upon adsorption at the interface. An explanation of this apparent anomaly lies in the fact that upon specific adsorption of the solute, displacement of several water molecules from the surface must occur, the adsorption of the organic additive being competitive with that of water, so that these values are relative rather than absolute ones. This release of water molecules will be accompanied, per mole, by a positive entropy change probably of the order of the entropy of fusion of water. Since, for example, the pyridine molecule will be equivalent in area to about five water molecules, it may be understood

how a net positive entropy change can result. Also the entropy of the molecule in water solution will in any case be less than in the gas phase.

(v) *Role of adsorbate size and structure*

Previously obtained data[13] on the relative adsorption isotherms for copper using pyridine, quinoline and acridine, indicated an expected trend that the degree of adsorption increases with the number of condensed conjugated rings in the molecule. Further attempts were made to correlate adsorbate structure with degree of adsorption.

Three characterised isomers of benzacridine and three of dibenzacridine were obtained from Professor A. ALBERT. The adsorption of these substances was examined at copper but their solubilities were far too low (less than 10^{-6} *M*) for them to be usefully employed. An analogous series (*i.e.*, of compounds differing from one another by a six-membered ring) comprising pyrrole, indole and carbazole was explored as a second possibility to study the effect of ring size on adsorption at copper. The solubility of carbazole was again found to be too low for practical use. A further restriction was the absence of any sharp absorption peaks in the u.v. spectrum of pyrrole.

A change of solvent from water to methanol was made in order to overcome the difficulties presented by the insolubility of the above compounds. Negligible amounts of 1,2-benzacridine and 3,4-benzacridine were adsorbed from methanolic solutions. With copper, only the isomer 2,3-benzacridine was significantly adsorbed (see Fig. 1 (b)). It may be observed that the linear 2,3-benzacridine has the most favourable structure for maximum adsorption in a planar configuration.

Methanolic solutions of acridine, pyridine and quinoline were examined with copper, silver and nickel. In all cases, the additives showed little adsorption at nickel and silver. Trace amounts were adsorbed by copper, which confirms the trend previously reported[13] that copper is the best adsorbent of the three metals in these experiments. These results also suggest a parallelism between the degree of adsorption and the solubility of the adsorbate. This is clearly not the only factor concerned, since quite soluble derivatives, *e.g.*, quaternary ions of the bases, are strongly adsorbed from water at mercury, even at the potential of zero charge.

An explanation of the negligible adsorption from methanolic solutions is that there exists the usual competition between the interphase* and the bulk phase for the solute, and in the methanolic solution the organic molecule probably has a higher energy of solvation than in water. Only with 2,3-benzacridine is the enhanced solubility in methanol sufficiently small for it to be possible to measure a significant extent of adsorption over a range of concentrations large enough to enable an isotherm to be obtained.

(vi) *Effect of variation of applied potentials*

The effect of variation of applied potentials was examined but satisfactory results could not be obtained (*cf.* Ref. 28) with copper and nickel electrodes over any appreciable range of potentials ($>$ 100 mV), because of the problems already stated concern-

* Here we prefer to use the term *interphase* rather than *interface* as it allows a better description of the two-phase equilibrium which occurs in adsorption. It also avoids the introduction of fictitious concepts such as adsorption in a two-dimensional interface (*cf.* GUGGENHEIM[27]), a term which is preferably to be restricted to the dividing boundary between the adsorbent and the solution.

ing the dissolution of the metals in acidic media, or electro-catalytic reduction of the conjugated adsorbate, which can be observed in the case of acridine by the appearance of a new absorption peak in the u.v. which can be followed quantitatively. A limited range of variation of potential has been followed using silver in a quinolinium chloride solution as shown in Fig. 4. Reduction still occurs, however, at cathodic potentials higher than -0.5 V *vs.* the 0.1 *N* HCl calomel electrode. Despite the difficulties in this

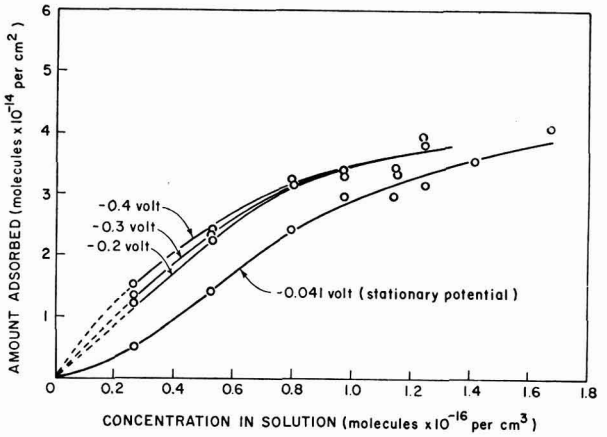

Fig. 4. Effect of electrode potential (measured *vs.* 0.1 *N* HCl calomel electrode) on adsorption of quinoline on silver (22°) below the potential where electrochemical reduction becomes significant.

aspect of the work, it can be expected that such studies could be made successfully with electrodes of more noble metals such as platinum, gold or iridium, at least at moderate anodic potentials. These experiments have not yet been pursued because of the prohibitive cost of making specially fabricated large gauze electrodes of sufficiently fine mesh from these metals.

ACKNOWLEDGEMENTS

We are indebted to the National Research Council for support of this and related work and to the Defence Research Board for support of the work on Grant No. 9530-16. We wish to thank Professor A. ALBERT for providing us with several benzacridine isomers.

SUMMARY

A spectrophotometric method developed previously has been applied to the examination of the adsorption of several organic adsorbates in neutral and ionic form at various solid electrode materials. Standard free energies and isosteric heats of adsorption have been evaluated and their apparent dependence on coverage examined. The behaviour of the adsorbates at the solid metals is compared with that of similar compounds at the mercury electrode. As in previous work, difficulties are encountered when adsorption at non-noble metals is studied over a range of potentials.

REFERENCES

1 B. E. CONWAY AND R. G. BARRADAS, *Electrochim. Acta*, 5 (1961) 319.
2 R. G. BARRADAS AND B. E. CONWAY, *ibid.*, 5 (1961) 349.
3 E. BLOMGREN AND J. O'M. BOCKRIS, *J. Phys. Chem.*, 63 (1959) 1475.
4 P. W. SCHAPINK, M. OUDEMAN, K. W. LEU AND J. M. HELLE, *Trans. Faraday Soc.*, 56 (1960) 415.
5 M. A. V. DEVANATHAN, *Proc. Roy. Soc. (London), Ser. A*, 264 (1961) 133.
6 R. PARSONS, *ibid.*, 261 (1961) 79.
7 E. BLOMGREN, J. O'M. BOCKRIS AND C. JESCH, *J. Phys. Chem.*, 65 (1961) 2000.
8 R. G. BARRADAS, *Ph.D. Thesis*, University of Ottawa (1960).
9 R. S. HANSEN AND B. H. CLAMPITT, *J. Phys. Chem.*, 58 (1954) 908; 60 (1956) 1185.
10 N. HACKERMAN AND J. S. STEPHENS, *ibid.*, 58 (1954) 904.
11 J. O'M. BOCKRIS AND B. E. CONWAY, *ibid.*, 53 (1949) 527.
12 B. E. CONWAY, AND J. O'M. BOCKRIS, *Proc. C.I.T.C.E. (Poitiers Meeting)* (1955) 207.
13 B. E. CONWAY, R. G. BARRADAS AND T. ZAWIDSKI, *J. Phys. Chem.*, 62 (1958) 676.
14 B. E. CONWAY AND R. G. BARRADAS, *Trans. Symposium on Electrode Processes 1959*, edited by E. YEAGER, John Wiley and Sons Inc., New York, 1961, p. 299.
15 R. J. NEWMILLER AND R. B. PONTIUS, *J. Phys. Chem.*, 64 (1960) 584.
16 A. ALBERT, *The Acridines*, Arnold, London, 1951.
17 N. HACKERMAN, *Trans. N. Y. Acad. Sci.*, (2) 17 (1954) 7.
18 N. HACKERMAN AND A. C. MAKRIDES, *Ind. Eng. Chem.*, 46 (1954) 523.
19 N. HACKERMAN AND H. KAESCHE, *J. Electrochem. Soc.*, 105 (1958) 191.
20 N. HACKERMAN, *Abstracts*, 118th Meeting of the Electrochemical Society, Houston, Texas (1960).
21 J. O'M. BOCKRIS AND B. E. CONWAY, *J. Chem. Phys.*, 28 (1958) 707.
22 M. GEROVICH, *Dokl. Akad. Nauk SSSR* 86 (1954) 543; 105 (1955) 1278.
23 B. E. CONWAY, R. G. BARRADAS AND J. M. PARRY, in course of publication.
24 McD. BAKER AND G. I. JENKINS, *Advan. Catalysis*, 7 (1955) 1.
25 C. KEMBALL, *Proc. Roy. Soc. (London), Ser. A*, 190 (1947) 117.
26 O. BEECK, *Advan. Catalysis*, 2 (1950) 151.
27 E. A. GUGGENHEIM, *Trans. Faraday Soc.*, 36 (1940) 397.
28 J. O'M. BOCKRIS AND E. BLOMGREN, *Nature*, 187 (1960) 504.

RADICAL ION INTERMEDIATES IN THE ELECTRO-REDUCTION OF TRIPHENYLMETHANE DYES

TERRY MILLER, BARBARA LAMB AND RALPH N. ADAMS

Department of Chemistry, University of Kansas, Lawrence, Kansas (U.S.A.)

(Received 24th July, 1963)

The reduction products of several triphenylmethane dyes have been investigated by means of electron paramagnetic resonance (EPR) studies. Previous reports[1-3] have indicated that the dyes are reduced through a free radical stage. This investigation has endeavoured to demonstrate conclusively the existence of such free radical intermediates by exhibiting their EPR spectra.

EXPERIMENTAL

Commercial DuPont dyes were used without further purification. Saturated solutions of the dyes were de-aerated by a stream of nitrogen and then filtered before spectroscopic investigation. Dimethylformamide (DMF) was used as co-solvent with Britton-Robinson buffers (pH values quoted throughout this paper are those of the aqueous buffer in the solution); tetraethylammonium perchlorate was the supporting electrolyte. The technique of *in situ* reduction, which has been described previously[4], was employed on these solutions using a Varian V-4500 EPR Spectrometer.

RESULTS AND DISCUSSION

The following dyes (Color Index number in parentheses) were examined: crystal violet (681), ethyl violet (682), malachite green (657), brilliant green (662), fuchsine (677), setoglaucine (658) and alphazurine G (712).

Solutions of crystal violet varying in pH from 3–6 and in DMF concentration from 15–35% were reduced at a potential of −1.3 V. The resulting spectrum was a singlet with a line width of 1.3 gauss. Further investigation disclosed solvent effects such as those noted by KEMULA[5]. The EPR resonance disappeared about 1½ h after dissolution of the dye, and no spectrum was detected in pure DMF solution.

Similarly, solutions of ethyl violet were reduced at −1.3 V. The pH of solutions examined ranged from 5–6 and the DMF concentration from 15–35%. The observed spectrum which also diminished with time was again a singlet having a line width of 1.7 gauss.

The reduction at −1.2 V of solutions of setoglaucine at pH 6 in 35% DMF produced a singlet with line width of 2.3 gauss. The singlet associated with setoglaucine likewise decayed, exhibiting a half-life of about 75 min. Reduction of a fuchsine solution at pH 6 in 35% DMF at −1.1 V produced a very broad, very weak singlet. The extensive line width — approximately 8 gauss — and the weakness of the singlet

make it impossible to attribute the resonance definitely to a free radical reduction product of fuchsine. However, no resonance was observed prior to application of the reduction potential. No distinguishable hyperfine structure was found with any of these dyes.

Using solutions of the other dyes — malachite green, alphazurine G, and brilliant green — no radical intermediates were detected by the EPR spectrometer. Investigations were carried out on saturated and also less concentrated solutions of these dyes. The pH of the solutions was varied from 3–6 , and the DMF concentration was varied from 15–35%. No complete explanation has yet been found to account for the failure of malachite green, etc. to yield an EPR spectrum upon reduction. However, it should be noted that the absence of an EPR spectrum does not preclude the existence of the radical intermediate in the reduction.

If, as mentioned above, the decay of the resonance of the radical intermediates in the cases of crystal violet, etc. is attributed to the solvation of the dye cation and the subsequent irreducibility of the solvated cation[5], a similar process might well occur with malachite green, etc. Since there is about a 15-min interval between the dissolution of the dye and the first scan on the EPR spectrometer, no EPR spectrum would be recorded if the solvation process in the cases of malachite green, etc. were sufficiently rapid, although a radical might be formed by the reduction of the dye cation, provided it remained unsolvated.

ACKNOWLEDGEMENTS

This work was supported by the Atomic Energy Commission through contract AT-(11-1)-686. The authors (B. LAMB and T. MILLER) gratefully acknowledge the support received for this work in the form of undergraduate research grants from the National Science Foundation and the Kansas Heart Association.

SUMMARY

The existence of radical intermediates in the reduction of several triphenylmethane dyes has been proved by observation of their EPR spectrum. Certain solvation effects concerning the reduction of the dyes have also been substantiated. Under equivalent conditions however, the expected spectra from the reduction of other similar triphenylmethane dyes have not been produced.

REFERENCES

1 R. C. KAYE AND H. J. STONEHILL, *J. Chem. Soc.*, (1952) 3232.
2 W. KEMULA AND A. AXT-ZAK, *Roczniki Chem.*, 36 (1962) 737.
3 C. G. BUTLER AND F. P. MARTIN, *J. Pharm. Pharmacol.*, 14 (1962) 103T.
4 L. H. PIETTE, P. LUDWIG AND R. N. ADAMS, *Anal. Chem.*, 34 (1962) 916.
5 W. KEMULA AND A. AXT-ZAK, *Roczniki Chem.*, 37 (1963) 113.

Short Communication

Current–Voltage Curves for Zirconium and Uranium in Molten Fluorides

A cathodic wave for the reduction of zirconium(IV) in molten LiF–NaF–KF (46.5–11.5–42 mole %) and an anodic wave for the oxidation of uranium(IV) in molten LiF–NaF–KF and also in molten $2LiF \cdot BeF_2$ have been observed. Zirconium and uranium were added as ZrF_4 and UF_4. Typical current–voltage curves are shown in Fig. 1.

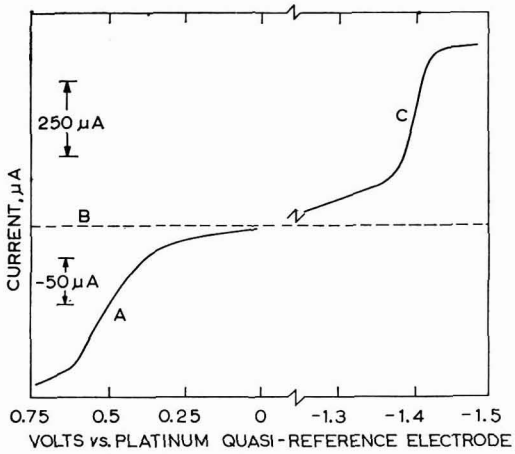

Fig. 1. Current–voltage curves for UF_4 and ZrF_4 in molten LiF–NaF–KF, temperature 498°: (A), oxidation of UF_4, concn. UF_4 approximately 0.01 *M*, Pt indicator electrode area 3.1 mm^2; (B), zero current line; (C), reduction of ZrF_4, concn. ZrF_4 approximately 0.06 *M*, tungsten indicator electrode area 9 mm^2.

As previously discussed[1], the molten LiF–NaF–KF was contained in a graphite cell which was enclosed in a quartz vessel to provide a vacuum or a controlled atmosphere. A similar technique was utilized for the molten $2LiF \cdot BeF_2$ except that the graphite cell was enclosed in a nickel apparatus.

A controlled-potential polarograph[2] was used to record the current–voltage curves. In the molten LiF–NaF–KF system the indicator electrode was connected with a platinum quasi-reference electrode and an isolated counter electrode. For the $2LiF \cdot BeF_2$ melt, the graphite cell which had a large surface area as compared to the platinum indicator electrode, was used for both the quasi-reference electrode and the counter electrode.

The reduction wave for zirconium at both platinum and tungsten micro-electrodes exhibits a half-wave potential of approximately −1.4 V *vs.* the platinum quasi-reference electrode. In general, the waves were better defined when the tungsten indicator electrode was used. That the zirconium undergoes a four-electron change

was indicated by reverse scans in which reasonably well-defined stripping curves were obtained in all cases. On reverse scans, the current passed through zero at approximately +1.25 V; however, the stripping curve exhibited no inflection in passing through zero current which suggests reversibility of the electrode process.

The oxidation of uranium(IV) at a platinum micro-electrode occurred at half-wave potentials of approximately +0.4 and +0.5 V *vs.* the graphite and platinum quasi-reference electrode, respectively. The slopes of logarithmic plots of log $(i_l - i)/i$ *vs.* E were in good agreement with theory[3] for a one-electron change. This suggests the oxidation of U(IV) to U(V) under the existing conditions.

In general, the correlation between the limiting current (wave heights) and the concentration of the electroactive species was erratic. This may be due in part to the surface condition of the electrode as well as traces of oxide impurity in the melt which may cause partial precipitation of UO_2 and ZrO_2. However, one of us (G. M.) is conducting further studies on the voltammetry and chronopotentiometry of uranium in molten fluorides and more detailed results will be presented in a subsequent report.

Analytical Chemistry Division,
Oak Ridge National Laboratory,
Oak Ridge, Tennessee (U.S.A.)

D. L. MANNING

Reactor Chemistry Division,
Oak Ridge National Laboratory, and
Chemistry Department,
University of Tennessee,
Knoxville, Tennessee (U.S.A.)

GLEB MAMANTOV

1 D. L. MANNING, *J. Electroanal. Chem.*, 6 (1963) in press.
2 M. T. KELLEY, H. C. JONES AND D. J. FISHER, *Anal. Chem.*, 31 (1959) 1475.
3 I. M. KOLTHOFF AND J. J. LINGANE, *Polarography*, Vol. 1, Interscience Publishers, Inc., New York, 1952, pp. 205–209.

(Received May 21st, 1963)

Book Review

Les Réactions Chimiques dans les Solvants et les Sels Fondu, by G. CHARLOT AND B. TRÉMILLON, Gauthier-Villars, Paris, 1963, xii + 602 pages. N.F. 94 ($20).

This is a remarkably compact collection of information about chemical reactions in different solvents. The use of thin paper has enabled the compression of 600 pages into a very convenient small book.

The first 150 pages introduce the subject in a general way, the overall view being stressed rather than the details. Thus the authors use the Born model for the interaction of ions with the solvent to illustrate general trends rather than attempting a more detailed physical interpretation which might satisfy the expert, but confuse the general reader. Three principal classes of reaction are considered: acid–base (in the Brønsted–Lowry sense), complex formation (transfer of atoms other than hydrogen) and oxidation-reduction (electron transfer) reactions. Limiting types of behaviour are described in strongly dissociating and weakly dissociating solvents. The use of generalised scales analogous to pH scales is extensively and clearly discussed. One of the few obscurities is the discussion on page 38 of the use of Onsager's conductance equation for the determination of dissociation constants. The equation quoted is incorrect for the conductance of a weakly dissociated electrolyte and the numerical constants in it are unidentified. Many references are given at the end of each section, but as they are not individually quoted they would be useful mainly for focussing a literature search.

The greater part of the book consists of data and lists of references for individual solvents, including 85 pages on fused salts. The number of references must run into several thousand and this book is therefore a most useful source of information, especially as some idea of the content of each paper is usually given in the text. The physical constants of the solvent given are the dielectric constant and the boiling point or freezing point. Most space is naturally given to the reactions which have been studied in the solvent and their equilibrium constants.

Prof. CHARLOT and M. TRÉMILLON have made a worthy start to the new series of monographs of Inorganic Chemistry under the general editorship of Prof. CHRÉTIEN. Many others besides inorganic chemists will find matter of interest to them in this book.

ROGER PARSONS, University of Bristol

THE POLAROGRAPHIC SOCIETY

President: Professor J. Heyrovsky

Chairman: H. M. Davis

THIRD INTERNATIONAL CONGRESS OF POLAROGRAPHY

SOUTHAMPTON, 19-25 JULY 1964

Chairman of Congress: Professor G. J. Hills

President and 1964 Medallist: Professor I. M. Kolthoff

The Third International Congress of Polarography has been organised to coincide with the tenth anniversary of the founding of the Polarographic Society. It is being held at the University of Southampton which provides excellent facilities for lectures, exhibitions and accomodation.

The Congress will be concerned with all aspects of polarography and will be open to members and non-members of the Society.

Contributed papers will be selected on the basis of a lengthy abstract which, in turn, will enable a Sub-Committee of Referees to select full papers for publication in a separate volume of proceedings.

Further details on the programme, contributed papers, exhibitions, fees, accomodation and social activities can be obtained from the Congress Secretary: Dr. D. A. Pantony, T.D., F.R.I.C., Department of Metallurgy, Imperial College of Science and Technology, London, S.W.7.

THE POLAROGRAPHIC SOCIETY

CONTENTS

ELSEVIER PUBLISHING COMPANY, AMSTERDAM

Printed in The Netherlands by

NEDERLANDSE BOEKDRUK INRICHTING N.V., 'S-HERTOGENBOSCH